DISSERTATION

INFLUENCE OF PROSODY AND EMOTIONAL CONGRUENCE IN EMOTION PERCEPTION

Submitted by

Katherine M. Becker

Department of Psychology

In partial fulfillment of the requirements

For the Degree of Doctor of Philosophy

Colorado State University

Fort Collins, Colorado

Summer 2020

Doctoral Committee:

Advisor: Donald C. Rojas

Deana B. Davalos
Dan J. Graham
Jaclyn Stephens

ABSTRACT

INFLUENCE OF PROSODY AND EMOTIONAL CONGRUENCE IN EMOTION PERCEPTION

Vocal emotion, or emotional prosody, is conveyed via suprasegmental changes to the acoustic qualities of a speaker's voice. Prosody is essential to affect perception as it can independently and instantaneously convey emotion. Prosody normally coincides with affective facial expressions and other non-verbal cues to form holistic emotional percepts. Prior research pairing emotional voices with affective faces found that emotion perception may be biased by emotional prosody, as affective faces presented with a happy voice were rated 'happier' than faces presented with an angry or neutral voice. While these findings indicate that emotion perception is biased by voice prosody, the precise mechanism of this bias remains unclear. Since vision predominates perception, much like in the more well-known McGurk effect, it is likely that visual cues in the speaker influence the prosodic bias. Visual modality cues in the face may moderate this bias via increased fixations to the mouth or eyes, potentially changing the influence of prosody as the perceiver is or is not directed to visual cues associated with auditory information. Thus, increased visual attention to moving mouths may increase the perceptual bias created by prosodic voices. Visual attention patterns will be directed to fixate on either the mouth or eyes of speaking faces paired with either emotionally congruent or incongruent voices. The current study will use behavioral measures, electroencephalography, and magnetoencephalography to assess the neural and behavioral correlates underlying the effects of emotional congruency and visual attention on prosodic perceptual biases.

ACKNOWLEDGEMENTS

This work would not have been possible without the support of my doctoral committee: Dr. Don Rojas, Dr. Deana Davalos, Dr. Dan Graham, and Dr. Jaclyn Stephens. Their expertise and insight enabled me to design and execute three research projects which I will present in my doctoral dissertation. Additionally, I would like to thank Dr. Michael Thomas for standing in on the day of my oral defense. This journey contained many stumbling points at which my enthusiasm began to falter, but the continued support of my advisor, committee, and family and friends enabled me to finish this endeavor.

TABLE OF CONTENTS

CHAPTER 1 – GENERAL INTRODUCTION

The ability to make inferences about the emotional state of another individual is facilitated by the decoding and identification of concurrently presented facial and vocal information. Deriving the contribution or role of each modality in affect perception is difficult as both faces and voices provide sufficient information to convey emotions independently (Ekman & Friesen, 1976; Schröder 2003; Belin, Fillion-Bilodeau, & Gosselin, 2008). Darwin (1872) was the first to recognize the innate correspondence of facial movements to the condition of one's internal emotional state. Ekman and Friesen (1976) expounded upon this concept, identifying six basic emotions (anger, happiness, sadness, disgust, fear, and surprise) which are associated with the stereotyped movements of groups of facial muscles (Bartlett, Viola, Sejnowski, Golomb, Larsen, Hager, & Ekman, 1996; Ekman, 1984). These facial expressions appear to be highly salient, as performance on tests evaluating the recognition and characterization of others' emotional state is consistent across cultures (Darwin, 1872; Ekman, 1993; Ekman, Friesen, & Wallace, 1971; Ekman & Frisen, 1976). This conservation implies that facial expressions are inherent and play an essential role in human communication. Yet, faces are rarely experienced naturally in silence; rather, they are typically accompanied by a vocal counterpart.

Vocal emotion, or emotional prosody, is conveyed via suprasegmental changes to the acoustic qualities of a speaker's voice (Belin, Fillion-Bilodeau, & Gosselin, 2008; Juslin & Laukka, 2003; Patel, Scherer, Björkner, & Sundberg, 2011), which can be combined to form auditory gestalts of emotion. Prosody is essential to affect perception as it can independently and instantaneously convey emotional information (Johnson, Emde, Scherer, & Klinnert, 1986). Prosody normally coincides with emotional facial expressions and other non-verbal cues to form

holistic emotional percepts. Thus, prosody appears to be embedded in human communication and may be considered the vocal analog of the six basic emotions originally identified by Ekman & Friesen (Ekman & Friesen, 1976; Schröder, 2003). These findings make intuitive sense, as vocalizations are produced through the coordinated action of vocal and facial muscles, which result in distinctive facial expressions (Schröder, 2003; Belin, Fillion-Bilodeau, & Gosselin, 2008). This congruency implies that vocalizations and facial expressions may be innately linked as visceral responses, simultaneously communicating affective audiovisual information to the eyes and ears of an observer. Previous research pairing emotional voices with emotional faces found that emotion perception may be biased by the prosody of a speaker's voice, as faces presented with a happy voice were rated 'happier' than faces presented with an angry or neutral voice (Becker & Rojas, submitted). Moreover, this perceptual bias was associated with a distinct anterior-posterior distribution of neural activity, with affective faces paired with angry voices exhibiting activity in right frontal areas and happy voices showing activity over right posterior parieto-occipital areas (Becker & Rojas, submitted).

The instantaneous and automatic integration of visual information with vocal information is best illustrated during speech communication, wherein auditory information from a speaker's voice is directly linked to the movements of a speaker's face to form one coherent percept (McGurk & MacDonald, 1976). One of the most influential experiments examining aberrant audiovisual integration is evidenced by the illusory percept formed (hearing /da-da/) by the fusion of two mismatched visual (spoken /ga-ga/) and auditory inputs (voiced /ba-ba/), commonly known as the McGurk Effect (McGurk & MacDonald, 1976). This phenomenon has been replicated in experiments of affect perception, where the vocal and facial cues of a stimulus contain conflicting emotional information (Massaro & Egan, 1996; de Gelder & Vroomen, 2000). These studies have

shown that while both facial expressions and affective vocalizations can bias emotion perception (Massaro & Egan, 1996; de Gelder & Vroomen, 2000), faces appear to have the greatest effect (Massaro & Egan, 1996; de Gelder & Vroomen, 2000; Abelin, 2007). Since vision predominates the perception, it is likely that visual cues in the speaker influence the prosodic bias. Faces are highly salient sources of information with visual attention focusing on three core facial regions: the eyes, nose, and mouth (Luria & Strauss, 1978; Stacey, et al., 2005). Visual fixations to these core regions may moderate the influence of prosody on bimodal emotion perception, as the perceiver may or may not be directed to cues strongly associated with auditory information. Increased visual attention to mouths may thus increase the perceptual bias created by prosodic voices by increasing the gain on vocal auditory information processing.

The vast majority of emotion perception research has only employed silent static face images to study affect recognition (de Gelder & Vroomen, 2000, Massaro & Egan, 1996; Ekman & Friesen, 1976; Bartlett, Viola, Sejnowski, Golomb, Larsen, Hager, & Ekman, 1996; Ekman, 1984; Ekman, 1993; Bruce & Young, 2000). These stimuli fail to accurately simulate affective states as emotions are multidimensional and fluid, accompanied by physiological changes that can instantaneously change the emotional prosody of a person's voice, their facial expression, and body language (Schirmer & Adolphs, 2017). Static faces present emotions as single frames representing one fixed point in time. These frozen images miss the unique information rich configural changes that differentiate emotions as they unfold across time (O'Toole, Roark, & Abdi, 2002). This difference is meaningful as motion facilitates face recognition by imparting supplementary information not provided by two-dimensional faces (O'Toole, Roark, & Abdi, 2002; Jiang, Blanz, & O'Toole, 2009; Lander & Bruce, 2003). Moreover, the brain differentially processes changeable and invariant facial features via a distributed network of neural areas

(Haxby, Hoffman, & Gobbini, 2000). These findings underscore the importance of using dynamic faces in affect perception research as they convey perceptual advantages that are associated with distinct neural substrates. This experimental oversight undermines our current understanding of emotion perception, as it predicates itself on the use of ecologically invalid silent static face images. This literature is further complicated as countless studies have used these stimuli in experiments which identified deficits in emotion perception in multiple clinical populations: autism spectrum disorder, schizophrenia, bipolar disorder, post-traumatic stress disorder, and depression. Many of these findings are confounded by the nature of their stimuli as they may reflect deficits in recognizing static faces rather than impairments in making holistic judgments about multimodal emotions encountered in the real world, as several studies have indicated that dynamic faces may convey a perceptual advantage regardless of an individual's clinical diagnosis as typically developing individuals (Ambadar, Schooler, & Cohn, 2005) and persons with autism spectrum disorders (Gepner, Deruelle, & Grynfeltt, 2001) were more accurate at recognizing dynamic faces over static ones.

This study contributes to the current literature by using dynamic face stimuli to investigate the neural and behavioral correlates underlying the effects of visual attention on prosodic perceptual biases, as well as the influence of emotional congruency on such biases. In the first experiment, visual attention was directed to different facial locations while viewing speakers' faces paired with either emotionally congruent or emotionally incongruent voices. Hypothesis 1: The authors predicted that individuals cued to the mouths of speaking faces would exhibit larger biases for each prosody condition as measured through two psychophysical measures of perception (the point of subjective equality (PSE) and the just noticeable difference (JND)). Functional neuroimaging was used to identify the underlying neural activity associated with this prosody-

related bias using electroencephalography (EEG) and magnetoencephalography (MEG). In the second experiment, subjects were presented with affective faces, voices, and emotional faces and voices paired together while their brain activity is measured using EEG. This activity was decomposed using independent component analysis to better deconstruct and localize this activity. Hypothesis 2a: Neural activity will be localized to the parietal, temporal, and occipital areas in the right hemisphere. Hypothesis 2b: Select neural components will be correlated with the conditions (happy, angry, neutral prosody) and/or stimulus types (face, voice, face and voice) of the experiment. In the third experiment, MEG was used to assess the effects of emotional congruency on right hemisphere activity. Hypothesis 3a: Emotionally incongruent face-voice pairs will exhibit greater activity in the right posterior superior temporal sulcus than emotionally congruent face-voice pairs. Hypothesis 3b: Neural activity will exhibit a posterior-anterior distribution of activity in the right hemisphere with emotionally congruent angry face-voice pairs being localized to anterior areas of the right hemisphere and congruent happy face-voices pairs being localized to posterior areas of the right hemisphere.

REFERENCES

Ambadar, Z., Schooler, J. W., Cohn, J. F. (2005). Deciphering the enigmatic face: the importance of facial dynamics in interpreting subtle facial expressions. *Psychological Science, 16*(5):403-410. PMID: 15869701

Bartlett, M.S., Viola, P.A, Sejnowski, T.J., Golomb, B.A., Larsen, J., Hager, J.C., Ekman, P. (1996). Classifying facial action. *Advances in Neural Information Processing Systems.* D. Touretzky, M. Mozer, & M. Hasselmo (Eds.), MIT Press, pp. 823-829.

Belin, P., Bestelmeyer, P.E.G., Latinus, Watson, R. (2011). Understanding Voice Perception. *British Journal of Psychology,* 102:711-725. doi:10.1111/j.2044-8295.2011.02041.x

Belin, P., Fillion-Bilodeau, S., Gosselin, F. (2008). The Montreal Affective Voices: a validated set of nonverbal affect bursts for research on auditory affective processing. *Behavioral Research Methods, 40*(2):531-9. PMID: 18522064

Bruce, V., Young, A. W. (2000). *In the eye of the beholder: The science of face perception*. Oxford, UK: Oxford University Press.

Calder, A.J., Young, A.W., Perrett, D.I., Etcoff, N.L., Rowland, D. (1996). Categorical Perception of Morphed Facial Expressions. *Visual Cognition, 3*(2): 81–118. doi:10.1080/713756735.

Campbell, R. (1996). Seeing Speech in Space and Time: Psychological and Neurological Findings. In *Spoken Language*, 3:1493–97. Philidelphia, United States: IEEE. doi:10.1109/ICSLP.1996.607899.

Darwin, C. (1872). *The expressions of emotion in man and animals.* London: John Murray.

de Gelder B., Vroomen, J. (2000). The Perception of Emotions by Ear and by Eye. *Cognition and Emotion, 14*(3): 289–311. doi:10.1080/026999300378824.

Ekman, P., Friesen, W.V. (1976). *Pictures of Facial Affect*. Palo Alto, CA: Consulting Psychological Press.

Ekman, P. (1992). An Argument for Basic Emotions. *Cognition and Emotion, 3*(4): 169–200. doi:10.1080/02699939208411068.

Ethofer, T., Pourtois, G., Wildgruber, D. (2006). Investigating audiovisual integration of emotional signals in the human brain. *Progress in Brain Research,* 156:345-361. PMID: 17015090

Fitch, W.T. (2000). The evolution of speech: a comparative review. *Trends Cognitive Sciences, 4*(7):258-267. PMID: 10859570

Gepner, B., Deruelle, C., Grynfeltt, S. (2001). Motion and emotion: a novel approach to the study of face processing by young autistic children. *J Autism Developmental Disorders 31*(1): 37–45. PMID: 11439752

Grandjean, D., Sander, D., Pourtois, G., Schwartz, S., Seghier, M.L., Scherer, K.R., Vuilleumier, P. (2005). The voices of wrath: brain responses to angry prosody in meaningless speech. *Nature Neuroscience, 8*(2):145-156. PMID: 15665880

Haxby, J.V., Hoffman, E.A., Gobbini, M.I. (2000). The distributed human neural system for face perception. *Trends Cognitive Science, 4*(6):223-233. PMID:10827445

Jiang, F., Blanz, V., O'Toole, A. J. (2009). Three-dimensional information in face representation revealed by identity aftereffects. *Psychological Science, 20*(3):318-325. PMID: 19207696

Kanwisher, N., McDermott, J., Chun, M. (1997). The fusiform face area: a module in human extrastriate cortex specialized for face perception. *J Neuroscience,* 17: 4302±4311. PMID: 9151747

Köchel, A., Plichta, M.M., Schäfer, A., Leutgeb, V., Scharmüller, W., Fallgatter, A.J., Schienle, A. (2011). Affective perception and imagery: A NIRS study. *Int J Psychophysiology, 80*(3):192-197. PMID: 21419180

Kreifelts, B., Ethofer, T., Shiozawa, T., Grodd, W., Wildgruber, D. (2009). Cerebral representation of non-verbal emotional perception: fMRI reveals audiovisual integration area between voice- and face-sensitive regions in the superior temporal sulcus. *Neuropsychologia, 47*(14):3059-3066. PMID: 19596021

Lander, K., Bruce, V. (2003). The role of motion in learning new faces. *Visual Cognition, 10*(8):897-912. DOI: https://doi.org/10.1080/13506280344000149

Massaro, D.W., Egan, P.B. (1996). Perceiving affect from the voice and the face. *Psychonomic Bulletin Review, 3*(2):215-21. doi: 10.3758/BF03212421. PMID: 24213870.

McGurk, H., MacDonald, J. (1976). Hearing lips and seeing voices. *Nature, 264*(5588):746-8. PMID: 1012311

Molholm, S., Ritter, W., Murray, M.M., Javitt, D.C., Schroeder, C.E., Foxe, J.J. (2002). Multisensory auditory-visual interactions during early sensory processing in humans: a high-density electrical mapping study. *Brain Res Cogn Brain Res*., *14*(1):115-28. PMID: 12063135

O'Toole, A. J., Roark, D., Abdi, H. (2002). Recognition of moving faces: a psychological and neural framework. *Trends in Cognitive Sciences, 6*(6):261-266. PMID: 12039608

Patel, S., Scherer, K.R., Björkner, Sundberg, J. (2011). Mapping emotions into acoustic space: The role of voice production. *Biological Psychology, 87*(1):93-98. PMID: 21354259

Roberson, D., Damjanovic, L., Pilling, M. (2007). Categorical perception of facial expressions: Evidence for a "category adjustment" model. *Memory & Cognition, 35*(7):1814-1829. PMID: 18062556

Scherer K.R., Johnstone T., Klasmeyer G. (2003). Vocal expression of emotion. In Davidson R.J., Scherer K.R., Goldsmith H.H. (Eds.), Handbook of affective sciences (pp. 433–456). New York: Oxford University Press.

Scherer, K.R., Kappas, A. (1988). Primate vocal expression of affective state. *Primate Vocal Communication,* 171-194. doi: 10.1007/978-3-642-73769-5_13

Schirmer, A., Kotz, S.A. (2006). Beyond the right hemisphere: brain mechanisms mediating vocal emotional processing. *Trends in Cognitive Sciences, 10*(1):24-30. PMID:16321562

Watson, R., Latinus, M., Noguchi, T., Garrod, O., Crabbe, F., Belin, P. (2014). Crossmodal Adaptation in Right Posterior Superior Temporal Sulcus during Face–Voice Emotional Integration. *J Neuroscience, 34*(20):6813-6821. PMID: 24828635

Wright, T.M., Pelphrey, K.A., Allison, T., McKeown, M.J., McCarthy, G., (2003). Polysensory interactions along lateral temporal regions evoked by audiovisual speech. *Cerebral Cortex,* 13: 1034–1043. PMID:12967920

Young, A. W., Rowland, D., Calder, A. J., Etcoff, N. L., Seth, A., Perrett, D. I. (1997). Facial expression megamix: Tests of dimensional and category accounts of emotion recognition. *Cognition*, 63:271-313. PMID: 9265872

CHAPTER 2 – THE ROLE OF SPATIAL ATTENTION IN BIMODAL AFFECT PERCEPTION

2.1 Introduction

2.1.1 Affective Faces and Voices. Facial expressions and vocalizations instantaneously convey information about the emotional state of another individual. In natural settings, these modalities are almost always experienced concurrently, but in lab settings, faces and voices provide sufficient information to effectively convey emotion independently (Ekman & Friesen, 1976; Schröder 2003; Belin, Fillion-Bilodeau, & Gosselin, 2008). Darwin (1872) was the first to identify the strong correspondence between an individual's facial movements and their internal emotional state. Ekman and Friesen (1976) further developed and refined this concept, identifying that affective states can be categorized into six basic emotions (anger, happiness, sadness, disgust, fear, and surprise), which are associated with the stereotyped and coordinated movement of specific groups of facial muscles (Bartlett, Viola, Sejnowski, Golomb, Larsen, Hager, & Ekman, 1996). Facial expressions appear to be highly salient, as these emotional states have been shown to be consistently identified and recognized across cultures (Darwin, 1872; Ekman, 1993; Ekman, Friesen, & Wallace, 1971; Ekman & Frisen, 1976). These findings indicate that facial expressions appear to be universally conserved, implying that facial expressions are inherent to and play an essential role in the basic foundation of human communication. However, emotion is multimodal, and faces are rarely experienced in silence but rather are typically paired with vocal information.

The vocal system transmits emotional information via changes in the articulatory gestures which alter the volume, stress, and intonation of a speaker's voice (Schröder, 2003; Grandjean, et. al, 2005). Vocal emotion, or emotional prosody, conveys emotion via the grouping of suprasegmental acoustic vocal features (amplitude, rhythm, and fundamental) to produce distinct,

unique, affective vocalizations (Belin, Fillion-Bilodeau, & Gosselin, 2008; Juslin & Laukka, 2003; Patel, Scherer, Björkner, & Sundberg, 2011). Linguistic cues appear to be processed independently from these acoustic vocal qualities as subjects can accurately identify and recognize a speaker's mood when semantically neutral sentences are read in different prosodies (Johnson, Emde, Scherer, & Klinnert, 1986) or spoken in a foreign language (Pell, Monetta, Paulmann, & Kotz, 2009; Scherer, Banse, & Wallbott, 2001; Thompson & Balkwill, 2006). Moreover, affective prosody has been considered the vocal analog of the six basic emotions originally identified by Ekman & Friesen (Ekman & Friesen, 1976; Schröder, 2003). These findings highlight the inherent correspondence between facial expressions and vocalizations, as changes in emotional prosody are produced through the coordinated action of vocal and facial muscles which result in distinctive facial expressions (Schröder, 2003; Belin, Fillion-Bilodeau, & Gosselin, 2008). This physical correspondence implies that vocalizations and facial expressions may be innately linked as visceral responses to external events, communicating complementary affective information to the eyes and ears of an observer.

2.1.2 Integration of Voices and Faces. The instantaneous and automatic integration of concurrently presented visual information and vocal information is best illustrated during speech communication, wherein auditory information from a speaker's voice is directly fused to the movements of a speaker's face to form one coherent multimodal percept (McGurk & MacDonald, 1976). One of the seminal experiments in aberrant audiovisual integration is evidenced by the illusory percept formed (hearing /da-da/) by the fusion of two mismatched auditory inputs (voiced /ba-ba/) and visual (spoken /ga-ga/), commonly known as the McGurk Effect (McGurk & MacDonald, 1976). This illusory percept has been replicated in experiments of bimodal affect perception, where the vocal and facial cues of a stimulus contain incongruent emotional cues

(Massaro & Egan, 1996; de Gelder & Vroomen, 2000). More recent studies have shown that while both facial expressions and affective vocalizations have the propensity to bias emotion perception (Massaro & Egan, 1996; de Gelder & Vroomen, 2000), each study reported that faces appear to have the greatest effect (Massaro & Egan, 1996; de Gelder & Vroomen, 2000; Abelin, 2007). This effect appears to be malleable, as the efficacy of each channel to bias perception appears to vary as a function of stimulus content, instructions, and response directions (Massaro & Egan, 1996; de Gelder & Vroomen, 2000; Abelin, 2007). Understanding how simultaneously presented conflicting visual and auditory input distorts perception may hold special significance when integrating nonverbal affective information.

Variations on the emotional McGurk experiment have provided critical insights into the integration of verbal and nonverbal affective vocal information with emotional faces. These studies typically utilize morphed continua created from two oppositely valenced, static end-point face images and a variation of semantically emotional sentences or affectively voiced prosodic stimuli (Massaro & Egan, 1996; de Gelder & Vroomen, 2000; Roberson, Damjanovic, & Pilling, 2007). Emotional facial expressions are perceived categorically (Ekman & Friesen, 1976; Calder, Young, Perrett, Etcoff, & Rowland, 1996; Young, et al., 1997; de Gelder & Vroomen, 2000; Fujimura, et al., 2012), which enables researchers to capture the perceptual changes that occur as stimuli incrementally change in equal physical amounts across a morphed continuum. Interestingly, people do not perceive linear morphs of physical stimuli as a continuum. Rather, morphed stimuli are perceived as belonging to one of two discrete categories, meaning that their responses exhibit what is known as categorical perception (Harnad, 1987). This phenomenon is pertinent to studies of audiovisual integration, where the perceptual boundary between two emotions can be quantified by a subject's identification responses, (Fujimura, et al., 2012; Calder, Young, Perrett, Etcoff, &

Rowland, 1996) with faces nearest to the center of the morph continuum being the most ambiguous and hardest to identify (Calder et al., 1996).

To characterize the perceptual boundary between two emotional categories, this study assessed two psychophysical measures, the point of subjective equality (PSE), associated with category identification and the just noticeable difference (JND), related to category discrimination. This study defined the PSE as the point at which a stimulus is equally likely to be judged as happy or not happy. The JND was measured as the percentage value of the amount of physical change needed to discriminate between two stimuli 50% of the time. The magnitude of the JND serves as an indication of the variance in subject responses, which can be interpreted as the participants' level of confusion in each condition.

These measures were used to assess the cross-modal effects of simultaneously presented affective vocal and facial expressions in emotion perception, with the intent of expanding upon a literature of bimodal emotion perception studies using nonverbal stimuli. Several studies have suggested that emotional prosody interferes with face perception, as subjects' identification of facial expressions becomes biased towards the emotion expressed in the vocal utterance (de Gelder & Vroomen, 2000; Massaro & Egan, 1996; Pourtois, de Gelder, Vroomen, Rossion, & Crommelinck, 2000; Campbell, 1996) and this effect persists even when instructed to ignore the auditory stimuli (de Gelder & Vroomen, 2000). Further, verbal interference appears to degrade the categorical perception of faces more than interference with incongruent faces during a vocal categorical perception task (Roberson & Davidoff, 2000). Findings from de Gelder & Vroomen (2000) indicated that the perception of affective faces is biased in the direction of a simultaneously presented prosodic voice, and that the impact of the voice increases as the emotions of the facial expressions become more ambiguous (Vroomen et al., 2001). Molholm and colleagues (2002)

suggested that these data indicate that early processing of visual inputs is modified by auditory inputs. Massaro & Egan (1996) found that while both facial expressions and affective vocal cues are effective in biasing responses from happy to angry, faces appear to exert a greater influence in bimodal integration emotion perception. Similarly, other findings have suggested that faces appear to play a greater role in biasing affect perception in bimodal conditions (Hess, Kappas, & Scherer, 1988), however this may vary by age (Bugenthal, Kaswan, Love, & Fox, 1970), emotion (Li, et al., 2013), directions (de Gelder & Vroomen, 2000), choice of stimuli, and subject characteristics (Massaro & Egan, 1996).

While the precise mechanism of this audiovisual perceptual bias is not clear, it seems that visual cues in the speaker's face may play a major role in influencing the prosodic bias. Faces are highly salient with individuals focusing visual attention on three core facial features: the eyes, nose, and mouth (Luria & Strauss, 1978; Stacey, Walker, & Underwood, 2005). Directing visual attention to these core regions may moderate the influence of prosody on bimodal emotion perception, as the perceiver may focus on both the visual and auditory channels associated with the vocal stimulus. Redirecting visual attention to fixate on moving mouths may thus increase the perceptual bias created by prosodic voices by increasing the focus on both the visual and auditory components of vocal auditory information processing.

2.1.3 The Current Study. This study investigated bimodal emotion perception using emotionally congruent and emotionally incongruent faces and voices paired together and preceded by fixation crosses placed at either the eyes or mouth. The authors elected to use short nonverbal affective bursts as vocal stimuli, as they are paralinguistic to avoid unintentionally engaging any additional cognitive processes (Schröder, 2003; Belin, Fillion-Bilodeau, & Gosselin, 2008). Additionally, these stimuli may be more ecologically valid as they were evoked by the actors so

that the actors' voices match their articulatory patterns and facial gestures (Schröder, 2003; Belin, Fillion-Bilodeau, & Gosselin, 2008). This study utilized a two-alternative forced choice task where subjects were instructed to indicate if the overall emotion they perceived for each trial was "happy" or "not happy" with no reference to attend to the voice or face.

We predicted that reaction times will be slowest for all conditions when they are at the category boundary or most ambiguous portion of the continuum (Massaro & Etcoff, 1996; de Gelder & Vroomen, 2000). Further, we hypothesized that reaction times for each prosody condition would vary as a function of their congruency with the emotion of the simultaneously presented face, with reaction times being faster when the faces and voices expressed the same emotion and slower when they are mismatched (de Gelder & Vroomen, 2000). The authors predicted that the PSEs for each condition would not only be biased in the direction of the simultaneously presented prosody, but that PSE values would indicate a stronger bias in the direction of the voice when cued to look at the mouths of face stimuli. JND values were interpreted as the level of confusion in subjects' responses, which together with the reaction time data could be used as indicators of how well defined the perceptual boundaries were between the two emotion categories. Additionally, JND values would be largest when subjects were cued to look at the eyes of stimuli.

2.2 Methods

2.2.1 Participants. Seventy participants, approximately half female were recruited from using the online survey platform MTurks (MTurks, Amazon, Seattle, Washington, United States). Subject demographics are shown in table 2.1. Subjects were compensated with $10.00. The protocol was approved by the Colorado State University Institutional Review Board and all participants will be provided informed consent before taking part in the procedures.

Table 2.1 *Subject Demographics*

n	Age	Gender	
	M(*SD*)	M	F
70	36.21(8.82)	33	37

2.2.2 Power Analysis. Mean point of subjective equality (PSE) values and standard deviations from the face only (M = 4.2, SD = 0.6) and neutral face+voice (M = 4.7, SD = 1.0) conditions were taken from an identical psychophysical experiment (Becker & Rojas, unpublished) and entered into an a priori power analysis to compute the required sample size in G*Power 3.1 (r = .299; Faul, Erdfelder, Lang, & Buchner, 2007; Faul, Erdfelder, Buchner, & Lang, 2009). The results of this analysis indicated that a sample size of N = 55 will be sufficient to detect a large effect (Cohen's dz = 0.50, power of .95 and alpha of .05 (two-tailed)).

2.2.3 Stimuli. Videos of two nonprofessional actors saying the vowel sound /a:/ in an angry or happy tone of voice were used to create morphed continua ranging from 100% happy to 100% angry. Means and standard deviations for the valence and arousal ratings for each stimulus are shown in table 2.2, analysis details in appendix A. The table also shows that there are no significant differences in the arousal and valence ratings of each stimulus depending on whether the videos

Table 2.2 *Arousal and Valence Rating for Male and Female Dynamic Models*

Actor	Emotion	Valence		*p*-value	Arousal		*p*-value
		AV	Silent		AV	Silent	
Male	Happy	4.28(0.74)	4.39(0.68)	0.278	3.52(0.96)	3.52(0.94)	0.423
	Angry	1.78(0.73)	1.48(0.76)	0.388	3.72(1.09)	3.95(0.97)	0.056
Female	Happy	4.16(0.80)	4.19(0.79)	0.727	3.28(0.98)	3.39(1.05)	1.000
	Angry	1.56(0.79)	1.69(0.69)	0.359	3.09(1.00)	3.39(0.94)	0.092

Note: Means and standard deviations are shown in parentheses for each emotion video for both the male and female dynamic video models. Ratings for each video presented with voices are indicated by the audiovisual (AV) stimulus condition and silent video ratings are indicated by the 'Silent' column. *p*-values are the result of dependent samples t-test between the AV and Silent conditions, alpha = .05. Arousal was rated on a 5-point scale (1-5), with 1 being the least arousing. Valence was rated on a 5-point scale (1-5), with 1 being the most negative valence.

arepaired with a congruent emotional voice or shown alone. Videos were filmed with actors sitting behind a green screen to eliminate any hair or clothing that may have been visible. All videos were created and edited at Colorado State University by Katherine Becker. Each continuum consists of two end-point prototype videos (angry or happy), which were morphed together to create seven videos. The seven videos contained two endpoint prototype videos and 5 morphs, which were morphed by approximately 16.67% per step so that the mid-point video was a 50% combination of each prototype video (Figure 2.1).

To create each continuum, two videos (one angry and one happy video) were selected from each actor (1 male) and edited in Adobe Premiere Pro (Adobe Premiere Pro CC 2019 release, Adobe, San Jose, CA, United States). Videos were exported as 40 frames to Adobe Photoshop (Adobe Photoshop 2019 release, Adobe, San Jose, CA, United States), saved as bitmaps, and imported to Psychomorph (Tiddeman, Burt, & Perrett, 2001; Tiddeman & Perrett, 2002). Within Psychomorph, each frame was associated with a unique template map made up of approximately 190 hand placed points outlining the actor's face shape and other major facial features (eyes, nose, lips, teeth). There was a total of 80 frames, 40 from each video sequence, each with their own template. Templates were used to spatially align each angry and happy frame for subsequent morphing to create one seven-step continuum of static images, ranging from 100% happy to 100% angry. This process was repeated 40 times, once for each frame in the video sequence.

Fourteen emotional videos were generated, one for each continuum step for each actor, face videos were paired with an angry or happy voice or shown in silence. These stimuli were preceded by a written cue (mouth, eyes) to pay attention to the mouth or eyes of the stimulus to create six conditions. Each written cue was followed by a fixation cross placed at the location indicated by the written cue (mouth, eyes).

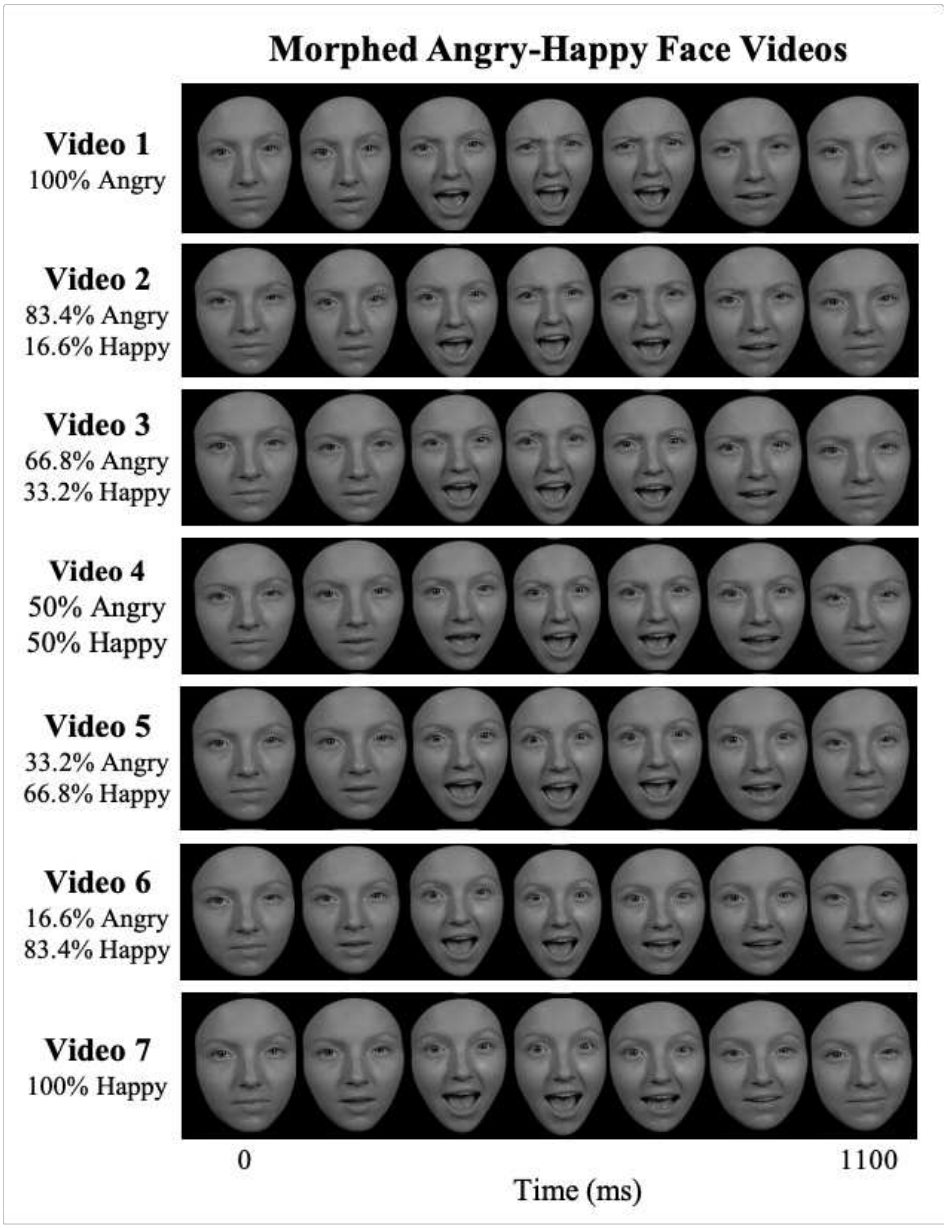

Figure 2.1: Exemplar timeseries created from seven frames taken from each morphed video from the angry-happy continua created from two end-point angry and happy videos for the female model. Time is shown on the x-axis. Videos becoming increasingly composed of happy physical features when moving from video 1 (top) to video 7 (bottom) on the continuum.

2.2.4 Experiment. Auditory stimuli were presented through computer speakers or audio headphones. Visual stimuli were presented on a computer or laptop monitor located in front of the subject. Morphed face stimuli were either shown in silence or simultaneously presented with an emotional voice using a custom experimental program created using JavaScript, CSS, and API. A password protected link to the experiment was published on the MTurks survey database

(MTurks, Amazon, Seattle, Washington, United States). Each trial began with a verbal cue (mouth, eyes) presented for 300 ms, which directed subjects to pay attention to either the eyes or mouth of the stimulus. This slide was followed by a white fixation cross on a black background which lasted 200 ms. The location of the fixation cross corresponded to the area of the face indicated by the verbal cue after which an audiovisual video clip of a morphed face video was presented for 1100 ms.

A black screen appeared for 750 ms after the stimulus ended, creating trials which totaled 2350 ms in duration (Figure 2.2a). All blocks contained 10 trials. Each block condition was indicated by the trial type that is in the majority. Seven of the trials were the same as the block emotion-fixation cue condition, and the remaining three trials were divided equally between the three-remaining emotion conditions preceded by the opposite cue. Each condition was shown in 12 blocks. The hybrid block design experiment contained a total of 720 trials (10 trials x 6 conditions x 12 blocks). Trials and blocks were presented in a pseudo-randomized order, to prevent subjects from easily predicting the condition within the blocks (Figure 2.2b). Each block was 23.5 seconds in duration with one 30 second break located halfway through the experiment. The total duration of the experiment was 28.5 minutes. Subjects were instructed to identify if the emotion expressed by the actor was “happy” or “not happy” for every trial in a 2-alternative forced choice procedure using keys 1 to indicate “happy” and 2 to indicate “not happy” on a keyboard with no specific reference to the face or voice. Subjects were asked to respond quickly, to ensure that their responses occurred within the stimulus window.

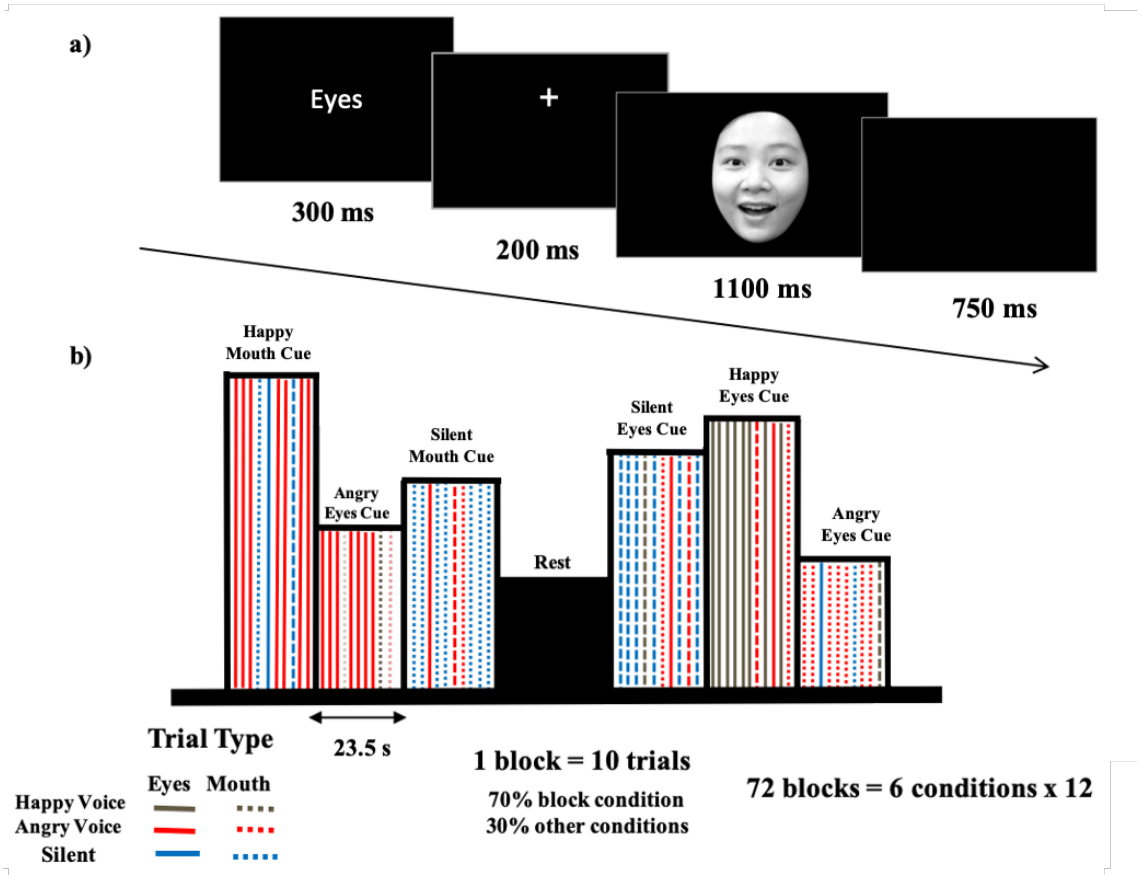

Figure 2.2: Experimental organization for the psychophysical experiment. a) Example of a single trial. Each trial begins with a word cue to either the Eyes or Mouth, followed by a fixation cue in the corresponding location, that was shown prior to viewing the morph stimulus. There was a 500 ms interstimulus interval. b) Diagram illustrating the pseudorandom trial and hybrid block organization for the six experimental conditions created from the Happy, Angry, and Silent voice conditions paired with either the Eyes or Mouth cue. One blank black rest block is situated in the middle of the blocks, at the mid-point of the experiment. Block height is arbitrary and is only meant to better differentiate between successive blocks.

2.3 Results

To analyze the hypothesized bias effects, data were fit using a logistic function to calculate point of subjective equality (PSE) and just noticeable difference (JND) values (calculations in appendix B), which were analyzed using two identical linear mixed effects models with fixation cue (mouth, eyes) and prosody (happy, angry, silence) entered as fixed factors and subjects entered as a random factor, see appendix C. Results for the first linear mixed model showed that mouth fixation cue (beta = 0.126, $t(68) = 2.21$, $p < .05$), happy prosody (beta = 0.338, $t(68) = .95$, $p <$

.000), and silent prosody (beta = 0.535, $t(68) = 9.28$, $p < .000$) were linearly related to PSE values. All voice-fixation cue conditions will be referred to by their prosody and their associated fixation cue location (i.e, Happy Eyes). Neither the Happy Mouth interaction (beta = -0.120, $t(68) = -1.50$, $p = .136$) nor the Silent Mouth interaction (beta = -0.117, $t(68) = -1.45$, $p = .148$) were linearly related to PSE values. Post hoc comparisons were performed using the Tukey HSD test and multiple comparisons were corrected

Table 2.3 *Multiple Comparison Tukey HSD PSE Contrast Results*

Contrast	Estimate	Std. Error	*z*-value	*p*-value
Angry M – Angry E	0.126	0.057	2.23	0.030
Happy E – Angry E	0.338	0.056	5.99	0.000
Happy M – Angry E	0.344	0.057	6.02	0.000
Silent E – Angry E	0.535	0.057	9.36	0.000
Silent M – Angry E	0.544	0.057	9.53	0.000
Happy E – Angry M	0.212	0.057	3.75	0.000
Happy M – Angry M	0.218	0.057	3.82	0.000
Silent E – Angry M	0.409	0.057	7.13	0.000
Silent M – Angry M	0.418	0.057	7.32	0.000
Happy M – Happy E	0.006	0.056	0.10	0.917
Silent E – Happy E	0.197	0.057	3.46	0.001
Silent M – Happy E	0..206	0.057	3.64	0.000
Silent E – Happy M	0.191	0.057	3.32	0.001
Silent M – Happy M	0.200	0.057	3.49	0.000
Silent M – Silent E	0.009	0.057	0.16	0.917

Note: Results of the post hoc pairwise comparisons for the PSE linear mixed model results. Fixation cue names have been abbreviated for each contrast to simplify the table and conserve space. Happy, Angry, and Silent indicate the voice condition. (E = “Eyes”, M = “Mouth”)

by FDR set at q = .05. PSE values for the Angry Eyes condition ($M = 3.51$, $SD = 0.59$) were significantly lower than the Angry Mouth condition ($M = 3.64$, $SD = 0.60$). There were no significant differences in PSE values between the Eyes and Mouth fixation cue conditions for either the Happy Eyes ($M = 3.82$, $SD = 0.50$) and Happy Mouth ($M = 3.85$, $SD = 0.58$) or Silent Eyes ($M = 4.02$, $SD = 0.52$) and Silent Mouth ($M = 4.05$, $SD = 0.57$) conditions were not

significantly different. However, both the Happy and Silent Eyes conditions exhibited significantly higher PSE values than the Angry Eyes condition, see table 2.3. This difference was also present for the Mouth condition, with the Happy and Silent conditions having higher PSE values than the Angry Mouth condition. When compared against one another, the Happy prosody condition exhibited significantly lower PSE values than the Silent prosody condition when paired with the Eye fixation cue, and this difference in PSE values was true for the Happy-Silent Mouth fixation cue comparison. Condition means and individual PSE scores are depicted as boxplots in Figure 2.3.

JND values were analyzed in a second identical linear mixed effects models with fixation cue (mouth, eyes) and prosody (happy, angry, silence) entered as fixed factors and subjects entered as a random factor. Results showed that Mouth fixation cue (beta = -0.713, $t(68) = -7.96$, $p < .000$), Happy prosody (beta = -0.537, $t(68) = -5.72$, $p < .000$), and Silent prosody (beta = -1.38, $t(68) = -14.67$, $p < .000$) conditions were linearly related to JND values. Both the Happy Mouth interaction (beta = 0.831, $t(68) = 6.52$, $p < .000$) and Silent Mouth (beta = 0.549, $t(68) = 4.33$, $p < .000$) interactions were linearly related to JND values. JND values for the Angry Eyes condition ($M = 3.65$, $SD = 0.74$) were significantly greater than the Angry Mouth condition ($M = 2.97$, $SD = 0.82$). The JND for the Happy Eyes ($M = 3.08$, $SD = 0.76$) condition was not significantly different than the Happy Mouth ($M = 3.23$, $SD = 0.65$). The difference between the Silent Eyes ($M = 2.27$, $SD = 0.89$) and the Silent Mouth ($M = 2.13$, $SD = 0.85$) condition was trending, but did not reach significance. The JND for Happy Mouth condition was significantly larger than both the Angry Mouth and Silent Mouth conditions. The Angry Eyes condition exhibited a significantly larger mean JND compared to all other conditions ($p < .000$). Conversely, the Silent Mouth condition exhibited a significantly smaller mean JND than every condition ($p < .000$) except for the Silent

Eyes condition (p = .917). Condition means and individual JND scores are depicted as boxplots in figure 4. A complete listing of all post hoc test results is listed in Table 2.4.

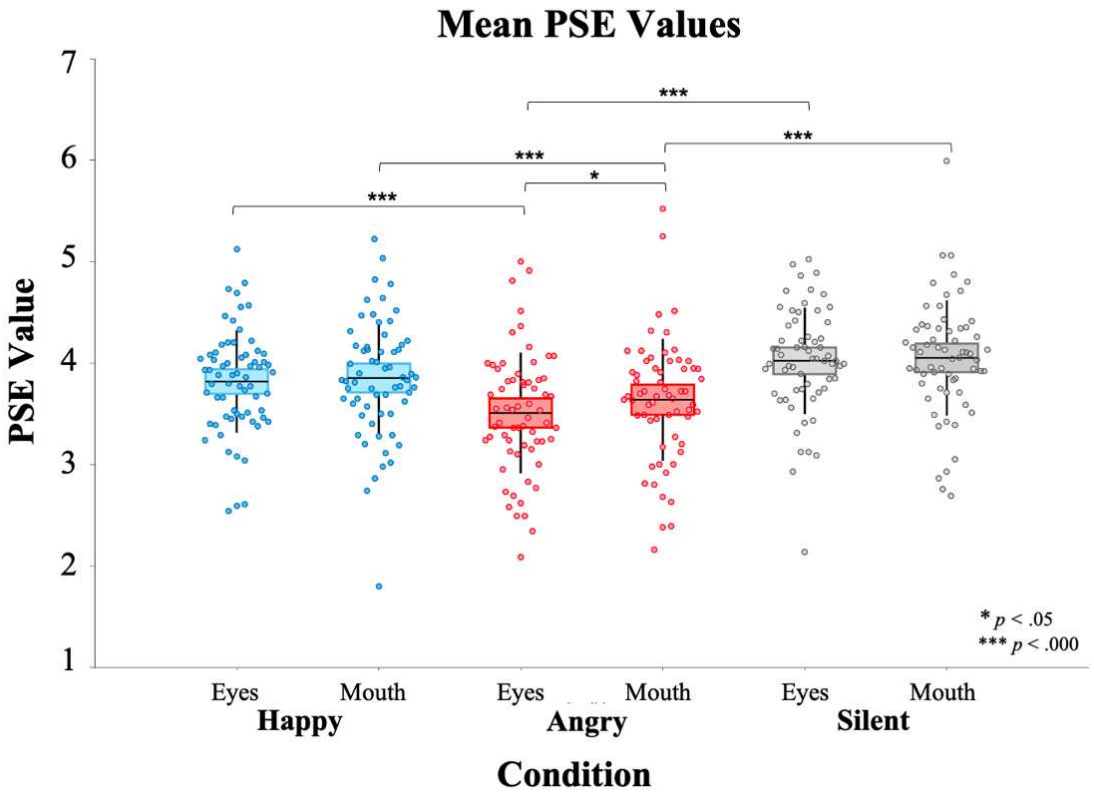

Figure 3.3: Group means and individual point of subjective equality (PSE) values for the Happy, Angry, and Silent voice conditions broken down by cue condition. Higher PSE values indicate that the stimuli were perceived to be happier than lower PSE values. Significance values indicated by p <.000 = ***, p < .05 = *.

A third linear mixed model was used to assess the effect of continuum step, voice prosody, and fixation cue on predicting reaction times, see appendix D. Results showed that Mouth fixation cue (beta = 18.47, t(68) = 2.03, p < .05), Step two (beta = 92.29, t(68) = 10.29, p < .000), Step three (beta = 46.95, t(68) = 5.23, p < .000), Step four (beta = 90.41, t(68) = 10.12, p < .000), and Step five (beta = 69.62, t(68) = 7.81, p < .000) were linearly related to JND values. Additionally, the interactions: Happy Mouth (beta = -25.52, t(68) = -2.02, p < .05), Step two Mouth (beta = -38.76, t(68) = -3.06, p < .01),

Table 2.4 *Multiple Comparison Tukey HSD JND Contrast Results*

Contrast	Estimate	Std. Error	*z*-value	*p*-value
Angry M – Angry E	-0.694	0.088	-7.89	0.00
Happy E – Angry E	-0.563	0.090	-6.24	0.000
Happy M – Angry E	-0.422	0.091	-4.64	0.000
Silent E – Angry E	-1.371	0.091	-15.14	0.000
Silent M – Angry E	-1.537	0.091	-16.93	0.000
Happy E – Angry M	0.131	0.089	1.46	0.144
Happy M – Angry M	0.272	0.91	3.00	0.003
Silent E – Angry M	-0.677	0.090	-7.52	0.000
Silent M – Angry M	-0.844	0.090	-9.34	0.000
Happy M – Happy E	0.141	0.089	1.59	0.120
Silent E – Happy E	-0.808	0.090	-8.95	0.000
Silent M – Happy E	-0.974	0.091	-10.76	0.000
Silent E – Happy M	-0.949	0.091	-10.43	0.000
Silent M – Happy M	-1.115	0.091	-12.22	0.000
Silent M – Silent E	-0.166	0.089	-1.87	0.071

Note: Results of the post hoc pairwise comparisons for the PSE linear mixed model results. Fixation cue names have been abbreviated for each contrast to simplify the table and conserve space. Happy, Angry, and Silent indicate the voice condition. (E = "Eyes", M = "Mouth")

Happy Step two (beta = -27.00, $t(68) = -2.14$, $p < .05$), Silent Step two (beta = -31.94, $t(68) = -2.52$, $p < .05$), Happy Step three (beta = -96.02, $t(68) = -7.56$, $p < .000$), and the three-way interaction Happy Mouth Step three (beta = 66.57, $t(68) = 3.071$, $p < .001$) were significantly linearly related to JND values. Reaction times for each prosody condition across the seven-step continuum are presented in five box plot figures. The mean of each condition is shown as a line drawn through the middle of each box and the raw values are displayed as markers. The size of each box indicates the standard deviation and the whiskers represent the 95% confidence interval. Two of the figures depict the average reaction times for all three prosody conditions across the seven steps of the morph continuum, separated by fixation cue condition. Mouth cue reaction times are displayed in figure 2.5 and Eyes cue reaction times are shown in figure 2.6. Across the continuum, reaction times appeared to be significantly longer for the Angry condition compared

to either the Happy or Silent prosody conditions, with the Silent prosody condition exhibiting the fastest reaction times for the Mouth cue condition. Reaction times for the Happy prosody condition were significantly faster than the Angry prosody condition at steps one, two, three, five, six, and

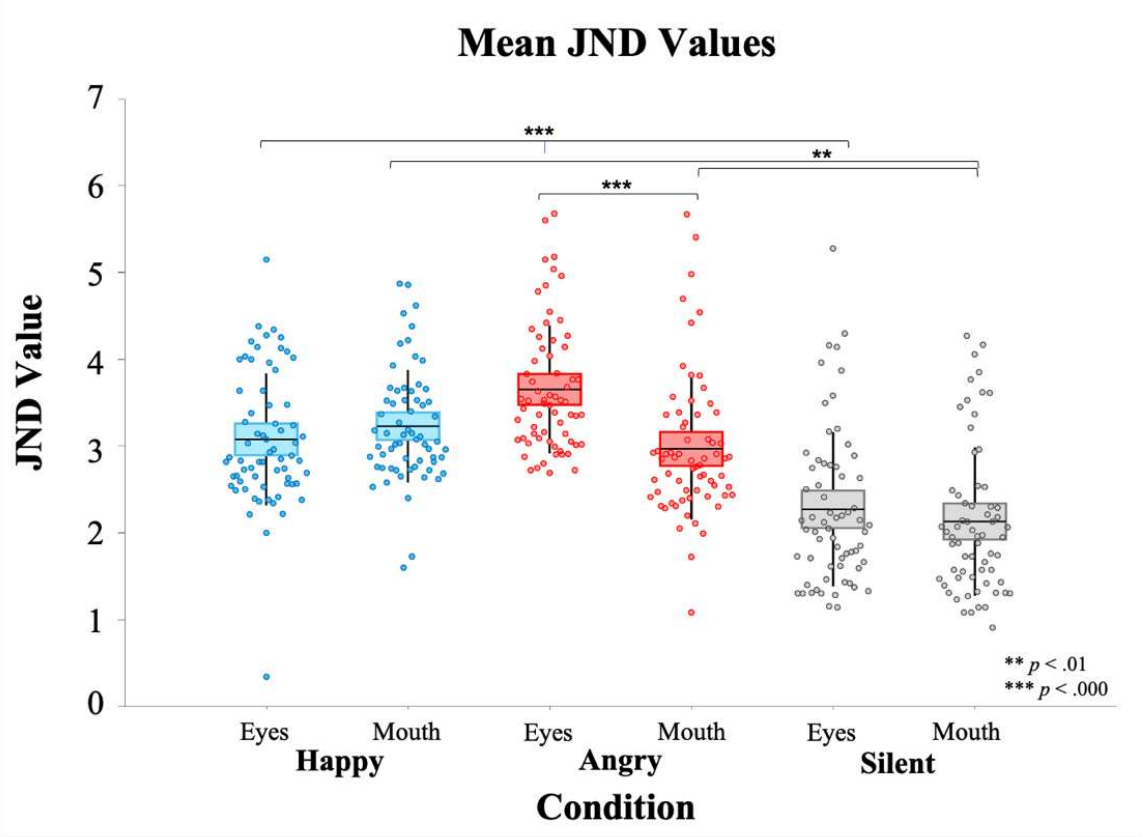

Figure 2.4: Group means and individual just noticeable difference (JND) values for the Happy, Angry, and Silent voice conditions separated by fixation cue. Higher JND values indicate greater variance in subjects' responses. Significance values indicated by p <.000 = ***, p < .01 = **.

seven, but were not significantly different at the midpoint of the continuum

Reaction time differences between the Angry and Happy prosody conditions were less consistent for the Eyes cue condition, with the Angry prosody condition exhibiting significantly longer reaction times than the Happy prosody condition at steps two and three, figure 2.6. Besides the first step of the continuum, both the Happy prosody and Angry prosody conditions were consistently significantly longer than the silent condition when the Eyes were cued. The one exception to this pattern was at step three where the average reaction time for the Happy prosody

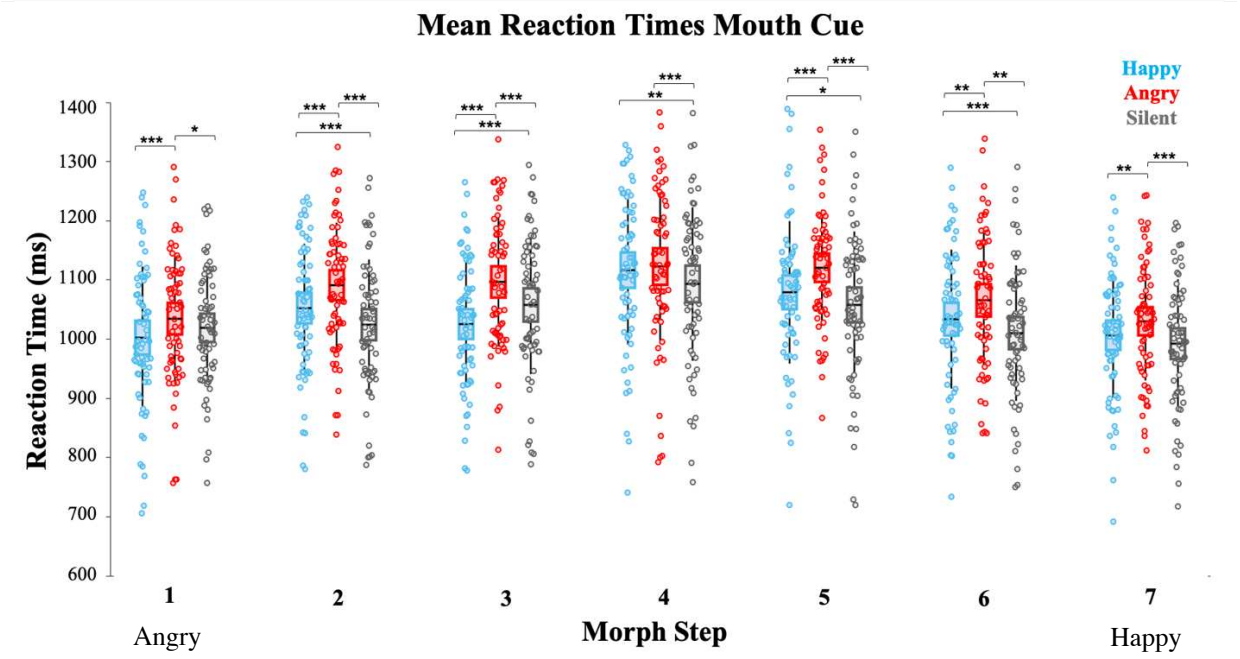

Figure 2.5: Mean reaction times for each prosody (Happy, Angry, Silent) condition across the morph continuum for the Mouth fixation cue. Means are plotted as horizontal bars, boxes indicate the size of the standard deviation, raw scores are plotted as circle markers, and confidence intervals are depicted by the whiskers above and below each box. Significance values indicated by p <.000 = ***, p < .01 = **, p < .05 = *.

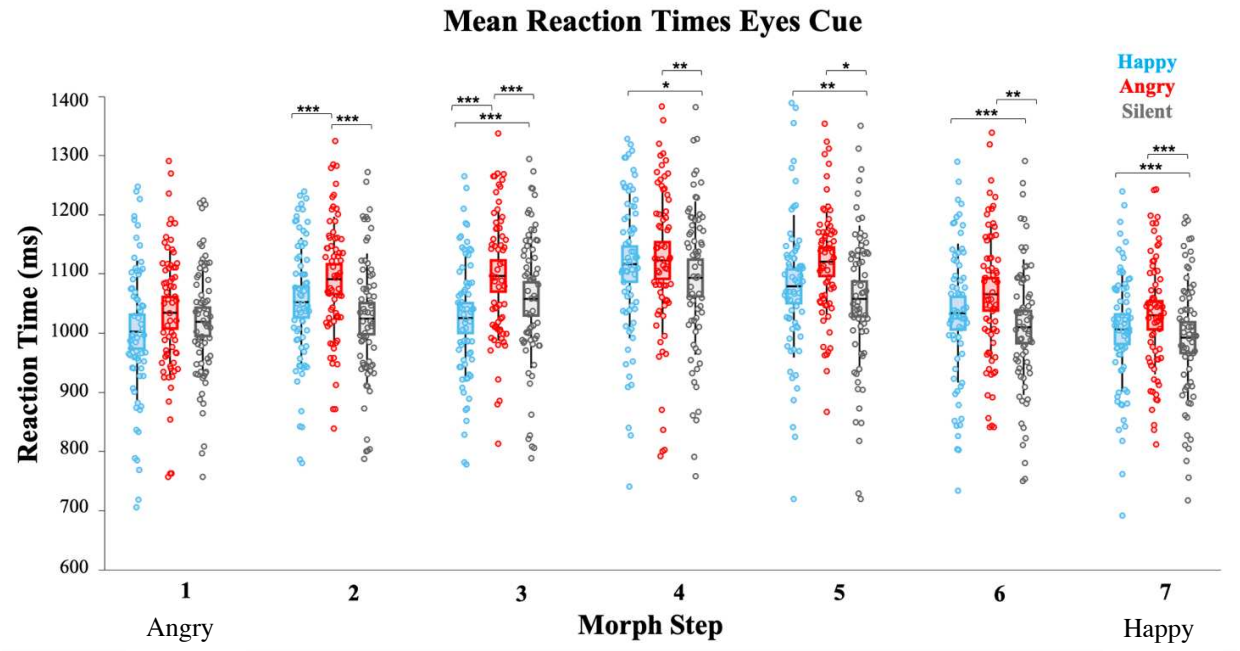

Figure 2.6: Mean reaction times for each prosody (Happy, Angry, Silent) condition across the morph continuum for the Eyes fixation cue. Means are plotted as horizontal bars, boxes indicate the size of the standard deviation, raw scores are plotted as circle markers, and confidence intervals are depicted by the whiskers above and below each box. Significance values indicated by p <.000 = ***, p < .01 = **, p < .05 = *.

condition was lower than the Silent prosody condition.

Individual graphs comparing the average reaction times for each fixation cue condition for each prosody are shown in figure 2.7. All three prosody conditions exhibited the longest reaction times at the midpoint of the continuum for both fixation cue conditions. The reaction times for the first and last steps of the continuum were significantly faster than the midpoint for all prosody and fixation cue conditions. The average reaction time for the Mouth fixation cue condition was significantly longer than the Eyes fixation cue condition for steps one, three, four, and five for the Angry prosody condition (Figure 2.7a). Reaction times for steps four and seven were also longer for the Angry Mouth fixation cue condition, but these differences did not reach significance. Reaction times for the Eyes fixation cue condition were only longer than the Mouth fixation cue for step two. Reaction times for the first and last step of the Angry prosody condition were not significantly different between fixation cue conditions. Reaction times significantly increased between steps one and four for both the Happy Eyes and Happy Mouth conditions and significantly decreased between steps four and seven (Figure 2.7b). Only two steps (two, three) of the Happy prosody condition exhibited significant differences between the Eyes and Mouth fixation cue conditions. The Silent prosody condition also exhibited an initial increase, peak, and then decrease in reaction times for both fixation cue conditions across the continuum (Figure 2.7c). Reaction times only differed at the second step of the continuum, where reaction times for the Eyes fixation cue were significantly slower than the Mouth fixation cue condition.

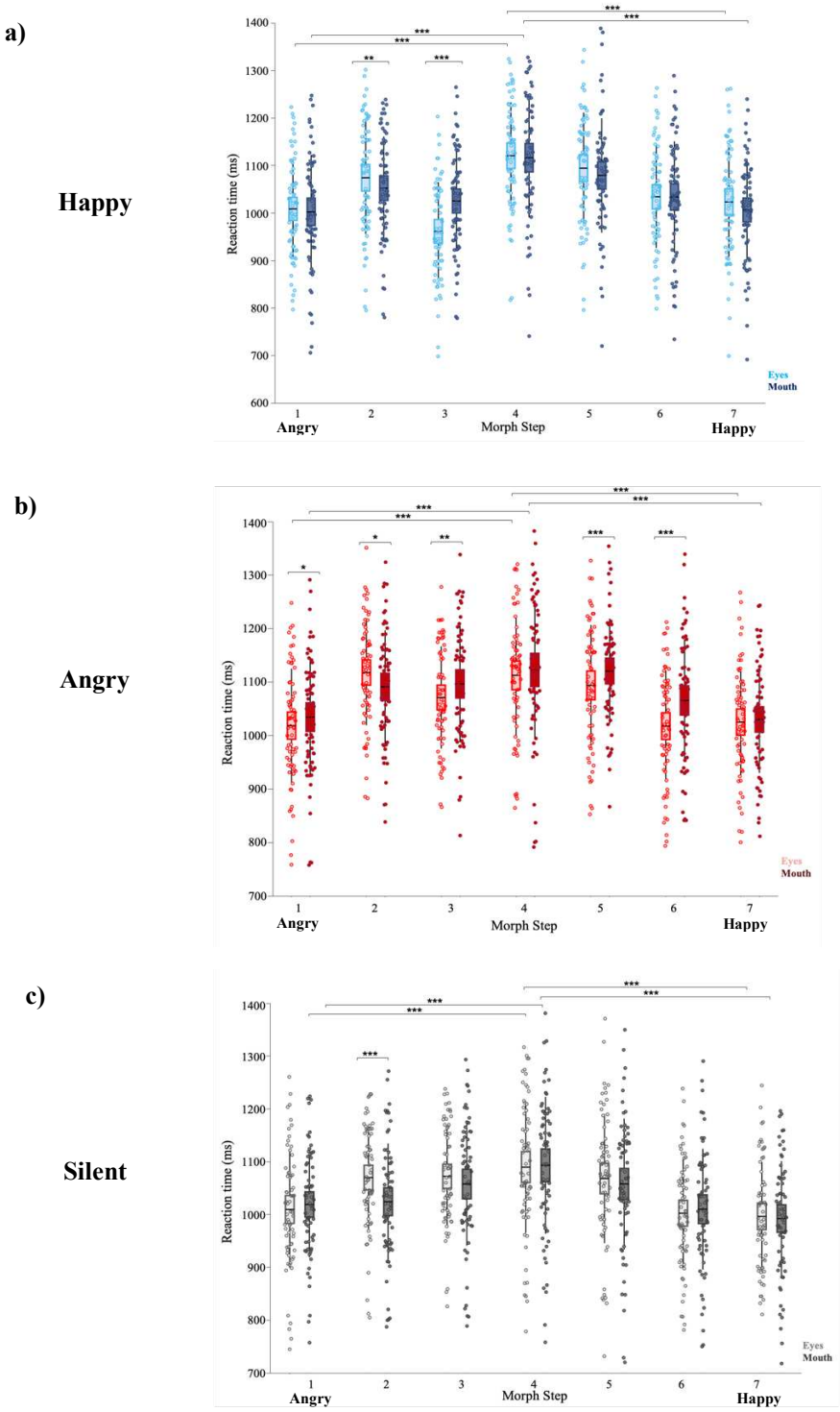

Figure 2.7: Mean reaction times for each fixation cue (Eyes, Mouth) for each prosody (Happy, Angry, Silent) condition across the morph continuum (100 % Angry to 100% Happy). Means are plotted as horizontal bars, boxes indicate the size of the standard deviation, raw scores are plotted as circle markers, and confidence intervals are depicted by the whiskers above and below each box. Significance values indicated by p <.000 = ***, p < .01 = **, p < .05 = *.

2.4 Discussion

The authors predicted that the PSEs for each condition would not only be biased in the direction of the simultaneously presented prosody, but that PSE values would indicate a stronger bias in the direction of the voice when cued to look at the mouths of face stimuli. Results showed that all three prosody conditions exhibited an increase in PSE values when cued to look at the mouth, with increased PSE values indicating a shift in the subjective judgments of affect perception to that morphed faces were perceived to be 'happier' than their physical condition. While these findings partially support the authors' hypothesis for the Happy condition, they were somewhat unexpected for the Angry prosody condition, as the authors had anticipated a decrease in PSE values between the Eyes and Mouth conditions as subjects were being presented with both the visual and auditory components of the vocalization (Figure 2.7b). Conversely, while both the Happy and Silent conditions exhibited an increase in PSE values, only the Angry prosody condition showed a significant increase between the Eyes and Mouth fixation cue conditions. These findings may reflect two a priori findings: 1) Visual information predominates perception (McDonald & McGurk, 1976) and 2) Mouths of happy faces are inherently more salient than other facial features across emotions (Calvo & Nummenmaa, 2008). These points indicate that happy faces may have given faces a greater advantage in biasing perception towards the happy end of the morph continuum, especially when subjects were cued to look at the mouths of stimuli. advantages which have been shown to have a detection advantage, as well as

This valence mediated perceptual bias may partially explain the decreased reaction times for both the Happy and Silent prosody conditions, which were perceived to be 'happier' based on significantly higher PSE values than the Angry prosody condition (Figure 3), with higher PSE values indicating a shift towards the happy end of the morphed angry-happy continuum so that

morphed faces appeared to be 'happier' than their physical composition. However, fixation cue location did not appear to effect PSE values for either the Happy or Silent prosody conditions (Figure 2.3). Surprisingly, the Silent voice condition exhibited significantly higher PSE values than the Happy and Angry prosody conditions for both fixation cues (Figure 2.3). This finding was somewhat surprising, as one would expect that faces paired with a Happy prosody would bias responses to have a higher mean PSE value than those presented in a silent condition. The Silent voice condition may have exhibited the highest PSE as it allowed subjects to view and evaluate the continuum based solely on its physical traits, which would have been equally biased by both the angry and happy physical features of the stimuli. This theory is supported by a comparison of the mean PSE values for the Silent Eyes ($M = 4.02$, $SD = 0.52$) and Silent Mouth ($M = 4.05$, $SD = 0.57$) conditions which occur nearly at the exact physical center of the morph continuum, where each video is equally composed of both happy and angry physical features.

While the authors did not take direct measures of the arousal and valence ratings of the actors' voices, a comparison of the arousal and valence ratings for the audiovisual and silent videos showed that these videos were not rated significantly different from one another for either prosody condition (Table 2.2). This may indicate that the prosody of the actor's voice did not determine the overall emotional percept conveyed by each video, but rather the video itself may have been driving the emotional percept as vision predominates bimodal perception (Hess, Kappas, & Scherer, 1988; McGurk & McDonald, 1976; Massaro & Egan, 1996; de Gelder & Vroomen, 2000; Abelin, 2007). Suggesting that while the Happy stimuli used in the experiment may have been equally as arousing and oppositely valenced as the angry stimuli, the Happy voices may not have been positively valenced enough to achieve a PSE that was "happier" than the Silent condition when presented without the Happy videos. However, one cannot definitively say that the happy

prosodic stimuli were completely ineffective as they did produce a PSE that was significantly higher than the angry prosody condition.

Perceptual confusion can be indexed by the just noticeable difference (JND). JND values were smallest for the Silent voice condition for both the Mouth and Eyes fixation cues, which may be related to decreased perceptual demands, as subjects are only presented with visual rather than mismatched audiovisual stimuli. This effect was somewhat surprising, as previous work has shown that morphed static faces presented in silence exhibited the largest JND values when compared to audiovisual face-voice stimuli (Becker & Rojas, submitted). The authors' interpretation had been that faces shown alone were perceived as being the most confusing because subjects only received one channel of affective information, producing the greatest variation in subjects' responses (Becker & Rojas, submitted). These conflicting results may be due to inherent differences in static versus dynamic faces, which differentially effect perceptual processing. Dynamic faces, for example, may provide more socially engaging salient features, which facilitate face recognition (Lander & Bruce, 2003). Some posit that facial movements are more effective in face recognition as they convey more information than static faces, which only provide a two-dimensional representation of an individual (Bassili, 1979). These findings necessitate further research using bimodal emotion perception paradigms, which employ static and dynamic faces to directly compare the perceptual advantages conveyed by using moving faces over static faces.

Similar to the current findings, Becker & Rojas (submitted) found that morphed static faces exhibited reaction times that were significantly faster than all of the bimodal face-voice conditions, lending further support to the idea that unimodal visual stimuli are processed more rapidly than audiovisual inputs. Collectively, these results indicate that while static and dynamic faces presented in isolation are rapidly processed, dynamic faces may have an inherent motion

advantage, which facilitates affect recognition, and this could be evidenced through faster reaction times and a lower JND score. While both the Angry and Happy prosody conditions exhibited greater JND values than the Silent condition for both the Eyes and Mouth fixation cues, the interaction between spatial cueing and emotional prosody in biasing response variability is not clear. The current results indicate that the size of the JND may be linked to both emotional valence and spatial cueing as the Angry prosody condition exhibited greater variability when cued to look at the Eyes but not the Mouth, and this pattern was reversed for the Happy prosody condition, but did not reach significance. These results may indicate that the most salient facial features used in affect recognition may differ by emotional valence. This notion is supported by eye-tracking studies, which have shown that individuals tend to spend more time fixating on the eyes of negatively valenced emotions and more time on the mouths of happy faces (Eisenbarth & Alpers, 2011; Bodenschatz, Kersting, & Suslow, 2019). Thus, differences in JND scores may indicate the existence of automatic emotion-specific detection mechanisms that are more sensitive to the distribution of key facial features.

Reaction time data results were in agreement with the author's hypotheses. The silent condition had significantly faster reaction times than both the Happy and Angry prosody conditions. Reaction times for all three voice conditions exhibited an inverted U shape, with the slowest reaction times occurring at the midpoint of the face continuum and the fastest reaction times appearing at the two end points. Specifically, reaction times at the two end points were significantly lower than the midpoint of the continuum but not significantly different from one another. Reaction times significantly increased and decreased as stimuli became more and less ambiguous from the beginning to the end of the continuum and this was true for all voice and fixation cue conditions (Figures 5, 6). This gradual increase in reaction times for all three voice

conditions may indicate greater confusion in responses as stimuli become more ambiguous. Additionally, audiovisual stimuli have been linked to longer reaction times as concurrently presented facial and vocal cues may require more processing time than faces presented alone (Massaro & Egan, 1996; Pell, 2005). This notion complements the current reaction time and JND findings, which showed that the Silent voice condition displayed significantly faster reaction times for both the Mouth and Eyes fixation conditions (Figures 5, 6) as well as significantly lower JND values compared to the Happy and Angry prosody conditions for both fixation cues (Figure 4). Indicating that subjects' responses to the Silent voice condition not only required less processing time but also exhibited less variance than subjects' responses to the Happy and Angry audiovisual conditions.

These findings coincide with those of an identical experiment which utilized static, rather than dynamic, faces (Becker & Rojas, submitted). Spatial cueing to the mouth appeared to prolong audiovisual processing of face-voice stimuli as faces paired with an Angry voice exhibited longer reaction times than both the Happy and Silent prosody conditions. Conversely, differences in reaction time for the Happy and Angry prosody conditions only appeared at steps two and three of the morph continuum for the Eyes fixation condition, whereas the Angry prosody condition displayed significantly longer reaction times than the Silent voice condition at steps two, three, four, five, six, and seven. These findings indicate that spatial cues to the mouth may enhance perceptual biases when processing emotional faces as they are visually salient and facilitate a detection advantage when differentiating between emotional faces (Calvo & Nummenmaa, 2008). This may be partially attributed to early attentional resources which direct subjects to fixate on the mouths of happy faces (Calvo & Nummenmaa, 2008). Additionally, some studies have suggested that happy faces may be inherently more discriminable than negative emotions because its

communicative intent is less ambiguous than the handful of emotions which fall under the umbrella of negatively valenced emotions (sad, disgust, fear, anger), which can often be confused with one another (Calvo & Nummenmaa, 2008; Becker, Anderson, Mortensen, Neufeld, & Neel, 2011). This is known as the happy superiority effect (Becker, Anderson, Mortensen, Neufeld, & Neel, 2011; Bortoloti, de Almeida, de Almeida, & de Rose, 2019) in which happy faces are categorized as happy faster than angry faces categorized as angry (Leppänen & Hietanen, 2003).

Given these findings, it is important to evaluate both the vocal and facial stimuli used in the current study, as it is imperative that both the angry and happy stimuli be equal in arousal and intensity, and oppositely valenced. This dynamic can be inherently difficult to achieve when using positively and negatively valenced stimuli (Tottenham, et al., 2009), especially under conditions where the emotional properties and overall intensity of each emotion ('hot anger' verses 'cool anger') are poorly defined or differentially produced (posed versus evoked), increasing variation in actors' portrayals (Gur, et al., 2002; Schröder, 2003). Thus, a limitation of the current study may have been that the emotions expressed by the actors were not as 'happy' as they needed to be, which may account for the differences in reaction times between the Angry and Happy prosody conditions, and the happy bias for the Silent voice condition. Moreover, video editing procedures may have prohibited the selection of videos with the most extreme intensity, arousal, and valence ratings, as these videos often featured dramatic differences in the physical features (face shape or length, number of teeth displayed, wincing or blinking) of the two end-point videos, which made them difficult to edit and morph together. Implementing such restrictions may have affected the ability of each face and voice to effectively convey the target emotion (Belin, Fillion-Bilodeau, & Gosselin, 2008), as affect recognition rates vary as a function of emotion, duration, (Pell, 2005; Cornew, Carver, & Love, 2009), valence, intensity, and arousal (Tottenham, et al., 2009).

These potential limitations may be more related to the prosody of the speaker's voice as they did not appear to hinder the formation of categorical boundaries for the morphed face continua when the faces were presented in silence. This point is supported by the pattern of subjects' reaction times, which were significantly faster one step before and after the most ambiguous point of the continuum for nearly every prosody-fixation cue condition (the Angry Mouth condition was not significantly different after), indicating a perceptual turning point at the most ambiguous point of the morphed continuum that was consistent for nearly every condition. These results suggest that, regardless of prosody or fixation cue, the video stimuli were effective in providing a set of dynamic visual stimuli that could be perceived categorically. Thus, the absence of a stronger 'happy' bias for the Happy prosody condition over the Silent condition may be linked to both the salient visual features of happy faces and the low arousal or valence ratings of the current prosodic stimuli. To gain more definitive insight into these findings the authors must collect arousal and valence ratings for each prosodic stimulus to evaluate their efficacy in accurately conveying the target emotions.

Additionally, it should be emphasized that this experiment was presented to subjects using an online research platform, which prevented the authors from controlling interindividual differences in viewing (screen size, resolution, distance from screen) and listening (sound level, binaural or monaural presentation, environmental noise) conditions during stimulus presentation. Differences in listening volume or environmental noise between-subjects may have attenuated or distorted the emotion-specific acoustic signatures that differentiate emotional voices (Scherer, 1986, Scherer, 2003; Belin, Fillion-Bilodeau, & Gosselin, 2008). Distortions to the acoustic profile of a particular vocalization may have made voices more emotionally ambiguous (Scherer, 1986; Scherer, 2003), potentially limiting the ability of a vocal utterance to positively or negatively bias

an emotional percept. These factors may have further confounded the ability of the happy prosody condition to produce a perceptual bias that was greater than the silent condition. Similarly, an inability to control the viewing conditions (screen or window size, resolution, distance from screen) may have limited the efficacy of the fixation cue to bias subjects' visual attention to either the eyes or mouth. This situation is further complicated as the author was unable to monitor subjects' eye movements during the task to verify that they were gazing at the correct facial features cued by the fixation crosses. Future studies should employ eye tracking to capture subjects' eye fixation patterns.

Overall, the findings of this study fit within a broader literature of affect perception research (Massaro & Egan, 1996; Etcoff & McGee, 1996; de Gelder & Vroomen, 2000; Pourtois, et al., 2000; Molholm et al. 2002; Campbell, 1996) which has demonstrated that auditory inputs modify the processing of visual stimuli. These findings add to the current literature as they showed that these perceptual biases persist when morphed dynamic stimuli are used in place of static faces. Moreover, reaction times showed that cueing spatial attention to the eyes hastens reaction times for all prosody conditions and this effect was most apparent for angry prosody. Additionally, visual cues to the mouth appear to differentially convey a detection advantage for happy voices over the angry and silent conditions. Although the arousal and valence ratings of the prosodic stimuli used in the current study are unknown, results showed that the processing of bimodal stimuli can be biased in the direction of a simultaneously presented affective voice. Additionally, this study adds to the current literature in showing that while two emotions may be oppositely valenced, and exhibit similar arousal ratings, the full efficacy of these emotions and sensory channels may depend on the stimuli of the experiment (Massaro & Egan, 1996, de Gelder & Vroomen, 2000).

REFERENCES

Abelin, A. (2007). Emotional McGurk effect – an experiment. Proceedings of the Seventh International Convergence on Epigenetic Robotics: Modeling Cognitive Development in Robotic Systems. *Lund University Cognitive Studies, 135*

Bassili, J. N. (1979). Emotion recognition: the role of facial movement and the relative importance of upper and lower areas of the face. *J Personality and Social Psychology, 37*(11):2049-2058. PMID: 521902

Becker, D. V., Anderson, U. S., Mortensen, C. R., Neufeld, S. L., Neel, R. (2011). The face in the crowd effect unconfounded: happy faces, not angry faces, are more efficiently detected in single- and multiple- target visual search tasks. *J Experimental Psychology General, 140*(4):637-59. PMID: 21744984

Becker, K. M., Rojas, D. C. (Submitted). The role of prosody in influencing emotion perception: a near-infrared spectroscopy study.

Belin, P., Fillion-Bilodeau, S., Gosselin F. (2008). The Montreal Affective Voices: a validated set of nonverbal affect bursts for research on auditory affective processing. *Behavioral Research Methods, 40*(2):531-9. PMID: 18522064

Bodenschatz, C. M., Kersting, A., Suslow, T. (2019). Effects of briefly presented masked emotional facial expressions on gaze behavior: an eye-tracking study. *Psychological Reports, 122*(4):1432-1448. PMID: 30032717

Bortoloti, R., de Almeida, R. V., de Almeida, J. H., de Rose, J. C. (2019). Emotional faces in symbolic relations/l a happiness superiority effect involving the equivalence paradigm. *Frontiers in Psychology, 10*:954. PMID: 31114529

Calvo, M. G., Nummenmaa, L. (2008). Detection of emotional face: silent physical features guide effective visual search. *J Experimental Psychology General, 137*:471–494. PMID: 18729711

Campbell, R. (1996). Seeing Speech in Space and Time: Psychological and Neurological Findings. In *Spoken Language,* 3:1493–97. Philadelphia, United States: IEEE. doi:10.1109/ICSLP.1996.607899.

Cornew, L., Carver, L., Love, T. (2009). There's more to emotion than meets the eye: A processing bias for neutral content in the domain of emotional prosody. *Cognition and Emotion, 24*(7):1133-1152. PMID: 21552425.

Darwin, C. (1872). *The expressions of emotion in man and animals.* London: John Murray.

de Gelder, B., Vroomen, J. (2000). The Perception of Emotions by Ear and by Eye. *Cognition and Emotion, 14*(3): 289–311. doi:10.1080/026999300378824.

Eisenbarth, H., Alpers, G. W. (2011). Happy mouth and sad eyes: scanning emotional facial expressions. *Emotion, 11*(4):860-865. PMID: 21859204

Ekman, P., Friesen., Wallace, V. (1971). Constants across cultures in face and emotion. *Journal of Personality and Social Psychology 17*(2),124-129. PMID: 5542557

Ekman, P., Friesen, W.V. (1976). *Pictures of Facial Affect*. Palo Alto, CA: Consulting Psychological Press.

Ekman, P. (1993). Facial expression and emotion. *American Psychologist.* 48, 384-392.

Elfenbein, H. A., Ambady, N. (2003). When familiarity breeds accuracy: cultural exposure and facial emotion recognition. *J Personality Social Psychology, 85*:276–290. PMID: 12916570

Etcoff, N. L., Magee, J. (1992). Categorical perception of facial expressions. *Cognition,* 44**,** 227-240. PMID: 1424493

Grandjean, D., Sander, D., Pourtois, G., Schwartz, S., Seghier, M.L., Scherer, K.R., Vuilleumier, P. (2005). The voices of wrath: brain responses to angry prosody in meaningless speech. *Nature Neuroscience 8*(2):145-156. PMID: 15665880

Gur, R.C., Sara, R., Hagendoorn, M., Marom, O., Hughett, P., Macy, L., Turner, T., Bajcsy, R., Posner, A., Gur, R. E. (2002). A method for obtaining 3-dimensional facial expressions and its standardization for use in neurocognitive studies. *J Neuroscience Methods, 115*(2):137-43. PMID: 11992665.

Harnad, S. (Ed.). (1987). *Categorical perception: The groundwork of cognition.* Cambridge University Press.

Lander, K., Bruce, V. (2003). The role of motion in learning new faces. *Visual Cognition, 10*(8):897-912. DOI: https://doi.org/10.1080/13506280344000149

Leppänen J. M., Hietanen J. K. (2003). Positive facial expressions are recognized faster than negative facial expressions, but why? *Psychological Research, 69*:22–29. PMID: 14648224

Li, A., Fang, Q., Jia, Y., Duang, J. *Chinese Computational Linguistics and Natural Language Processing Based on Naturally Annotated Big Data*: *Emotional McGurk Effect? A Cross-Cultural Investigation on Emotion Expression under Vocal and Facial Conflict*., edited by M. Sun et al.: Springer-Verlag Berlin Heidelberg, 2013, pp. 214–226, DOI: 10.1007/978-3-642-41491-6_20.

Luria, S. M., Strauss, M. S. (1978). Comparison of eye movements over faces in photographic positives and negatives. *Perception, 7*(3):349-358. PMID: 693234

Massaro, D.W., Egan, P. B. (1996). Perceiving affect from the voice and the face. *Psychonomic Bulletin Review, 3*(2):215-21. doi: 10.3758/BF03212421. PMID: 24213870.

McGurk, H., MacDonald, J. (1976). Hearing lips and seeing voices. *Nature, 264*(5588):746-8. PMID: 1012311.

Molholm, S., Ritter, W., Murray, M.M., Javitt, D.C., Schroeder, C.E., Foxe, J.J. (2002). Multisensory auditory-visual interactions during early sensory processing in humans: a high-density electrical mapping study. *Brain Res Cogn Brain Res*, *14*(1):115-28. PMID: 12063135.

Pell, M.D. (2005). Nonverbal Emotion Priming: Evidence from the Facial Affect Decision Task. 29(1): 45–73. doi:10.1007/s10919-004-0889-8.

Pourtois, G., de Gelder, B., Vroomen, J., Rossion, B., Crommelinck, M. (2000). The time-course of intermodal binding between seeing and hearing affective information. *Neuroreport, 11*(6):1329-33. PMID: 10817616.

Scherer, K. R. (1989). Vocal correlates of emotion. In: Wagner, H., Manstead, A. (Eds.), Handbook of Psychophysiology: Emotion and Social Behavior. Wiley, London, pp. 165–197.

Scherer, K. R. (2003). Vocal communication of emotion: A review of research paradigms. *Speech Communication, 40*(1-2):227-256. DOI: https://doi.org/10.1016/S0167-6393(02)00084-5

Schröder, M. (2003). Experimental study of affect bursts. *Speech Communication,* 40:99-116. doi.org/10.1016/S0167-6393(02)00078-X

Silveira, M. V., Aggio, N. M., Cortez, M. D., Bortoloti, R., Rico, V. V., de Rose, J. C. C. (2016). Maintenance of equivalence classes and transfer of functions: the role of the nature of

stimuli. *The Psychology Record, 66*:65–74. DOI: https://doi.org/10.1007/s40732-015-0152-1

Stacey, P. C., Walker, S., Underwood, J. D. M. (2005). Face processing and familiarity: evidence from eye-movement data. *British Journal of Psychology, 96*(Pt 4):407-422. PMID: 16248933

Tottenham, N., Tanaka, J.W., Leon, A.C., McCarry, T., Nurse, M., Hare, T.A., Marcus, D.J., Westerlund, A., Casey, B.J., Nelson, C. (2009). The NimStim set of facial expressions: judgments from untrained research participants. *Psychiatry Research*, *168*(3):242-9. PMID: 19564050

CHAPTER 3 – DISENTANGLING THE INTEGRATION OF EMOTIONAL FACES AND VOICES IN MULTIMODAL EMOTION PERCEPTION: AN INDEPENDENT COMPONENT APPROACH TO ELECTROENCEPHALOGRAM (EEG) DATA ANALYSIS

3.1 Introduction

3.1.1 Affective Faces and Voices. Emotion is multimodal, communicated via the fusion of audiovisual cues arising from the coordinated action of multiple facial muscles and concurrently expressed vocalizations (Schirmer & Adolphs, 2017). This correspondence is underscored by the fact that both vocalizations and facial expressions have been categorized as belonging to one of six basic emotions (happiness, sadness, fear, anger, surprise, and disgust; Ekman & Friesen, 1976; Schröder, 2003; Belin et al., 2008). This indicates that an individual's emotional state may be expressed via separate complementary modalities, which can independently impart the same, or similar, holistic perceptual experience to the observer (Schirmer & Adolphs, 2017). This perceptual convergence suggests that multimodal emotional stimuli may engage a constellation of spatially segregated and functionally diverse areas associated with sensory, perceptual, and cognitive processes (Schirmer & Adolphs, 2017).

3.1.2 Electroencephalography and Emotion. The neural correlates of audio, visual, and tactile dimensions of emotion have been characterized by research using electroencephalography (EEG). Alternatively, the blood oxygenation level dependent (BOLD) response measured by functional magnetic resonance imaging (fMRI) (Ogawa, Lee, Nayak, & Glynn, 1990; Belliveau et al., 1991; Kwong et al., 1992) has been used to localize patterns of brain activity with excellent spatial resolution. However, the temporal resolution of fMRI is relatively poor compared to EEG due to the inherent delay in the hemodynamic response, which is offset by several seconds relative to the onset of neural activity (Logothetis et al., 2001; Lewin, 2003). Due to its superior temporal

resolution EEG has enabled researchers to study these features as temporally distinct event-related potentials (ERPs). These events are stimulus specific with a collection of ERPs being selectively evoked by faces (Roisson et al., 2003; Hajcak, Weinberg, MacNamara, & Foti, 2011; Eimer & Holmes, 2007), voices (Hajcak, Weinberg, MacNamara, & Foti, 2011), and emotional stimuli (Cacioppo et al., 1993; Foti & Hajcak, 2008; Bernat, Bunce, & Shevrin, 2001). These components are temporally coincident, occurring within one to two hundred milliseconds of one another and sometimes sharing similar spatial distributions (Pratt, 2011; Hajcak et al., 2011).

3.1.3 ERPs of Face Processing. Visual processing of affective faces is principally characterized by two ERP components occurring between 100-200 ms after stimulus presentation. The first component, P100, appears as a positive deflection over parieto-occipital electrodes, peaking between 100-130 ms post stimulus presentation (Hajcak et al., 2011). The P100 has been attributed to the early coarse analysis of low-level facial features (Rossion & Caharel, 2011; Regan, 1989; Lou et al., 2010). Higher order face processing has been linked to the N170 component, which occurs approximately 130-200 ms after stimulus onset over a network of parieto-temporal-occipital areas in the right hemisphere (Hajcak et al., 2011). The N170 has been associated with more fine-grained visual analysis the configural changes which characterize different emotions as the amplitude and latency of the N170 may be mediated by the emotionality of a facial expression (Batty & Taylor, 2003; Luo et al., 2010).

3.1.4 ERPs of Voice Processing. Vocalizations can enhance or alter the meaning of a facial expression (de Gelder & Vroomen, 2000) and are processed and represented via a series of discrete neural events (Pell et al., 2015; Jiang, 2017). Early acoustic analysis occurs approximately 100 ms after stimulus presentation appearing as a negative going deflection over fronto-central electrodes and has been associated with sensory-perceptual processing of vocal stimuli (Paulmann & Kotz,

2008). Acoustic attributes appear to be integrated shortly after initial perceptual processing as the amplitude of the fronto-central P200 response differs between vocal emotions (Paulmann, Seifert, & Kotz, 2010; Paulmann, Bleichner, & Kotz, 2013; Pell et al., 2015). Emotional evaluation of vocalizations has been linked to the N300, which peaks in frontocentral electrodes (Paulmann & Kotz, 2008). Later elaboration of emotional meaning been associated with the sustained activity of the late centro-positivity (LPC), which peaks approximately 500 ms after stimulus onset (Paulmann, Bleichner, & Kotz, 2013).

3.1.5 Multimodal ERPs. Several components appear to respond more generally to affective stimuli and may reflect attentional processes associated with the motivational significance of stimuli. The N2 appears 200-300 ms post stimulus onset over occipital sites and is associated with increased selective attention to emotional content (Hajcak et al., 2011). The P300 has been associated with processing the motivational significance of emotional stimuli, occurring 300-500 ms post stimulus onset over midline parietal electrodes (Hajcak et al., 2011). Emotional faces, words, and pictures elicit a late positive potential (LPP) that appears to migrate from parietal to midline electrodes, appearing 300 ms after stimulus presentation and persisting even after stimulus removal (Hajcak & Olvet, 2008; MacNamara & Hajcak, 2010). These ERPs represent the complex perceptual and cognitive processing that occurs after initial audiovisual analysis and categorization of affective stimuli.

3.1.6 Multimodal Perception. The complexities of this dynamic process are underscored by research on multimodal integration in emotion perception, wherein emotional voices are shown to bias the perception of simultaneously presented affective faces in the direction of the emotion presented in the speaker's voice (de Gelder & Vroomen, 2000). This perceptual bias was reversed when subjects were instructed to pay attention to the emotional faces, as voices were perceived to

be more similar to the emotion of the simultaneously presented facial expression (de Gelder & Vroomen, 2000). These findings illustrate that faces and voices are integrated in the brain in a bidirectional manner that appears to be mediated by attention. Indicating that unimodal influences can shape multimodal perception.

3.1.7 Neural Correlates of Emotion Perception. While the neural activity associated with the independent processing of these two channels is well defined (Hajcak et al., 2011), the when and where of the concomitant processing and integration of multimodal stimuli remains unclear. This question is further complicated by EEG's relatively poor spatial resolution as ERPs are a measure of the summed activity of field potentials (Zhukov, Weinstein, & Johnson, 2000; Pascual-Marqui, 2009). Findings from fMRI suggest that face-voice integration may occur in the posterior superior temporal sulcus (pSTS), which has been shown to be sensitive to unimodal and multimodal representations of emotion (Beauchamp, 2004; Campanella & Belin, 2007). These findings may reflect fMRI's superior spatial resolution as multiple temporally coincident ERPs appear in parietal-temporal-occipital areas surrounding the pSTS (Hajcak et al., 2011).

3.1.8 Independent Component Analysis. Independent component analysis has been used to resolve the subtle differences in evoked responses by differentiating the spatiotemporal patterns underlying several sensory and perceptual processes (Onton, Westerfield, Townsend, & Makeig, 2006; Vigario et al., 2000). However, it should be emphasized that EEG components do not represent isolated neural processes even when stimuli are unimodal. This issue is further complicated by the presentation of multimodal stimuli, which exacerbates the spatiotemporal overlap typically seen during the processing of unimodal stimulus. Source localization techniques have been used to further increase the spatial resolution of this activity and dissociate the neural responses associated with processing emotional images (Liu & Tian, 2007). The temporally

coincident, and sometimes spatially overlapping, functionally separable subprocesses underlying face and voice processing necessitates the use of advanced data reduction and source localization techniques to disentangle and further characterize the neural underpinnings of multimodal emotion perception.

3.1.9 The Current Study. The current study sought to identify the neural substrates underlying multimodal emotion integration using a two-step ICA-sLORETA analysis. To examine the unimodal and multimodal aspects of affect perception, subjects were presented with affective faces and voices, presented separately or simultaneously. Subjects' responses were used to quantify changes in emotion perception using two psychophysical metrics: the point of subjective equality (PSE) and just noticeable difference (JND). These metrics can be used to evaluate the magnitude of the perceptual biases elicited by each prosody condition and estimate the variance in subjects' responses. We hypothesized that the perception of emotionally ambiguous faces paired with prosodic voice would be biased in the direction of the emotional voice, with faces appearing 'happier' with happy voices and 'angrier' or 'less happy' than when presented with an angry or neutrally toned prosodic voice. Moreover, reaction times were expected to be fastest to the face only condition compared to the bimodal conditions and subjects would exhibit the lowest variance in responses for the bimodal conditions, as they convey more affective information than the face only condition. We hypothesized that ICA components would be lateralized to parietal-temporal-occipital areas in the right hemisphere surrounding the pSTS, as this region has been identified as a major locus of multimodal integration (Beauchamp, 2004; Campanella & Belin, 2007). Further, these component time-courses would be correlated with one or more stimulus modalities (face, voice, or face and voice) or emotional prosody conditions (happy, angry, neutral).

3.2 Methods

3.2.1 Participants. Thirty undergraduate students (15 female) from Colorado State University participated in this study. The mean age for participants was 21.03 (3.35) years. All participants were provided informed consent before taking part in the procedures. All participants filled out three brief questionnaires regarding general and mental health, as well as drug and alcohol use. The Duke health profile (DUKE) was used to gauge subjects' perceived level of physical, mental, social, and overall health (Parkerson, Broadhead, & Tse, 1990). One subject chose not to complete the DUKE general health questionnaire; this is indicated under the questionnaires completed column. Alcohol use was measured using the Alcohol Use Disorders Identification Test (AUDIT; Babor, de la Fuente, Saunders, & Grant, 1992), and drug use was assessed using the Drug Abuse Screening Test (DAST-10; Skinner, 1982). Questionnaire results and scoring cutoffs are shown in table 3.1. The protocol was approved by the Colorado State University Institutional Review Board and the experiment was conducted in accordance with all relevant guidelines and regulations. Exclusion criteria were based on self-report and included: past or current neurological or psychiatric diagnosis, history of developmental disability or traumatic brain injury, current tobacco use, visual acuity of worse than 20/20 without correction, and chronic or current substance abuse within three months of taking part in the experiment.

3.2.2 Face Stimuli. Face stimuli consisted of a set of nonprofessional actors with natural hair and makeup taken from the NimStim database (Tottenham et al., 2009). One happy and one angry closed-mouth image were selected from a subset of 20 actors (10 men) from the database. Images were transformed to grayscale and cropped so that only the actor's face was visible. Psychomorph software was used to generate two continua, one for each actor (Tiddeman, Burt, &

Table 3.1 *Mean Questionnaire Scores Concerning Drug and Alcohol Use, and General Physical and mental health*.

Scale	Variables		Age		Score	
			M	*SD*	*M*	*SD*
DUKE		*n* = 29(15)	21.10	3.38		
Health Measures						
	Physical health				83.45	13.17
	Mental health				82.50	15.78
	Social health				84.83	15.26
	General health				83.57	9.99
	Perceived health				83.93	23.78
	Self-esteem				87.50	11.10
Dysfunction Measures						
	Anxiety				20.69	14.88
	Depression				22.50	17.56
	Anxiety-depression				19.39	14.53
	Pain				17.24	24.19
	Disability				3.45	12.89
DAST-10		*n* = 30(15)	21.03	3.35		
	Drug abuse				1.74	1.44
AUDIT		*n* = 30(15)	21.03	3.35		
	Alcohol use				3.84	2.85

Note: Parentheses indicate number of female participants. Scores for the DUKE are raw scores from a scale of 0.0-100.0. High scores for health measures indicate good health, high scores for the dysfunction measures equates to poor health. DAST-10 contains 10 items with scores ranging from 0.0-10.0, lower scores (1-5) indicating lower to moderate drug use, and higher scores (6-10) suggesting substantial to severe drug use. Total AUDIT scores greater than 8 indicate dangerous and harmful alcohol consumption, with scores ranging from 0.0-40.0.

Perrett, 2001; Tiddeman & Perrett, 2002). continuum consisted of two end-point prototype images (angry or happy), Each which were morphed together in seven steps (two endpoints and 5 morphs, in 12.5% steps) so that the image at the mid-point step would be a 50% combination of each prototype image (Figure 3.1).

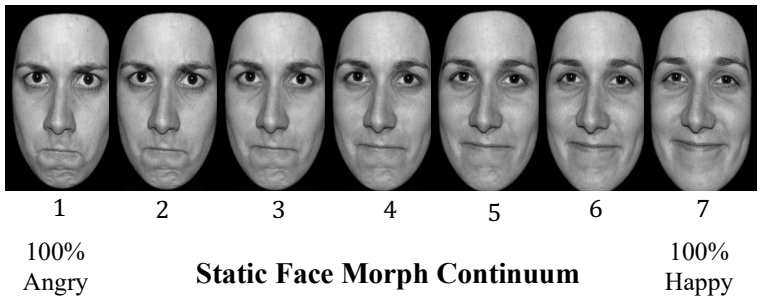

Figure 3.1: Example of one morphed continuum created from two static end-point angry and happy images, which are represented by two 100% Angry and Happy images. Individual images were taken from these continua and used as the visual face stimuli for the experiment and were either shown alone or presented with an Angry, Happy, or Neutral prosody. The image at the center of the continuum is a 50/50 composite image of the Angry and Happy face images.

Individual morphing templates were created from each end-point image using 182 manually placed control points. Closed mouth images were selected to facilitate morphing. Face stimuli were presented on an LED monitor with a 240 Hz refresh rate located 45 cm in front of the subject. Face stimuli subtended 7.62 degrees of visual angle vertically and 5.72 degrees horizontally.

3.2.3 Voice Stimuli. Auditory stimuli consisted of short, nonverbal affective interjections of the vowel /a:/ "ah" obtained from the Montreal Affective Voices database (Belin, Fillion-Bilodeau, & Gosselin, 2008). These vocalizations were produced by professional actors in spoken English. These stimuli were chosen because they effectively convey emotion, are created from authentic human voices, and are paralinguistic rather than linguistic. Three vocalizations expressed in an angry, happy, and neutral prosody were chosen for each actor (1 male and 1 female), resulting in six unique vocalizations. These stimuli have previously been matched and validated for valence (negative, positive), arousal and perceived intensity (Belin, Fillion-Bilodeau, & Gosselin, 2008). All vocal stimuli were cropped to be 993 ms in length (Audacity Team (2017), Audacity(R): Free Audio Editor and Recorder; 32-bit float, 44100 Hz, see table 2.2 for individual SPL values) and were attenuated individually in E-Prime 2 presentation software (Psychology Software Tools,

Pittsburgh, Pennsylvania, United States). Auditory stimuli were delivered binaurally (70 dB SPL) via EAR 3a foam insert earphones.

3.2.4 EEG Experiment. Participants were presented with three classes of stimuli, face only (FO), voice only (VO), and face+voice (F+V), to create seven conditions, one for each prosody (happy, angry, neutral) for the F+V and VO conditions with one condition for the FO stimuli (Figure 3). Morphed face stimuli were presented concurrently with auditory stimuli or were shown alone. Each trial began with a white fixation cross on a black background for 300 ms, followed by a 200 ms pause, after which a VO, FO, or F+V stimulus was presented for 993 ms, followed by a 500 ms inter-stimulus interval, which featured a blank black screen, for a total trial time of 1993 ms (Figure 3.2a). For each trial, subjects were instructed to indicate if the emotion expressed by the actor was "happy" or "not happy" using a X-box controller (Microsoft, Inc., Redmond, Washington, United States) without specific reference to the face or voice. Button press responses were analyzed for the proportion of happy responses and reaction times for each prosody condition and face. Reaction times were measured at the onset of each stimulus presentation. Reaction times were excluded if they were less than 200 ms or greater than 994 ms.

Table 3.2 *Sound Pressure Level (SPL) for Individual Vocal*

Emotion	Sex	SPL (dB)
Happy	Female	-23.33
Angry	Female	-13.44
Neutral	Female	-10.81
Happy	Male	-19.21
Angry	Male	-14.20
Neutral	Male	-14.62

Stimuli were presented in blocks of 14 trials defined by their condition (Happy F+V, Angry F+V, Neutral F+V, Happy VO, Angry VO, Neutral VO, FO) and stimulus type (FO, F+V, VO). Block condition was indicated by the trial type that was in the majority. For the three F+V conditions, and the VO conditions, 70% of the trials were the same as the block prosody condition,

with the remaining 30% being divided equally between the two remaining prosody conditions. Each condition was repeated in 10 blocks, for a total of 70 blocks (7 conditions x 10 blocks) (Figure 3.2b). Faces and voices were matched for gender for the F+V conditions. The total experiment therefore comprised 980 trials (20 actors x 7 conditions x 7 faces on a continuum), with VO, FO, and F+V condition blocks presented pseudo-randomly (14 trials per block x 70 blocks = 980 trials).

The total duration of the experiment was 32.5 minutes.*3.2.5 EEG Acquisition and Preprocessing.* Electrophysiological data were continuously acquired from 39 passive, sintered

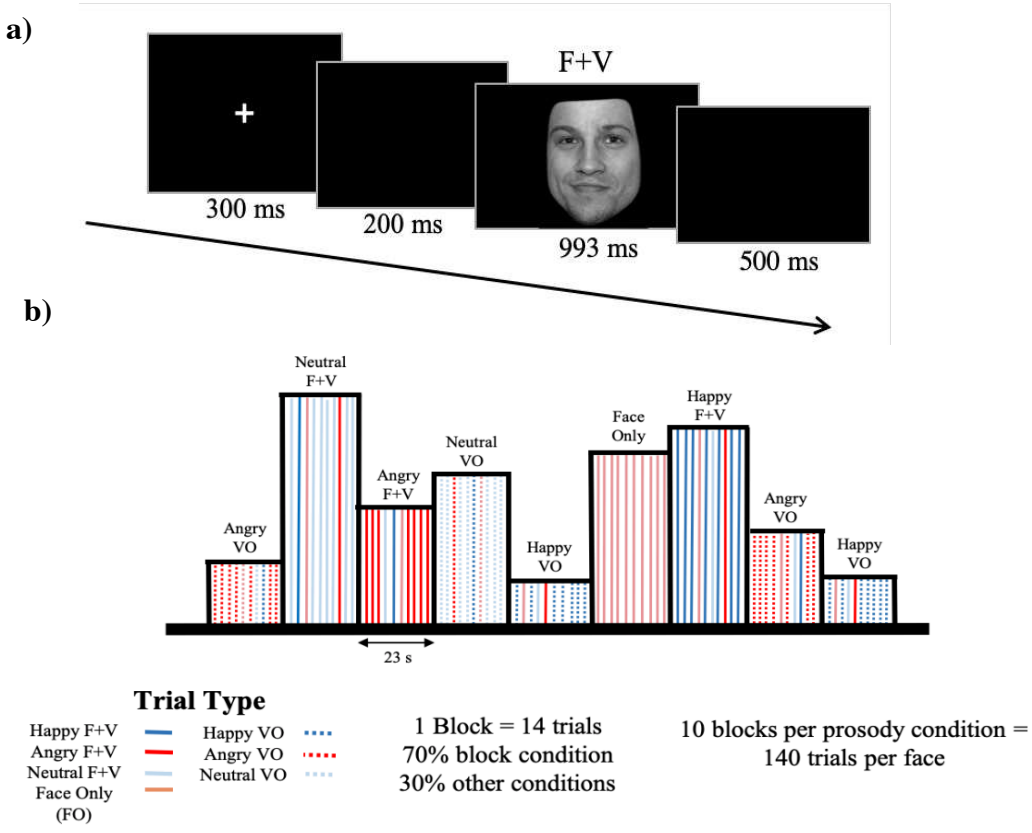

Figure 3.2: Experimental organization for the multimodal emotion perception EEG experiment. a) Example of a single trial showing the Face+Voice (F+V) condition. Each trial begins with a fixation cross, followed by a short blank black period, and then a stimulus (Voice only (VO), F+V, Face only (FO)), and then a 500 ms interstimulus interval. b) Diagram illustrating the pseudorandom trial and hybrid block organization for the seven experimental conditions. Block height is arbitrary and is only meant to better differentiate between successive blocks.

Ag/AgCl ring electrodes using a Neuroscan SynAmp 2 amplifier (Compumedics USA, El Paso, Texas, United States). Electrodes were arranged in the standard 10-10 system (Nuwer, Comi, Emerson, Fuglsang-Frederiksen, Guerit, et al., 1998). A conductive gel was injected into each electrode in order to minimize impedances, which were kept at 10 kΩ or less for the experiment. Data were sampled at 1000 Hz. The open source EEGLAB toolbox (eeglab13_6_5b, Delorme & Makeig, 2004) and custom Matlab code was used to analyze the data, see appendix E. Vertical and horizontal EOG electrodes were simultaneously recorded and used in eye artifact removal. The data were re-computed to an average reference, excluding EOG channels, and any remaining eye artifact remnants were removed using the independent component analysis (ICA) algorithm runica (Makeig, Jung, Ghahremani, Bell, & Sejnowski, 1997). EEG recordings were divided into 2000 ms epochs (-500 ms pre- to 1500 ms post-stimulus presentation) and baseline corrected for the entire 2000 ms time period and band-pass (0.1-35.0 Hz, linear finite impulse response (FIR)) and notch (60.0 Hz) filtered.

3.2.6 Behavioral Data Analysis. Reaction times were analyzed using a two-way, 3 (prosody) x 7 (face) repeated measures ANOVA with Greenhouse-Geisser correction for both the prosody and condition factors. Significant main effects and interactions were subsequently examined using Bonferroni adjusted Fisher LSD post-hoc tests at alpha = .05. Response choices to each face were analyzed in a classical psychophysical framework. A logistic function was applied to the percentage happy face classifications for the 7 faces to determine the point of subjective equality (PSE, or 50% angry/happy point) and just-noticeable difference (JND, or 25+75% points, divided by 2). PSE and JND were entered into two, separate one-way, repeated measures ANOVAs with a single factor of prosody to examine the potential bias of voice prosody on face perception in SPSS (IBM SPSS Statistics for Windows, Version 24.0. Armonk, NY).

3.2.7 Independent Component Analysis and Correlations. Individual preprocessed data files were merged into a common time series for group ICA using the Infomax ICA algorithm in EEGIFT (Eichele, Rachakonda, Brakedal, Elkeland, & Calhoun, 2011) implemented in Matlab (Matlab 2016b, The MathWorks, Inc., Natick, Massachusetts, United States). Components were then back reconstructed into the individual data. ICA decomposition resulted in 37 independent components. While the data were acquired using 39 passive recording electrodes, the top two eye components were removed from the dataset so only 37 components were specified in the ICA decomposition. Individual component time courses were correlated (Pearson's r) with each stimulus type (FO, VO, F+V) and emotion condition (Happy, Angry, Neutral), see appendix F. Multiple comparisons were corrected by FDR set at q = .05. Components were selected for further analysis based off of their significant correlation with either the emotion or stimulus condition and physiological plausibility as discussed by Delorme and colleagues (2012). Physiological plausibility was defined by the approximate number of dipoles that could be realistically fit to each component, as each individual component, in theory, should only have one singular source of activity generating each component (Delorme, Palmer, Onton, Oostenveld, & Makeig, 2012). Additionally, t-tests were used to eliminate components, which exhibited no significant changes from baseline between 100-600 ms post stimulus onset, see appendix G. This time period was selected based off of *a priori* literature, which has indicated that processes related to auditory, visual, multimodal integration, and emotion processing appear to occur between these two time points (Hajcak, Weinberg, MacNamara, & Foti, 2012; Rossion & Jacques, 2012).*3.2.8 Component Source Localization.* sLORETA analysis was performed using the scalp component topographies generated from EEGIFT. Component time courses were exported as text files to LORETA-KEY (Pascual-Marqui, Michel, & Lehmann, 1994; Pascual-Marqui, 1999) using the LORETA-KEY

plugin in EEGLAB. Electrode positions were based on a subset of channels from the spherical 10-10 BESA coordinate system (BESA Research, BESA GmBH, Gräfelfing, Germany; PO7, FC5, CPz, POz, P1, PO3, AFz, FT7, T3, AF7, C3, F3, CP5, TP7, FC1, T5, P5, P3, FC2, P2, FC6, PO4, FT8, AF8, T4, T6, C4, F4, CP8, TP8, PO8, P6, P4, AF4, O1, Fz, O2, AF3, Cz). A transformation matrix was calculated using the electrode coordinates, which were warped into Talairach space. The EEG electrode coordinates were warped into Talairach space using a transformation matrix created from the EEG electrode coordinates. Current source density values were calculated for each voxel in the reference brain, under the assumption that spatially adjacent voxels should show similar patterns of electrical activity. These values were then saved into a LORETA file which could be mapped onto the standardized brain.

3.3 Results

3.3.1 Behavioral Results. To analyze the hypothesized bias effects of prosodic voices on emotion perception, the data were fit using a logistic function (Fechner, 1966) to calculate the point of subjective equality (PSE) and just noticeable difference (JND) values, which were analyzed using two identical one-way repeated measures ANOVAs with condition (F+V prosody, face) as the within-subjects factor. Results showed that there was a significant difference in PSE values between conditions $F(3,115) = 8.48$, $p = .000$ with the Happy F+V condition exhibiting the lowest PSE, which was significantly different ($3.78 \pm .946$) than both the Angry (4.87 ± 1.14, $p = .000$) and Neutral ($4.70 \pm .966$, $p = .000$) F+V conditions. The PSE for the Face Only condition($4.15 \pm .628$) was also significantly different than the Neutral ($p = .028$) and Angry ($p = .003$) F+Vconditions, but it was not significantly different from the Happy F+V condition ($p = .132$), see figure 3.3.

The ANOVA for JND revealed a statistically significant difference in JND values between conditions $F(3,115) = 13.39$, $p = .000$. The Face Only condition exhibited a significantly larger JND (3.32 ± .939) than all F+V conditions (Happy, 1.77 ± .689, $p = .000$; Angry, 2.04 ± 1.20, $p =$

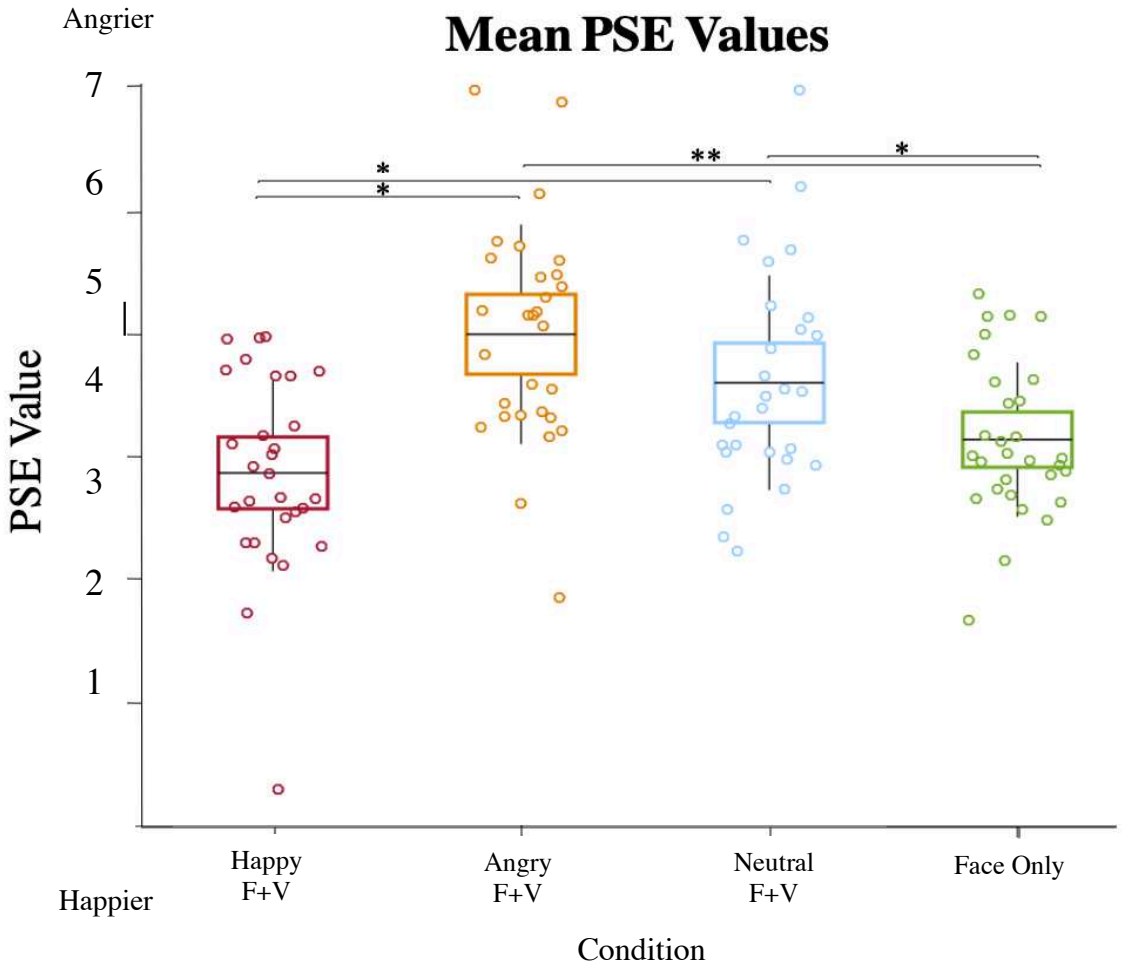

Figure 3.3: Group means and individual point of subjective equality (PSE) values for the Face Only, Happy, Angry, and Neutral Face+Voice (F+V) conditions. Lower PSE values indicate that the stimuli were perceived to be happier than higher PSE values. Horizontal lines indicate condition means, boxes illustrate the standard error of the mean, individual PSE values are shown as circles, and confidence intervals are shown as whiskers. Significance values indicated by p <.000 = ***, p < .005 =**, p < .05=*

.000; Neutral, 2.16 ± 1.20, $p = .0$ (3.32 ± .939). The JND for the Happy F+V condition was not significantly different from the Angry ($p = .313$) or Neutral ($p = .149$) F+V conditions, which also did not significantly differ from one another ($p = .656$), see figure 3.4.

Subject reaction times were analyzed using an ANOVA with the same within subjects factors and levels, which revealed a significant main effect for face step $F(6,162) = 2.89$, $p = .010$, $\eta_p^2 = .301$, condition $F(3,81) = 20.01$, $p = .000$, $\eta_p^2 = .426$, and a significant interaction between face step and condition $F(18,486) = 3.15$, $p = .000$, $\eta_p^2 = .105$.

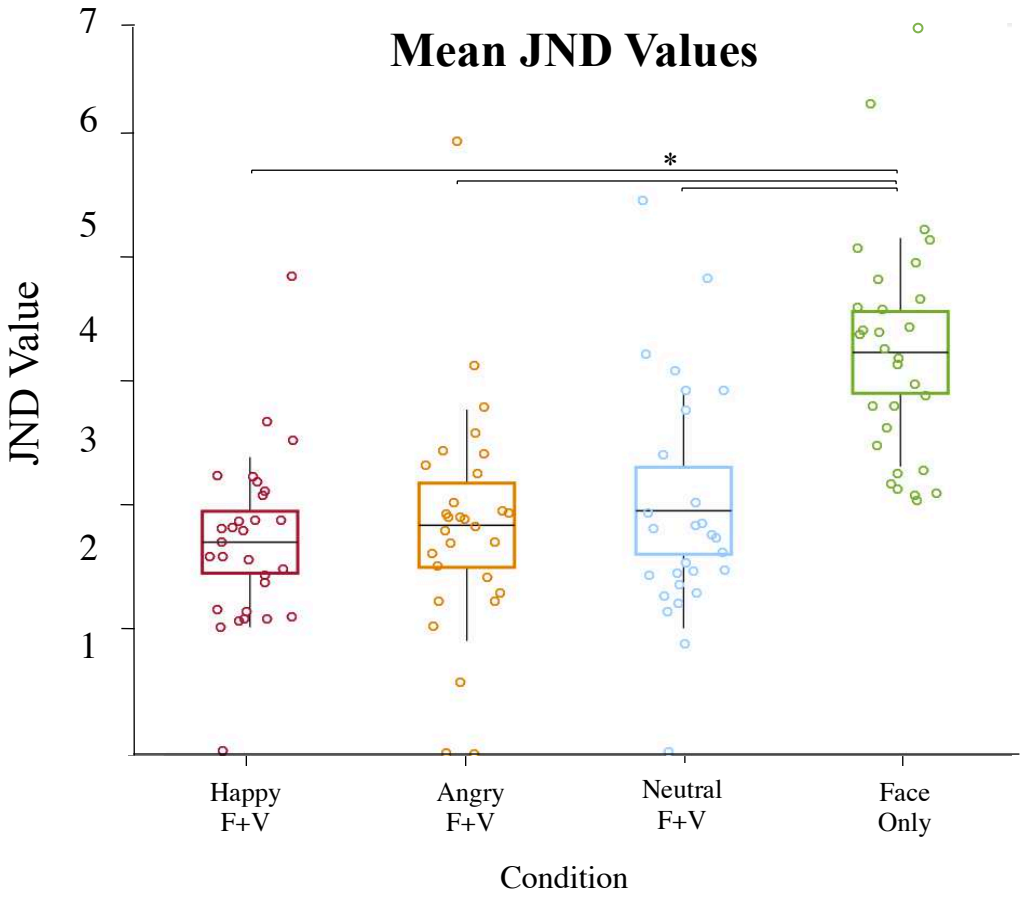

Figure 3.4: Group means and individual just noticeable difference (JND) values for the Face Only, Happy, Angry, and Neutral Face+Voice (F+V) conditions. Lower JND values indicate less variance in responses than higher JND values. Horizontal lines indicate condition means, boxes illustrate the standard error of the mean, individual PSE values are shown as circles, and confidence intervals are shown as whiskers. Significance values indicated by p <.000 = ***, p < .005 =**, p < .05=*

Pairwise comparisons revealed significantly faster reaction times for the Face Only condition when compared to all F+V conditions (Happy, 709.53 ± -51.08, $p = .000$; Angry, 709.53 ± -40.57,

p = .000; Neutral, 709.53 ± -44.20, p = .000). There were no significant differences between the F+V conditions.

While there were no significant differences in the average reaction times for each F+V condition, three one-way within subjects ANOVAs, one for each F+V condition, with face step as the within subjects factor were used in an exploratory analysis to see if gains in reaction time across the continuum varied as a function of the emotional congruency of the face and voice. Reaction times for the Happy F+V condition (F(6,199) = .774, p = .591) and the Neutral F+V condition (F(6,196) = 1.51, p = .177) were not significantly different across the face continuum (Figure 3.5). However, while the ANOVA for the Angry F+V condition did not reach significance (F(6,203) = 2.02, p = .064), post hoc comparisons revealed that reaction times for the first face

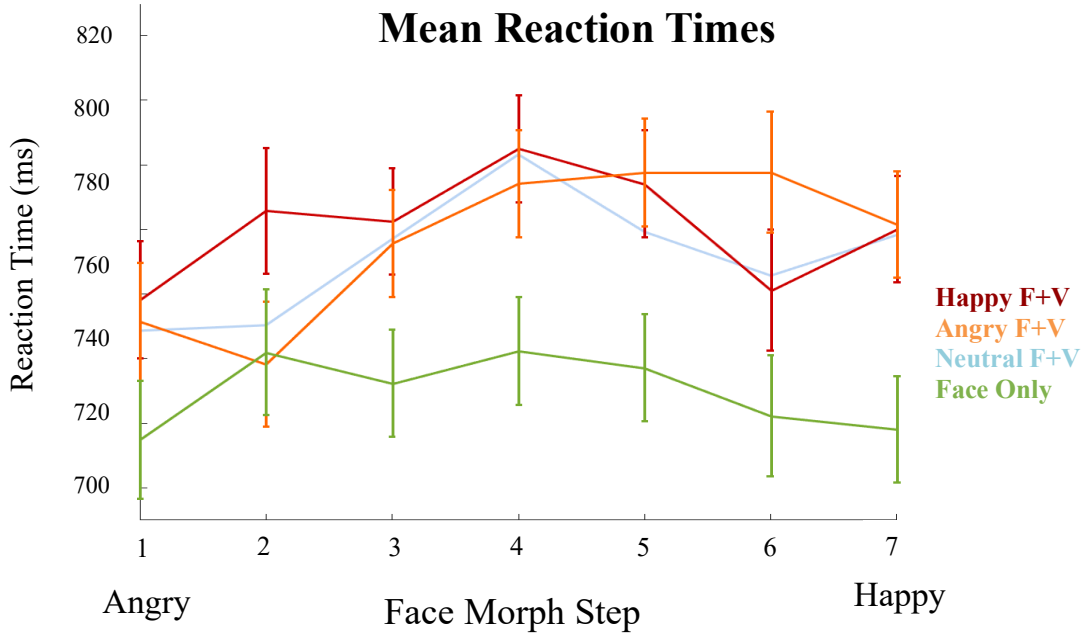

Figure 3.5: Mean reaction time (ms) values for each face step across the face morph continuum. Confidence intervals are plotted as vertical bars. Reaction times are shown for tconditions of the experiment containing face stimulus (Face Only, Happy, Angry, and Neutral F+V).

step were significantly faster than steps five (731.39 ± -46.25, p = .05) and six (731.39 ± -46.35,

= .05) and reaction times for the second step were significantly faster than steps four (718.28 ± -55.87, $p < .05$), five (718.28 ± -59.36, $p < .01$), and six (718.28 ± -59.46, $p < .01$).

3.3.2 ICA Component Results. While 39 passive electrodes were used to acquire the EEG data, only 37 components were used in the final analysis because the top two eye components were removed from each subjects' data after running the runICA algorithm to identify eye artifacts. All 37 components are shown in figure 3.7.

.

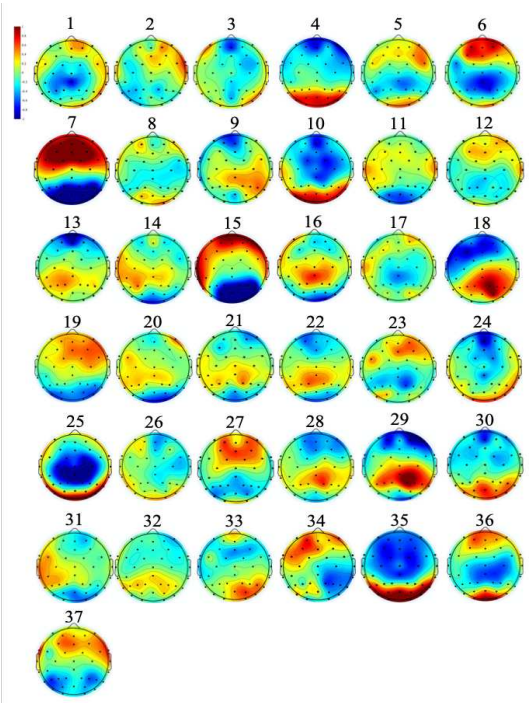

Figure 3.7: Results of the independent component analysis decomposition. Thiry-seven scalp topographies show the spatial distribution of increases (red) and decreases (blue) in activity collapsed across time. Component numbers are shown above each topoplot for organizational purposes. Component numbers are used only to numerically label each component.

3.3.3 Stimulus Type and Prosody Condition Correlation Results. Individual component time courses were correlated (Pearson's r) with each stimulus type (FO, VO, F+V) and emotion condition (Happy, Angry, Neutral). Multiple comparisons were corrected by FDR set at q = .05. Significant correlations and significant changes from baseline time periods are listed in tables 3.3 and 3.4.

Table 3.3 *Significant Correlation Time Periods Between Each Component Time-course and Condition.*

Component #	Condition	Significant Time Periods (ms)
1	Face Only	0-10; 330-363; 460-465; 895-911
5	Face Only	149-192; 252; 345-850; 868-930; 961-1010; 1037-1075; 1131-1157; 1219-1280; 1313-1333; 1220-1491
	Face+Voice	400-458; 497-514; 567-629; 685-712; 1138
7	Face Only	0-1500
	Face+Voice	0-36; 100-1500
	Voice Only	0-1500
	Angry	59-123; 197-234; 378-431; 498-518; 1232-1245; 1431
	Happy	79; 105-150; 300-106
	Neutral	40-405; 692-704; 1232-1245; 1432
8	Face Only	17-35; 67-71; 141-169; 208-415; 437-527; 556-579; 639-661; 684-711; 918-954; 1021-1030; 1149-1184; 1219-1238; 1292-1371; 1397-1481
	Face+Voice	133-155; 208-346; 366-386; 447-458
	Happy	257-271
9	Face+Voice	32-47; 152-177; 218-258; 310-375; 411-431; 662; 689-731; 847-899; 912-970; 983-1069; 1088-1149; 1213-1249; 1284-1348; 1365-1386; 1396-1473;1487-1500
12	Face Only	172-204
	Face+Voice	156-185; 263-495
15	Face Only	12-53; 325-690; 707-720; 1346
	Face+Voice	12-619
	Voice Only	260-290
	Angry	0-24; 79-146; 171-690; 711-736; 761-828; 847-875; 939-965; 1036-1059; 1318-1338
	Happy	421-687; 722; 767-779; 815-829; 855-971
	Neutral	90-127; 497-524; 641-651

Note: Each component is listed with the experimental element(s), which it was significantly $p < .05$ correlated with (Pearson's r), corrected for multiple comparisons using FDR, $q = .05$. Significant time periods for each correlation are listed on the right.

Table 3.4 *Significant Correlation Time Periods Between Each Component Time-course and Condition (Continued).*

Component #	Condition	Significant Time Periods (ms)
18	Face+Voice	163-189
21	Face Only	177-237; 256-316
	Angry	816
25	Face Only	44-96; 119; 121-163; 250; 467
	Face+Voice	0-68; 112-171; 183-218; 312-395; 439-481; 610-687; 737-760; 832; 854; 1020-1066; 1122-1136;1221; 1248-1261; 1313-1333
	Voice Only	75-104; 121-163; 655-690
	Angry	58-101
	Happy	54-82; 111-154; 314-342; 357-384; 452-537; 548-623; 653-745; 780-817; 834-901; 944-963; 974-989
28	Face+Voice	123-153; 167-174; 481-762; 767-804; 808-836; 856-893; 922-951; 968-1046;1073-1133; 1160-1178; 1234-1260; 1292-1299; 1323-1333; 1356-1379; 1439-1453
	Angry	37-46; 100-198; 580-636; 655-678; 711-747; 794-862; 886-837; 956; 1011-1040; 1054-1101; 1119-1196; 1209-1257; 1272-1300; 1321-1500
31	Face+Voice	57; 130-155; 185; 334-409; 447-491; 503-630; 651-666;
	Voice Only	48-62; 136-149; 178-190; 226; 268-422; 448-625; 637-713; 781-798; 853-864; 903; 963-980; 1045; 1109-1139; 1186-1211; 1224-1250; 1304-1321; 1344-1361; 1424
	Angry	121-153; 1041-1062; 1123-1146
35	Face Only	155-252
	Face+Voice	138-202; 275-307; 328; 1283-1299; 1364-1376
	Happy	130-159

Note: Each component is listed with the experimental element(s), which it was significantly $p < .05$ correlated with (Pearson's r), corrected for multiple comparisons using FDR, $q = .05$. Significant time periods for each correlation are listed on the right.

3.3.4 Component Baseline Comparison and Source Localization Results. Dependent t-tests comparing component time-course activity to baseline activity were performed on this final thirteen components, which had exhibited a significant correlation with one or more experimental elements (stimulus type or prosody condition). Results were corrected for multiple comparisons using a Bonferroni correction set at alpha = .01. Periods of significant change from baseline are highlighted in red on each component time-course as shown in the second column of figures 3.8 and 3.9. All components exhibited a significant increase or decrease from baseline activity prior to 300 ms as shown in figures 3.8 and 3.9.

These components were then source localized using the standardized low brain electromagnetic tomography (sLORETA; Pascual-Marqui, 2002) algorithm using LORETA-KEY (Pascual-Marqui, Michel, & Lehmann, 1994; Pascual-Marqui, 2002). Scalp topography, time-courses, and source localization results are shown in figures 3.8 and 3.9. Component activity was primarily lateralized to the right hemisphere, with some anterior frontal, occipital, and parietal activity appearing in components: 5, 8, 15, and 31. The majority of components exhibited activity in bilateral somatosensory or parietal areas: 1, 7, 12, 15, 18, 21, 25, 28, 31, 35. Only two components (5 and 12) exhibited activity in anterior temporal and inferior areas in the right hemisphere and these components were significantly correlated with both the face only and face and voice stimulus conditions. These components were significantly correlated with the face only condition during an overlapping time period (149-204 ms) that's strongly associated with face processing in the EEG literature (Hajcak, Weinberg, MacNamara, & Foti, 2012). Additionally, both components showed a brief significant decrease in activity between approximately 260-270 ms. Activity for components exhibiting significant activity post 300 ms (1, 7, 9, 15, 35) were primarily localized to somatosensory and parietal association areas

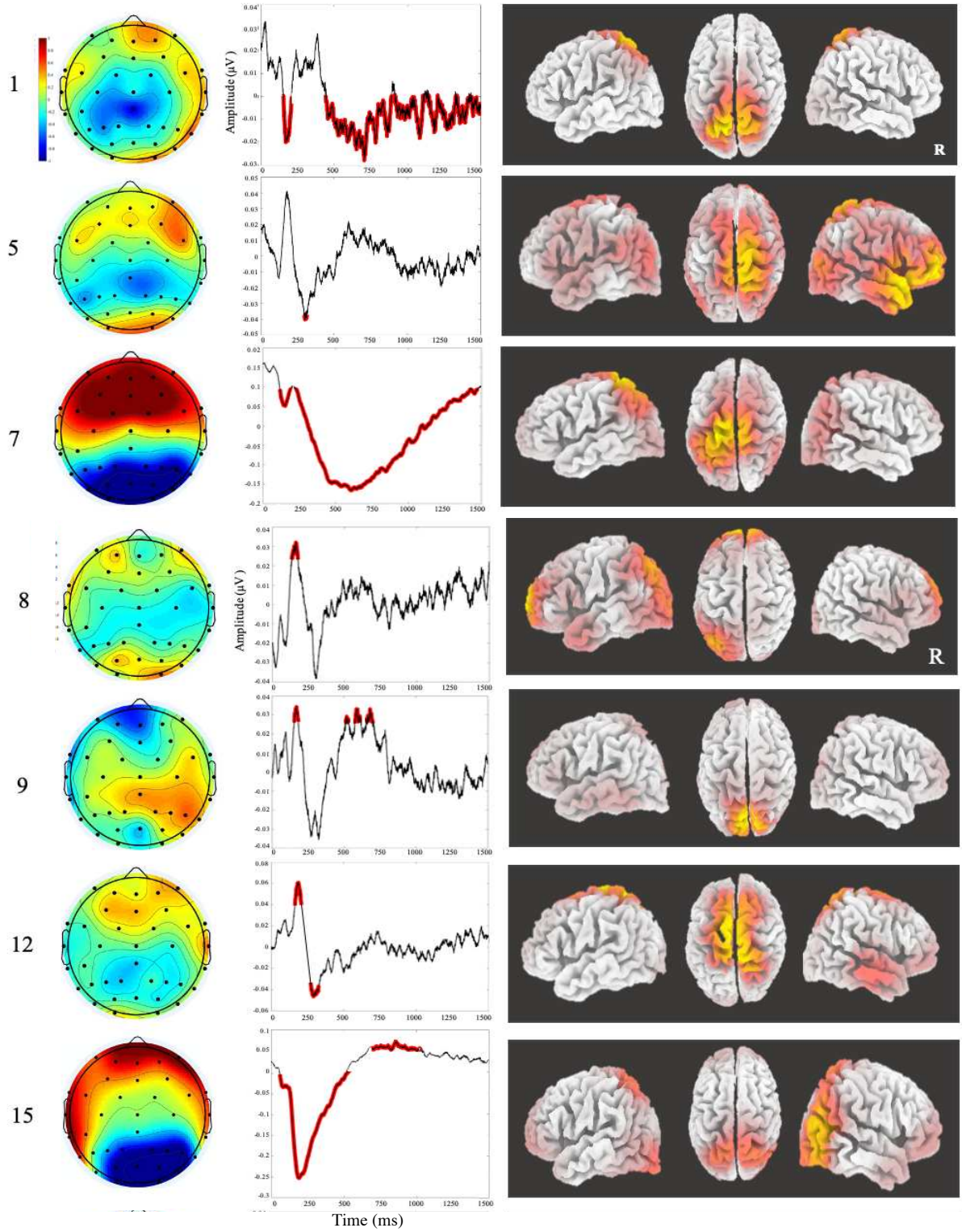

Figure 3.8: Component numbers shown on far left. Component topographies in column one show the spatial distribution of component activity collapsed across time. Column two shows component time-courses, time periods (ms) significantly different from baseline are shown in red, Bonferroni corrected at $p < .01$. Source localization results are shown in the third column.

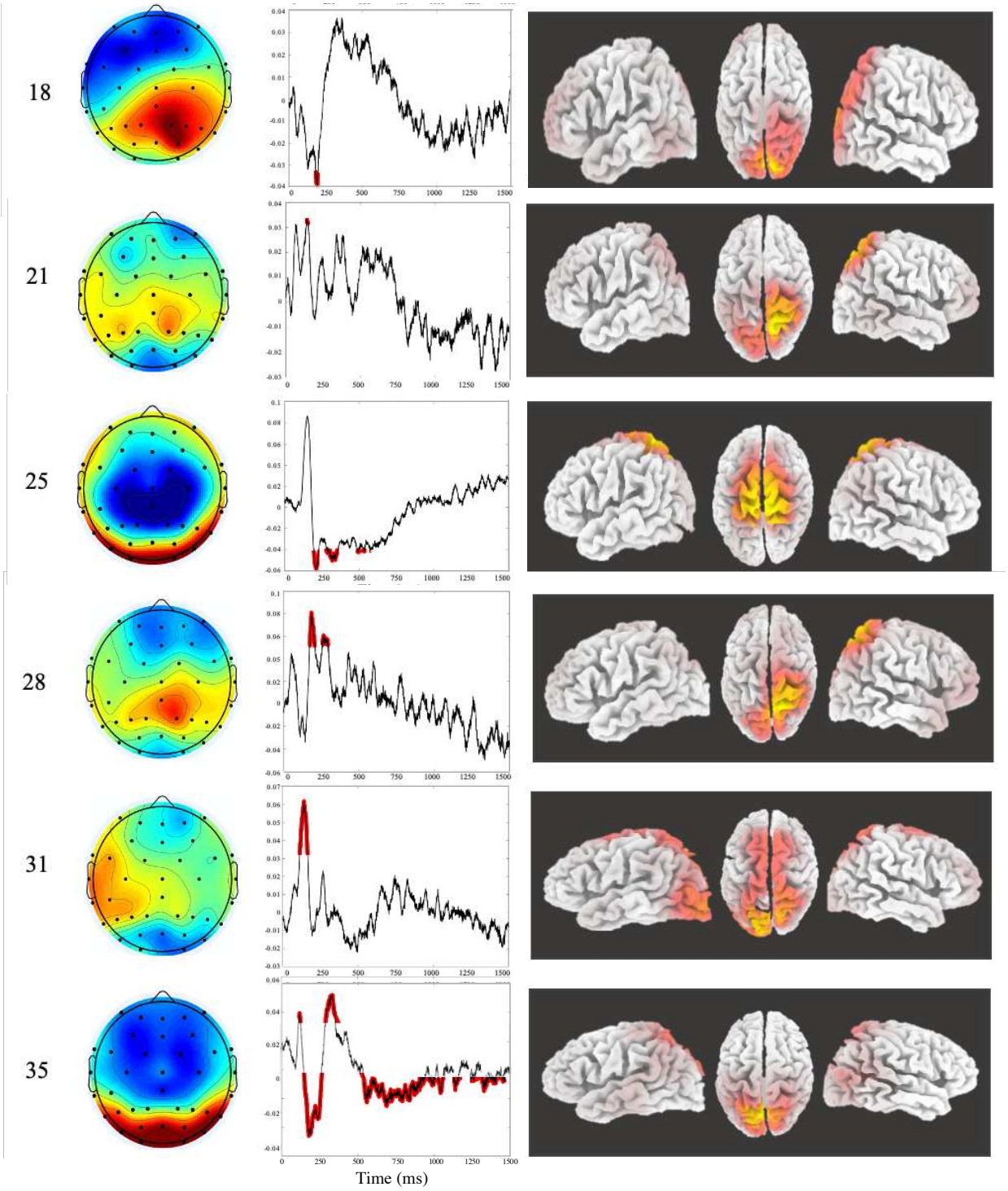

Figure 3.9: Component numbers shown on far left. Component topographies in column one show the spatial distribution of component activity collapsed across time. Column two shows component time-courses, time periods (ms) significantly different from baseline are shown in red, Bonferroni corrected at $p < .01$. Source localization results are shown in the third column.

3.4 Discussion

Emotion perception is the seemingly instantaneous integration of vocal and facial cues that together form a whole percept. While affective information can be gleaned from and identified in either modality independently, the relative contribution and interaction of these channels is unclear. While the brain processes underlying the independent processing of voices and faces has been well documented (Kanwisher, McDermott, & Chun, 1997; Schirmer & Kotz, 2006 Adolphs, Damasio, & Tranel, 2002; Belin, Zatorre, & Ahad, 2001) less research has focused on disentangling the neural correlates underlying bimodal emotion perception. Moreover, even fewer studies have focused on the role of emotional valence in mediating the combination of multimodal stimuli in the brain (Pourtois, de Gelder, Vroomen, Rossion, & Crommelinck, 2000). The current study confirmed the authors' hypotheses that activity would be localized to the pSTS and surrounding occipital, temporal, and parietal areas in the right hemisphere.

Three components (5, 7, 15) were localized to the right pSTS, an area which has been identified as the locus of affective multimodal integration (Adolphs, Damasio, & Tranel, 2002; Beauchamp, Argall, Bodurka, Duyn, & Martin, 2004; Robins, Hunyadi, & Schultz, 2009; Campanella & Belin, 2007). Two of the three components exhibited significant correlations with all of the stimulus types and prosody conditions. These findings are in accordance with the results of a high-resolution fMRI study that showed that voices, faces, and simultaneously presented voices and faces elicited physically distinct but spatially adjacent patterns of activation within the pSTS (Beauchamp, Argall, Bodurka, Duyn, & Martin, 2004). Affective vocal and facial information is relayed to the pSTS via a diverse constellation of direct and indirect connections between the amygdala and occipital, temporal (Blank, Anwander, & von Kriegstein, 2011; Haxby,

Hoffman, & Gobbini, 2000), and fronto-parietal areas of the right hemisphere (Pelphrey & Carter, 2008). This widespread connectivity may indicate that the pSTS works as a multifaceted hub for several components of social communication including: affect recognition (Haxby, Hoffman, & Gobbini, 2000; Campanella & Belin, 2007), social perception (Isik, Koldweyn, Beeler, & Kanwisher, 2017), and emotion cognition (Burnett & Blakemore, 2009). Moreover, the pSTS responds to both domain specific (faces and voices, language, emotion) and more general socially relevant (theory of mind, biological motion) stimuli (Deen, Koldewyn, Kanwisher, & Saxe, 2015). Tasks involving emotion perception may engage several perceptual and cognitive processes simultaneously, which may jointly and differentially recruit the pSTS. This general yet specialized processing capability may partially explain how two components localized to the pSTS could be significantly correlated with every prosody condition and stimulus modality as the pSTS may act as a point of multimodal convergence where information gleaned from affective facial expressions and vocalizations is integrated to enable holistic emotional judgments (Schirmer & Adolphs, 2017).

In addition to activity in the right pSTS, several other areas of brain activity emerged in the left hemisphere, which may reflect the interaction between emotion, attention, and perception in the brain. Components 5 and 8 exhibited activity in left intraparietal sulcus, orbitofrontal cortex, the superior frontal gyrus, and occipital lobe (Figure 3.8). These brain areas have been associated with the visceral modulation of emotion (Price, 2006), cognitive evaluation functions and attentional mechanisms which modulate visual processing (Pessoa & Ungerleider, 2004). Additionally, these regions are connected via subcortical structures including the amygdala (Vuilleumier & Driver, 2007), basal forebrain, and hypothalamus (Pessoa & Ungerleider, 2004). These structures are thought to exert top-down attentional and emotional modulation on visual

processing by evaluating the affective value of incoming stimuli (Pessoa & Ungerleider, 2004; Vuilleumier & Driver, 2007). The top-down modulatory effect of these areas on visual processing complements the conceptual correlations between components 5 and 8 and the visual Face Only and audiovisual Face+Voice conditions. The current study invoked both attentional and emotional modulation of visual processing as subjects were required to attend to and evaluate the affective properties of each visual stimulus. This top-down modulation may have led to increased or prolonged brain activity in the visual cortices while processing the emotional images (Vuilleumier & Driver, 2007), with attentional and emotional influences ultimately shaping the formation of each emotional percept. This pattern of activity appeared manifest in components 8, 15, 18, and 31, all of which exhibited occipital activity that was significantly correlated with the Face+Voice stimulus condition.

Several components were localized to right somatosensory areas (components: 5, 18, 21, 28, figures 3.8, 3.9) with multiple components exhibiting bilateral activity (components: 1, 7, 12, 15, 25, 31, figures 3.8, 3.9). While these results were not hypothesized, they fit within a wider literature indicating that the right somatosensory cortex plays an essential role in embodied emotion (Kragel & LaBar, 2016). Embodied emotion is the visceral bodily experience of an emotion. Representations in the somatosensory cortex have been associated with linking emotion perception to the subjective experience of observing affective vocal and facial expressions (Kragel & LaBar, 2016). One theory posits that the somatosensory cortex contains neural representations of emotional vocal and facial expressions, which facilitate affect recognition by connecting external emotional stimuli to internal emotion categories (Damasio, 1996). This viewpoint is bolstered by findings that damage to or interruption of activity in right somatosensory areas appears to interfere with the recognition of both vocal (Adolphs, Damasio, & Tranel, 2002;

Banissy et al., 2010) and facial (Adolphs, Damasio, Tranel, Cooper, & Damasio, 2000; Pitcher, Garrido, Walsh, & Duchaine, 2008) expressions of emotion. Additionally, one fMRI study showed that multivoxel activations were correlated with self-report measures of emotional experiences when viewing or hearing affective stimuli (Kragel & LaBar, 2016), indicating that the somatosensory cortex exhibits emotion-specific patterns of activity that coincide with subjects' subjective emotional states. In this study, 11 of the final 13 components showed some activity in either primary or secondary somatosensory cortices.

These findings are complemented by the behavioral data, which showed that happy and angry prosodic voices appear to shift subjective judgments of emotion perception so that morphed faces will appear to be 'happier' or 'angrier' than their physical composition. These results indicate that subjects may have experienced some form of emotional embodiment as their internal representation of each emotion was biased by the prosody of the simultaneously presented voice. While there were no significant differences between the Happy Face+Voice and Face Only condition (Figure 3.4) this may have been due to the highly salient nature of happy faces, which may not have benefited from the presence of a prosodic voice. Additionally, the PSE values between the Neutral and Angry Face+Voice conditions were not significantly different (Figure 3.4). These data could suggest an inherent negativity bias which made the voices for the Neutral and Angry Face+Voice conditions appear 'angrier' than the Happy Face+Voice and Face Only conditions. Further, a negativity bias may account for a potential ceiling effect that prevented the Angry Face+Voice condition from being perceived as 'angrier' than the Neutral Face+Voice condition.

The current study used JND values and reaction time scores to quantify both the variance in subjects' responses, as well as, the perceptual processing speed for each Face+Voice and Face

Only stimulus category. Results showed that although the Face Only condition exhibited the lowest reaction times (Figure 3.6), they also exhibited the highest JND values. Indicating that while bimodal stimuli may require more perceptual processing time than faces shown in isolation, faces and voices appear to increase sensitivity to differences in emotional expression. Additionally, the Happy Face+Voice condition had the lowest mean JND value, which may be related to the increased emotional salience of happy stimuli. These behavioral data illustrate that unimodal and multimodal stimuli are differentially perceived and processed, and that this perceptual processing may not only be dependent on the modality of the stimulus but also upon its emotional valence. Additionally, these results may suggest that emotional embodiment is facilitated by the presentation of affective faces as voices, with voices playing an essential role in the subjective experience of emotion recognition.

If replicated in a future study, these results may suggest that embodied emotion may be an essential element of emotion identification, as subjects were presented with affective audio, visual, and audiovisual stimuli and then asked to make subjective ratings of each stimulus. Thus, regardless of the stimulus modality or prosody condition subjects were presented with some form of emotional content, which would have been internally associated with an emotional category represented in the somatosensory cortex (Damasio, 1996; Kragel & LaBar, 2016). These effects may have resulted in multiple seemingly identical areas of activation that are differentially involved in the subjective experience of emotion. While difficult to physically parse apart, this notion of component specialization may be supported by differences in the component time-course correlations, which often varied in both the number and type (stimulus modality or emotional valence) of correlation between components with similar spatial distributions. However, due to the inferior spatial resolution of the imaging modality employed in the current study these nuanced

patterns of activity may have gone undetected. Future work with brain stimulation methods could experimentally manipulate suppression or enhancement of somatosensory brain regions in conjunction with presentation of multimodal emotional stimuli.

Collectively, these components characterize distinct aspects of multimodal integration, emotion perception, and the subjective experience of emotion. While multiple components (7, 8, 15, 21, 25, 28, 31, figures 3.8, 3.9) were significantly correlated with either the Happy or Angry prosody condition it was uncertain which neuroanatomical regions or cognitive, perceptual, or attentional processes these emotions were associated with. While the localization of emotional in the brain was somewhat ambiguous, studies of emotional prosody have provided invaluable evidence as to how affective voices are represented in the brain. Previous functional near-infrared spectroscopy (fNIRS) work using an identical task showed that happy and angry voices paired with affective faces exhibited a posterior-anterior distribution of activity in the right hemisphere that appeared to be dependent on the valence of the spoken prosody (Becker & Rojas, submitted). This functional organization parallels that described for prosodic language (Ross & Monnot, 2008) with posterior parietal areas being associated with the reception and comprehension of prosody and anterior frontal areas being associated with the expression of prosody. Of the 13 components, only component 5 appeared to exhibit a similar posterior-anterior distribution of activity, but it was not correlated with either prosody condition.

One of the goals of the current study was to use EEG and independent component analysis to isolate and source localize activity to structures that may be involved in multimodal affect recognition and which may be specialized to a single modality. These results reaffirm previous work showing that unimodal and multimodal information processing and integration occurs within a distributed network of brain areas within the right hemisphere (Adolphs, Vuilliemier & Driver;

Kragel & LaBar, 2016). Additionally, they build upon the current literature by demonstrating that neural activity can be decomposed and correlated with task elements (sensory modality and emotional valence) to further refine the role of each component. Limitations of the current study include an inability to record subcortical structures, which may serve as important components in the networks underlying bimodal affect recognition. In particular, the results presented herein could have benefitted from imaging the amygdala as multiple studies have identified it as a core structure in models of emotion perception (Baxter & Croxson, 2012; Adolphs, Damasio, & Tranel, 2002; Price & Friston, 2005), as it plays an essential role in the elaboration of emotion for higher cognitive functions (Baxter & Croxson, 2012; Price & Friston, 2005). The use of dynamic as opposed to static faces could have furthered the ecological validity of the current study as dynamic faces have been shown to specifically engage anterior areas of the pSTS (Robins, Hunyadi, & Schultz, 2009). This may have aided in the differentiation of the specialization of areas within the parietal lobe. The current study represents an important step toward furthering our understanding of the neural basis of dynamic emotion perception.

REFERENCES

Adolphs, R., Damasio, H., Tranel, D. (2002) Neural systems for recognition of emotional prosody: a 3-D lesion study. *Emotion, 2*(1):23–51. PMID: 12899365

Adolphs, R., Damasio, H., Tranel, D., Cooper, G., Damasio, A. R. (2000) A role for somatosensory cortices in the visual recognition of emotion as revealed by three-dimensional lesion mapping. *J Neuroscience, 20*(7):2683–2690. PMID: 10729349

Banissy, M. J,, Sauter, D. A., Ward, J., Warren, J. E., Walsh, V., Scott, S. K. (2010). Suppressing sensorimotor activity modulates the discrimination of auditory emotions but not speaker identity. *J Neuroscience, 30*(41):13552– 13557. PMID: 20943896

Batty, M., Taylor, M. J. (2003). Early processing of the six basic facial emotional expressions. *Brain Research Cognition Brain Research, 17*(3):613-20. PMID: 14561449

Baxter, M. G., Croxson, P. L. (2012). Facing the role of the amygdala in emotional information processing. *Proceedings of the National Academy of Sciences, 109*(52):21180-21181. PMID: 23243143

Beauchamp, M. S., Argall, B. D., Bodurka, J., Duyn, J. H., Martin, A. (2004). Unraveling multisensory integration: patchy organization within human STS multisensory cortex. *Nature Neuroscience, 7*(11);1190-1192. PMID: 15475952

Belin, P., Fillion-Bilodeau, S., Gosselin, F. (2008). The Montreal Affective Voices: A validated set of nonverbal affect bursts for research on auditory affective processing. *Behavior Research Methods*, *40*(2):531-539. DOI: doi.org/10.3758/BRM.40.2.53

Belin, P., Zatorre, R. J., Ahad, P. (2001). Human temporal-lobe response to vocal sounds. *Cognitive Brain Research, 13*(1):17-26. PMID: 11867247

Belliveau, J. W., Kennedy, D. N., McKinstry, R. C., Buchbinder, B. R., Weisskoff, R. M., Cohen, M. S., et al. (1991). Functional mapping of the human visual cortex by magnetic resonance imaging. *Science,* 254, 716–719. DOI: 10.2307/2879286

Bernat, E., Bunce, S., Shevrin, H. (2001). Event-related brain potentials differentiate positive and negative mood adjectives during both supraliminal and subliminal visual processing. *International Journal of Psychophysiology*, *42*(1):11-34. PMID: 11451477

Blank, H., Anwander, A., von Kriegstein, K. (2011). Direct Structural Connections between Voice- and Face-Recognition Areas. *J Neuroscience, 31*(36):12906-12915. PMID: 21900569

Burnett, S., Blakemore, S. (2009). Functional connectivity during a social emotion task in adolescents and in adults. *Cerebral Cortex, 29*(6):1294-1301. PMID:19302165

Cacioppo, J., Crites, S., Jr., Berntson, G., Coles, M. (1993). If attitudes affect how stimuli are processed, should they not affect the event-related brain potential? *Psychological Science*, 4(2):108-112. DOI: https://doi.org/10.1111/j.1467-9280.1993.tb00470.x

Campanella, S., Belin, P. (2007). Integrating face and voice in person perception. *Trends in Cognitive Science, 11*(2):535-543. PMID: 17997124

Damasio, A. R. (1996). The somatic marker hypothesis and the possible functions of the prefrontal cortex. *Philosophical Transactions of the Royal Society of London B Biological Sciences, 351*(1346):1413–1420. PMID: 8941953

Deen, B., Koldewyn, K., Kanwisher, N., Saxe, R. Functional Organization of Social Perception and Cognition in the Superior Temporal Sulcus. *Cerebral Cortex, 25*(11):4596-4609. PMID: 26048954

Delorme, A., Makeig, S. (2004). EEGLAB: an open source toolbox for analysis of single-trial EEG dynamics. *Journal of Neuroscience Methods,* 134:9-21. PMID: 15102499

Eichele, T., Rachakonda, S., Brakedal, B., Elkeland, R., Calhoun, V. (2011). EEGIFT: Group Independent Component Analysis for Event-Related EEG Data. *Comput Intell Neurosci*. DOI: 10.1155/2011/129365

Eimer, M., Holmes, A. (2007). Event-related brain potential correlates of emotional face processing. *Neuropsychologia*, 45(1):15-31. PMID: 16797614

Fechner, G. (1966). *Elements of psychophysics. Vol. 1.* Holt, Rinehart and Winston: New York.

Foti, D., Hajcak, G. (2008). Deconstructing reappraisal: Descriptions preceding arousing pictures modulate the subsequent neural response. *Journal of Cognitive Neuroscience*, 20(6):977-988. PMID: 18211235

Grech, R., Cassar, T., Muscat, J., Camilleri, K. P., Fabri, S. G., Zervakis, M., Xanthopoulos, P., Sakkalis, V., Vanrumste, B. (2008). Review on solving the inverse problem in EEG source analysis. *J Neuroengineering Rehabilitation*, *5*(25). DOI: 10.1186/1743-0003-5-25

Hajcak, G., Weinberg, A., MacNamara, A., Foti D. (2011). ERPs and the Study of Emotion. The Oxford Handbook of Event-Related Potential Components.

Haxby, J. V., Hoffman, E. A., Gobbini, M. I. (2000). The distributed human neural system for face perception. *Trends in Cognitive Sciences, 4*(6):223-233. PMID: 10827445

Isik, L., Koldewyn, K., Beeler, D., Kanwisher, N. (2017). Perceiving social interactions in the posterior superior temporal sulcus. *Proceedings of the National Academy of Sciences, 114*(43):E9145-E9152. PMID: 29073111

Jiang, X. (2017). Tracking the Sound of Human Affection: EEG Signals Reveal Online Decoding of Socio-Emotional Expression in Human Speech and Voice. Emotion and Attention Recognition Based on Biological Signals and Images, pp. 47-58. DOI: http://dx.doi.org/10.5772/66418

Kanwisher, N., McDermott, J., Chun, M. M. (1997). The Fusiform Face Area: A Module in Human Extrastriate Cortex Specialized for Face Perception. *J Neuroscience, 17*(11):4302-4311. PMID: 9151747

Kragel, P. A., LaBar, K. S. (2016). Somatosensory representations link the perception of emotional expressions and sensory experience. *eNeuro, 3*(2):e0090-15.2016 1-12. PMID: 27280154

Kwong, K. K., Belliveau, J. W., Chesler, D. A., Goldberg, I. E., Weisskoff, R. M., Poncelet, B. P., et al. (1992). Dynamic magnetic resonance imaging of human brain activity during primary sensory stimulation. *Proceedings of the National Academy of Sciences,* 89:5675–5679. DOI: 10.1073/pnas.89.12.5675

Lewin, J. S. (2003). Functional MRI: An introduction to methods. *J Magn. Reson. Imaging,* 17:383. DOI: 10.1002/jmri.10284

Liu, J., Tian, J. (2007). Physiology, Function, and Structure from Medical Images; 651121 (2007). Spatiotemporal analysis of single-trial EEG of emotional pictures based on independent component analysis and source location. *Medical Imaging*, 6511. DOI: https://doi.org/10.1117/12.709288

Logothetis, N. K., Pauls, J., Augath, M., Trinath, T., Oeltermann, A. (2001). Neurophysiological investigation of the basis of the fMRI signal. *Nature,* 412:150–157. DOI: 10.1038/35084005

Luo, W.,Feng, W., He, W., Wang, N. Y., Luo, Y. J. (2010). Three stages of facial expression processing: ERP study with rapid serial visual presentation. *NeuroImage, 49*(2):1857–1867. PMID: 19770052

Neumann, D., Spezio, M. L., Piven, J., Adolphs, R. (2006). Looking you in the mouth: abnormal gaze in autism resulting from impaired top-down modulation of visual attention. *Social, Cognitive and Affective Neuroscience, 1*(3), 194–202. DOI:10.1093/scan/nsl030

Ogawa, S., Lee, T. M., Nayak, A. S., Glynn, P. (1990). Oxygenation-sensitive contrast in magnetic resonance image of rodent brain at high magnetic fields. *Magn. Reson. Med.,* 14:68–78. DOI: 10.1002/mrm.1910140108

Onton, J., Westerfield, M., Townsend, J., Makeig, S. (2006). Imaging human EEG dynamics using independent component analysis. *Biobehavioral Reviews*, 30:808-822. DOI: doi:10.1016/j.neubiorev.2006.06.007

Pascal, H., Henrique, S. (2013). Time course of brain activation elicited by basic emotions. *Neuroreport, 24*(16):898-902. PMID: 24025800

Pascual-Marqui, R. D. (2009) Theory of the EEG Inverse Problem. in Tong, S. and Thakor, N. V., (eds.) Quantitative EEG Analysis: Methods and Clinical Applications, Boston, MA: Artech House. pp. 121-140

Paulmann, S., Seifert, S., Kotz, S. A. (2010). Orbito-frontal lesions cause impairment during late but not early emotional prosodic processing. *Social Neuroscience*, *5*(1):59-75. DOI: 10.1080/17470910903135668

Paulmann, S., Kotz, S. A. (2008). An ERP investigation on the temporal dynamics of emotional prosody and emotional semantics in pseudo- and lexical-sentence context. *Brain and Language, 105*(1), 59–69. DOI: http://doi.org/10.1016/j.bandl.2007.11.005

Paulmann, S., Bleichner, M., Kotz, S. (2013). Valence, arousal, and task effects in emotional prosody processing. Frontiers in Psychology, 4, 345. DOI: 10.3389/fpsyg.2013.00345.

Pell, M. D., Rothermich, K., Liu, P., Paulmann, S., Sethi, S., Rigoulot, S. (2015). Preferential decoding of emotion from human non-linguistic vocalizations versus speech prosody. *Biological Psychology, 111*:14–25. DOI: http://doi.org/10.1016/j.biopsycho.2015.08.008

Pelphrey, K. A., Carter, E. J. (2008). Charting the typical and atypical development of the social brain. *Development and Psychopathology, 20*(4):1081-1102. PMID: 18838032

Pessoa, L., Ungerleider, L. G. (2004). Neuroimaging studies of attention and the processing of emotion-laden stimuli. *Progress in Brain Research, 144*:171-182. PMID: 14650848

Pitcher, D., Garrido, L., Walsh, V., Duchaine, B. C. (2008). Transcranial magnetic stimulation disrupts the perception and embodiment of facial expressions. *J Neuroscience, 28*(36):8929–8933. PMID: 18768686

Pourtois, G., de Gelder, B., Vroomen, J., Rossion, B., Crommelinck, M. (2000). The time-course of intermodal binding between seeing and hearing affective information. *Neuroreport, 11*(6):1329-1333. PMID: 10817616

Pratt, H. (2011). Sensory ERP Components. The Oxford Handbook of Event-Related Potential Components.

Price, C. J., Friston, K. J. (2002). Functional ontologies for cognition: the systematic definition of structure and function. *Cognitive Neuropsychology, 22*(3/4):262-275. PMID: 21038249

Price, J. L. (2006). Architectonic structure of the orbital and medial prefrontal cortex. In D. H. Zald and S. L. Rauch, eds., *The Orbitofrontal Cortex,* 3-17. Oxford: Oxford University Press.

Regan, D. (1989). *Human brain electrophysiology: Evoked potentials and evoked magnetic fields in science and medicine.* New York: Elsevier.

Robins, D. L., Hunyadi, E., Schultz, R. T. (2009). Superior temporal activation in response to dynamic audio-visual emotional cues. *Brain and Cognition, 69*(2):269-278. PMID: 18809234

Ross, E. D., Monnot, M. (2008). Neurology of affective prosody and its functional-anatomic organization in right hemisphere. *Brain and Language, 104*(1):51-74. PMID: 17537499

Rossion, B., Joyce, C. A., Cottrell, G. W., Tarr, M. J. (2003). Early lateralization and orientation tuning for face, word, and object processing in the visual cortex. *Neuroimage, 20*(3):1609–24. PMID: 14642472

Rossion, B., Caharel, S. (2011). ERP evidence for the speed of face categorization in the human brain: Disentangling the contribution of low-level visual cues from face perception. *Vision Research*, *51*(12):1297-1311. PMID: 21549144

Schirmer, A., Kotz, S. A. (2006). Beyond the right hemisphere: brain mechanisms mediating vocal emotional processing. *Trends in Cognitive Sciences, 10*(1):24-30. PMID: 16321562

Tottenham, N., Tanaka, J. W., Leon, A. C., McCarry, T., Nurse, M., Hare, T. A., Marcus, D. J., Westerlund, A., Casey, B. J., Nelson, C. (2009). The NimStim set of facial expressions: Judgments from untrained research participants. *Psychiatry Research, 168*(3):242-249. DOI: 10.1016/j.psychres.2008.05.006

van den Broek, S. P., Reinders, F., Donderwinkel, M., Peters, M. J. (1998). Volume conduction effects in EEG and MEG. *Electroencephalography and Clinical Neurophysiology, 106*(6):522-534. PMID: 9741752

Vigario, R., Sarela, J., Jousmiki, V., Hamalainen, M., Oja, E. (2000). Independent component approach to the analysis of EEG and MEG recordings. *IEEE Transactions on Biomedical Engineering, 47*(5):589-593. PMID: 10851802

Vuilleumier, P., Driver, J. (2007). Modulation of visual processing by attention and emotion: windows on causal interactions between human brain regions. *Philosophical Transactions of the Royal Society B, 362*:837-855. PMID: 17395574

Zuhkov, L., Weinstein, D., Johnson, C. (2000). Independent component analysis for EEG source localization. *IEEE Engineering in Medicine and Biology*, *19*(3):87-96. PMID: 10834122

CHAPTER 4 – THE EFFECT OF EMOTIONAL CONGRUENCY ON MULTIMODAL EMOTION PERCEPTION: AN MAGNETOENCEPHALOGRAPHY (MEG) STUDY

4.1 Introduction

4.1.1 Perceptual Integration of Affective Faces and Voices. Emotion is communicated via the simultaneous integration of affective facial and vocal expressions, which provide complementary or incongruent information that can influence emotion perception (Kayser & Logothetis, 2007; de Gelder & Vroomen, 2000) and behavioral performance (de Gelder & Vroomen, 2000; Schröger & Widmann, 1998). These two channels appear to be strongly connected as illustrated by the famous McGurk Effect (McGurk & MacDonald, 1976), in which an illusory auditory percept is formed through the simultaneous presentation of two mismatched visual (spoken /ga-ga/) and auditory inputs (voiced /ba-ba/). The aberrant percept underscores the dynamic interplay of these two channels in bimodal perception and suggests that faces and voices are not processed independently in the brain. Rather, simultaneous presentation of incongruent audio and visual stimuli may disrupt the neural processes underlying normal multimodal integration to distort or bias perception (de Gelder & Vroomen, 2000) to form a third illusory percept that does not match the information presented in either the visual or auditory modality alone (McGurk & MacDonald, 1976). While this phenomenon has been well established in the behavioral literature (Campanella & Belin, 2007; de Gelder & Vroomen, 2000; McGurk & MacDonald, 1976; Schröger & Widmann, 1998), research examining the neural correlates of incongruent audiovisual integration in emotion perception has been lacking (Chen, Edgar, Holroyd, Dammers, Thönneßen, Roberts, & Mathiak, 2010).

4.1.2 Neural Substrates of Multimodal Emotion Perception. Affective information gleaned from faces and voices appears to be processed via a distributed network of brain regions which

exhibit connections involve fusiform gyrus (FG), occipital face area (OFA), the amygdala, the orbitofrontal cortex, and the posterior superior temporal sulcus (pSTS) of the right hemisphere (Gainotti, 2019), which lies at the intersection of primary auditory and visual cortices (Adolphs, Tranel, & Damasio, 2003; Adolphs, 2002). This lateralization appears to be related to the direct (orbitofrontal cortex, amygdala) and indirect (FG, OFA) connections to areas in the right hemisphere associated with processing affective socially relevant stimuli (Leppänen & Nelson, 2008; Adolphs, 2002).

Neuroimaging findings have provided ample evidence that the pSTS may be at the center of this network as it has been strongly associated with the convergence and integration of affective auditory and visual information (Beauchamp, Argall, Bodurka, Duyn, & Martin, 2004; Hagan, Woods, Johnson, Calder, Green, & Young, 2009; Hagan, Woods, Johnson, Green, & Young, 2013; Kreifelts, Ethofer, Grodd, Erb, & Wildgruber, 2007). Evidence from high resolution functional magnetic resonance imaging (fMRI) further refines the role of the pSTS in multimodal perception as it showed that the pSTS exhibits a patchy organization of separate groups of cells that are maximally responsive to both unimodal (auditory-only, visual-only) and multimodal inputs (Beauchamp, Argall, Bodurka, Duyn, & Martin, 2004). Non-human primates exhibit a homologous pattern of partially overlapping and nonoverlapping cortical projections connecting polysensory and unisensory brain regions to the pSTS (Seltzer, Cola, Gutierrez, Massee, Weldon, & Cusick, 1996), Cyto- and myeloarchitectonic parcellation of the pSTS in the rhesus monkey also demonstrated a similar pattern of afferent cortical connections arising in primary auditory and visual cortices, with some ventral areas of the pSTS receiving input from multiple cortical sources (Seltzer & Pandya, 1978). This organization may facilitate the integration of multimodal inputs

derived from auditory and visual brain areas (Seltzer, Cola, Gutierrez, Massee, Weldon, & Cusick, 1996; Beauchamp, Argall, Bodurka, Duyn, & Martin, 2004).

This physiological convergence supports the notion that the pSTS is essential to audiovisual integration and social communication, with one model of face processing hypothesizing that the pSTS is specialized in processing the dynamic changeable features of faces (eye gaze, mouth and cheek movements), which characterize not only visual speech but also the minute physical changes that differentiate different affective facial expressions (Haxby, Hoffman, & Gobbini, 2000). This model is further reinforced by fMRI studies which have shown that physically distinct, but overlapping areas of the STS respond to both the visual and auditory features of moving faces, with activations appearing while viewing dynamic faces, listening to emotional voices (Hoffman & Haxby, 2000; Yang, Rosenblau, Keifer, & Pelphrey, 2015), or during silent lip reading (Calvert, et al., 1997). Thus, the pSTS may play an integral role in combining separate sources of information to detect the physical changes in facial and vocal expressions that characterize different emotions (Calder & Young, 2005; Calder, Young, Keane, & Dean, 2000). These results reinforce the idea that the pSTS may possess a more holistic representation of emotion, which responds to both the changeable aspects of faces and their concomitant vocalizations. Such findings indicate that while the pSTS responds to both unimodal and bimodal sources of affective information, the pSTS exhibits heightened expertise in analyzing concurrently presented affective visual and auditory information conveyed by simultaneously presented faces and voices.

4.1.3 Neural Correlates of Emotional Congruence Detection. The initial processing and integration of faces and voices has a rapid time course, with electroencephalogram (EEG) findings showing that early (<100 ms post-stimulus onset) auditory processing of a vocal stimulus may be modulated by a concurrently presented affective facial expression (Pourtois, de Gelder, Vroomen,

Rossion, & Crommelinck, 2000). Additionally, two studies have reported that the amplitude of the auditory N1 and N140 components is greater when the emotion conveyed by the face is congruent with that communicated by the voice (Pourtois, de Gelder, Vroomen, Rossion, & Crommelinck, 2000; Puce, Epling, Thompson, & Carrick, 2007), suggesting that auditory processing is enhanced when presented with a congruent visual stimulus as visual context may modulate how auditory information is processed. Interestingly, while visually evoked N170 face component was elicited in one study it was not affected by the congruency manipulation (Puce, Epling, Thompson, & Carrick, 2007). Some researchers have suggested that later visual components may be less affected by manipulations to audiovisual stimuli as auditory information gleaned from the stimulus has already been processed via other sensory pathways or in unisensory auditory brain areas (Ghazanfar & Schroeder, 2006; Ghazanfar, Chandrasekaran, & Logothetis, 2008).

While only a subset of neuroimaging studies has directly examined the neural underpinnings of emotional congruence this study will touch on a related aspect of emotional cognition known as emotional conflict. Emotional conflict refers to situations in which the emotional expression displayed by the face is not congruent with that expressed in the voice (Müller, Habel, Derntl, Schneider, Zilles, Turetsky, & Eickhoff, 2011). Few studies have focused on the effects of emotional conflict (Müller, Habel, Derntl, Schneider, Zilles, Turetsky, & Eickhoff, 2011), which have been associated with increased cognitive processing and longer reaction times for incongruent bimodal stimuli (de Gelder & Vroomen, 2000; Wittfoth, Schroder, Schardt, Dengler, Heinze, & Kotz, 2010). Emotional conflict may take many forms and can be studied using a variety of paradigms which examine emotional and cognitive control mechanisms (Xu, Xu, & Yang, 2016; Song, Zilverstand, Song, d'Oleire Uquillas, Wang, Xie, Cheng, & Zou, 2017). Meta-analyses examining the effect of strong emotional conflict during emotional Stroop tasks have consistently

reported activity in the dorsolateral prefrontal cortex (DLPFC), inferior frontal gyrus, and dorsal anterior cingulate cortex (dACC), which has been associated with conflict detection (Xu, Xu, & Yang, 2016; Song, Zilverstand, Song, d'Oleire Uquillas, Wang, Xie, Cheng, & Zou, 2017). Additionally, one fMRI study reported that incongruent affective face-voice stimuli were associated with increased activity in a network of cingulate-fronto-parietal areas, which appear to be involved in conflict monitoring and resolution (Müller, Habel, Derntl, Schneider, Zilles, Turetsky, & Eickhoff, 2011).

4.1.4 Limitations of Existing Neuroimaging Findings. While a number of fMRI (Müller, Habel, Derntl, Schneider, Zilles, Turetsky, & Eickhoff, 2011; Kreifelts, Ethofer, Grodd, Erb, & Wildgruber, 2007) and EEG (Pourtois, de Gelder, Vroomen, Rossion, & Crommelinck, 2000; Puce, Epling, Thompson, & Carrick, 2007) studies have provided critical insights into the neural substrates underlying multimodal emotion perception, few studies have utilized magnetoencephalography (MEG; Hagan, Woods, Johnson, Calder, Green, & Young, 2009; Chen, Edgar, Holroyd, Dammers, Thönneßen, Roberts, & Mathiak, 2010). MEG measures the minute magnetic fields emanating from populations of active neurons in the cortex unencumbered by the effects of volume conduction which complicate interpretation of EEG results (Baillet, 2017). Additionally, MEG boasts excellent temporal precision and good spatial resolution, enabling researchers to delineate the neural activity underlying emotion perception on a fine time scale with reasonable spatial accuracy (Baillet, 2017). Experimentally, other studies investigating multimodal integration of affective faces and voices have used static stimuli (Hagan, Woods, Johnson, Calder, Green, & Young, 2009; Müller, Habel, Derntl, Schneider, Zilles, Turetsky, & Eickhoff, 2011; Chen, Edgar, Holroyd, Dammers, Thönneßen, Roberts, & Mathiak, 2010), which may have limited not only their ecological validity but also differentially effected the pSTS as it responds to

changeable, rather than invariant, facial features (Haxby, Hoffman, & Gobbini, 2000). This limitation may detract from the interference effects associated with incongruent dynamic stimuli as static stimuli lack the articulatory changes that normally coincide with affective vocalizations.

4.1.5 Current Study. The current study investigated the neural substrates involved in processing congruent and incongruent affective voices paired with dynamic faces. Dynamic face stimuli were used to increase both the ecological validity of the study and to potentially further engage the pSTS during the congruent and incongruent conditions as it is specialized in processing dynamic facial expressions and articulatory speech (Haxby, Hoffman, & Gobbini, 2000). Participants were presented with videos of actors portraying a happy or angry face while saying the vowel /:a/ in an emotionally congruent or emotionally incongruent tone while their brain activity was measured using MEG. Based on prior studies, a beamformer approach was used to analyze evoked and induced broadband responses across space and time between 0.1 and 80 Hz (Hagan, Woods, Johnson, Green, & Young, 2013; Hagan, Woods, Johnson, Calder, Green, & Young, 2009). This frequency range was chosen as both low (theta, alpha) and high (gamma) oscillations have been linked to integrating multimodal affective stimuli. Increased gamma activity (30-80 Hz) in the right STS has been implicated in integrating affective faces and voices (Hagan, Woods, Johnson, Calder, Green, & Young, 2009), sensorimotor integration (Roelfsema, Engel, König, & Singer, 1997; Senkowski, Schneider, Foxe, & Engel, 2008), and top-down attentional control related to auditory processing (Kaiser, Lutzenberger, Ackermann, & Birbaumer, 2002; Debener, Herrmann, Kranczioch, Gembris, & Engel, 2003). Multimodal integration may be modulated by attentional mechanisms associated with alpha band activity (Fu, Foxe, Murray, Higgins, Javitt, & Schroeder, 2001) that also subserve working memory processes and short-term memory retention (Palva & Palva, 2007; Senkowski, Schneider, Foxe, & Engel, 2008). Frontal theta oscillations have been

associated with working memory, emotional arousal, and may even facilitate communication between neuronal populations to promote sensory integration (Senkowski, Schneider, Foxe, & Engel, 2008). Given these findings, the authors predicted that emotional congruency of the simultaneously presented face-voice pair would impair the participant's perception of the stimulus and that this would be evidenced by increased gamma activity in right pSTS to both the incongruent angry and happy face-voice combinations compared with the congruent face-voice pairings. The gamma and theta frequency bands will exhibit overlapping patterns of activity in frontal and visual cortices for the congruent face-voice condition. Additionally, the authors hypothesized that the incongruent condition would show increased activity in the theta and alpha bands would appear in bilateral DLPFC, and ventral occipitotemporal and inferior frontal areas of the right hemisphere when compared to the congruent condition.

4.2 Methods

4.2.1 Participants. Twenty-four subjects were recruited from Denver, Fort Collins, and their surrounding areas. Subjects were excluded if they reported any history of developmental, learning, psychiatric, or neurological disorder, traumatic brain injury, current substance abuse, metal implantations, or were not native English speakers. Additionally, in order to participate, subjects were required to have normal or corrected-to-normal vision and hearing. Subjects filled out several questionnaires to gather information about current or past previous drug (Drug Abuse Screening Test (DAST), Gavin, Ross, & Skinner, 1989) and alcohol use (Alcohol Use Disorders Identification Test (AUDIT), Saunders, Aasland, Babor, de la Fuente, & Grant, 1993), as well as,

Table 4.1 *Mean Questionnaire Scores Concerning Drug and Alcohol Use, and General Physical and mental health*.

Scale	Variables		Age		Score	
			M	*SD*	*M*	*SD*
DUKE		*n* = 24(13)	30.43	6.32		
Health Measures						
	Physical health				80.43	11.22
	Mental health				80.83	14.11
	Social health				77.08	17.06
	General health				79.45	11.19
	Perceived health				91.67	19.03
	Self-esteem				85.83	14.12
Dysfunction Measures						
	Anxiety				23.61	13.82
	Depression				22.92	14.88
	Anxiety-depression				22.32	14.02
	Pain				29.17	25.18
	Disability				2.08	10.21
DAST-10		*n* = 24(13)	30.43	6.32		
	Drug abuse				0.46	.66
AUDIT		*n* = 24(13)	30.43	6.32		
	Alcohol use				4.38	3.66

Note: Parentheses indicate number of female participants. Scores for the DUKE are raw scores from a scale of 0.0-100.0. High scores for health measures indicate good health, high scores for the dysfunction measures equates to poor health. DAST-10 contains 10 items with scores ranging from 0.0-10.0, lower scores (1-5) indicating lower to moderate drug use, and higher scores (6-10) suggesting substantial to severe drug use. Total AUDIT scores greater than 8 indicate dangerous and harmful alcohol consumption, with scores ranging from 0.0-40.0.

information about general mental and physical health Duke Health Profile, Parkerson, Broadhead, & Tse, 1990). Questionnaire results and scoring cutoffs are shown in table 4.1.

4.2.2 Face Stimuli. Face stimuli consisted of a set of nonprofessional actors with natural hair and makeup taken from the NimStim database (Tottenham et al., 2009). Sixteen (8 men) were selected from the NimStim database. Two images were selected for each actor, one closed- and open-mouth happy and one angry facial expression. Images were transformed to grayscale and

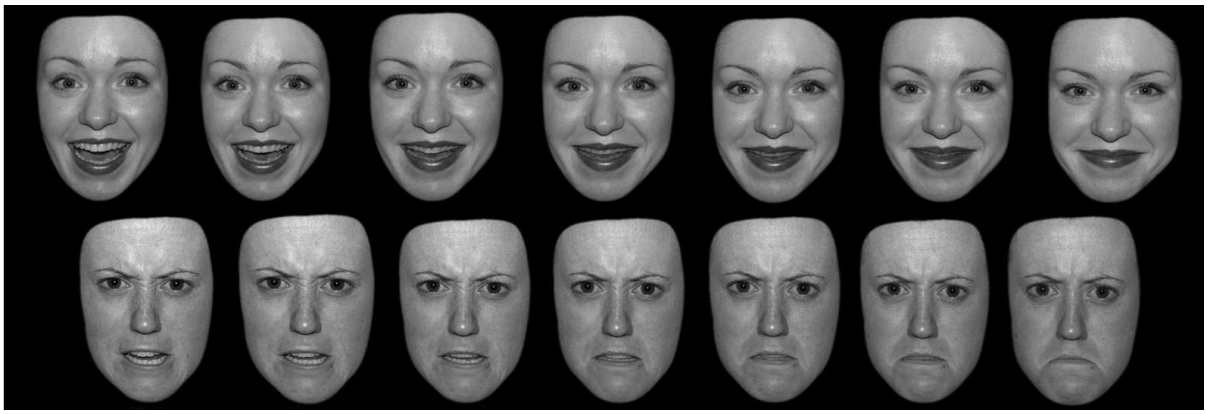

Figure 4.1: Morphed video stimuli presented during the MEG experiment. Two exemplar morphed continua created from one open mouth and one closed mouth image taken from the same actor expressing either a happy (top) or angry (bottom) face. The faces were combined together to create short videos so that it appeared as though the actor was opening and closing their mouth. These videos were then paired with voices saying /a:/ in either an angry or happy tone.

cropped so that only the actor's face was visible. Psychomorph software was used to generate 32 continua, one for each actor and each emotion (Tiddeman, Burt, & Perrett, 2001; Tiddeman & Perrett, 2002). Each continuum consisted of two end-point closed- and open-mouth prototype images of the same emotion, which were morphed together in seven steps (two endpoints and 5 morphs, in 16.6% steps, Figure 4.1), so that it appeared as though the actor was opening their mouth when the images were combined. Morphed images were created as described previously in Experiment 1 using individual morphing templates made up of manually placed control points. Morphed images were then concatenated in and exported using iMovie (iMovie 10.1.12, Apple Inc., Cupertino, California, United States). Face stimuli were presented on an LCD projector onto a screen located 45 cm in front of the subject. Face stimuli subtended 6.02 degrees visual angle vertically and 7.27 degrees horizontally*4.2.3 Voice Stimuli.* Auditory stimuli consisted of short, nonverbal affective interjections of the vowel /a:/ "ah" which were identical to those used in Experiment 2 (see Table 2). One happy and one angry vocalization was taken from each actor (1 male and 1 female), for a total of four vocal stimuli. Auditory stimuli were individually

attenuated in E-Prime 2 presentation software (Psychology Software Tools, Pittsburgh, Pennsylvania, United States) and delivered binaurally (70 dB SPL) via EAR 3a foam insert earphones (VIVOSONIC Inc., Toronto, Ontario, Canada).

4.2.4 MEG Experiment. Subjects were presented with a series of affective faces and voices while laying supine on a table while their brain signals were acquired using a MEG. During the scan, subjects were instructed to indicate if their overall impression of each trial was "happy" or "angry", with no reference to the face or voice. Each trial consisted of a 300 ms blank black screen, a 300 ms black screen with a vertically and horizontally centered white fixation cross, followed by a 1000 ms affective face-voice stimulus which was shown for 1900 ms, and a 500 ms interstimulus interval. Each stimulus contained a dynamic affective face and an emotional voice, which was either happy or angry, which resulted in the creation of two congruent (happy-happy and angry-angry) and two incongruent (happy-angry, angry-happy) stimulus conditions. Each of the four stimulus conditions was shown 150 times for a total of 600 trials. The experiment lasted 30-minutes with a two-minute break occurring halfway through the experiment, for a total duration of 32-minutes. There was a 34 ms auditory delay.

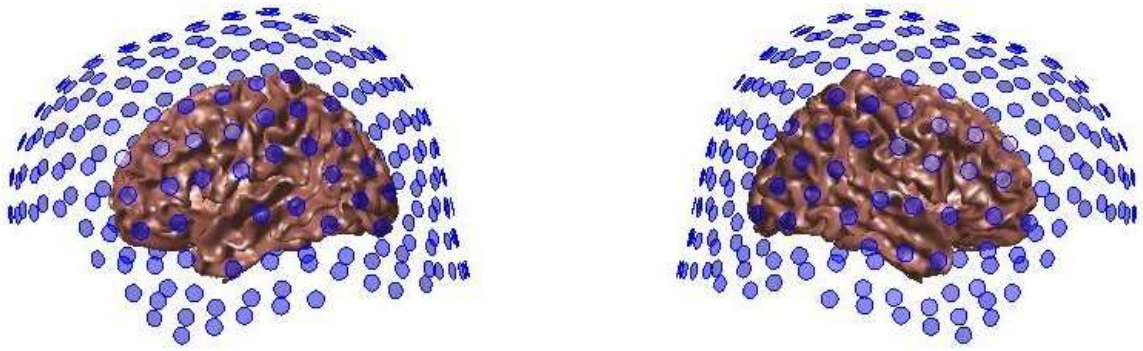

Figure 4.2: A standard head model is shown positioned within a three-dimensional rendering of the arrangement of the 248 first-order axial-gradiometers along the inner surface of the 4D Magnes magnetoencephalogram helmet, shown as gold vertices.

4.2.5 MEG Instrumentation. Data were acquired using a Magnes 3600 WH whole-head MEG instrument (4-D Neuroimaging, San Diego, California, United States). The helmet array consisted of 248 first-order axial-gradiometers (Figure 4.2). Changes in head position during the MEG scan were monitored using five head position indicator (HPI) coils, which were attached to the participant's scalp. The five coils were placed at the naison, left and right preauricular points and two non-fiducial points. Coil positions and a trace of the scalp surface were digitized using a 3D digitizer device (Polhemus, Colchester, Vermont, United States). MEG data were acquired within a 0.1-200 Hz bandwidth and sampled continuously at 508 Hz.

4.2.6 MEG Preprocessing. MEG data were pre-processed and analyzed using the Fieldtrip toolbox in Matlab (2016b, MathWorks, Inc., Natick, Massachusetts, United States). Data were bandpass filtered from 0.1-80.0 Hz, with a notch filter applied at 60 Hz to eliminate electrical powerline noise. Continuous data were segmented into 1.25 s epochs, with a 250 ms baseline (-250-0 ms) and 1000 ms post-stimulus active period. Epochs were adjusted for a 34 ms auditory delay. Eye blinks and saccades were removed using independent component analysis using the FastICA algorithm (Hyvarinen, 1999). Data were baseline corrected and epochs containing amplitudes exceeding ±3000 fT were rejected from further analysis (appendix H).

4.3.7 MEG Source Analysis. Time-frequency analysis was performed in Fieldtrip and data were decomposed into six frequency bands of interest: delta (0.1-3.5 Hz), alpha (4-7 Hz), theta (8-12 Hz), beta (13-30 Hz), gamma 1 (31-55 Hz), and gamma 2 (56-80 Hz), appendix I. Power spectra were based on a fast Fourier transformation (FFT) after application of a discrete prolate spheroidal sequences (dpss) taper. Prior to source localization, the MEG sensors were co-registered to a standard T1 structural image in MNI (SPM8, Wellcome Centre for Human Neuroimaging, United College London, London, United Kingdom). A single sphere head model was calculated and lead

fields were computed with a resolution of 1 cm. Source analysis was performed on each frequency band using a partial and canonical correlation (PCC) common filter beamformer, which calculates phase information and allows for higher specificity in post-processing of source activity. Sources were combined and then separated by condition and contrasted (i.e., ((Happy Face and Happy Voice)+(Angry Face and Angry Voice)-((Happy Face and Angry Voice)+(Angry Face and Happy Voice)) is equivalent to (HH+AA)-(HA+AH)), see appendices J and K. Condition comparisons, condition-congruency comparisons, and main effects for each frequency band were statistically compared using cluster-based nonparametric dependent samples t-tests that were cluster-corrected for multiple comparisons, with alpha set at .05. Statistically significant positive and negative sources were then interpolated and plotted onto a standard brain in MNI space, see appendix L.

4.3 Results

4.3.1 Beamformer Results. Cluster-based nonparametric statistical maps were generated from face-voice congruency pair comparisons [i.e., ((Happy Face and Happy Voice) + (Angry Face and Angry Voice)) – (Happy Face and Angry Voice) + (Angry Face and Happy Voice)) = ((HH+AA) – (HA+AH))] to localize the neural sources of increases and decreases in power observed between 0.1–80 Hz, broken down into six frequency bands of interest: delta (0.1-3.5 Hz), alpha (4-7 Hz), theta (8-12 Hz), beta (13-30 Hz), gamma 1 (31-55 Hz), and gamma 2 (56-80 Hz) across the entire duration of the stimulus.

Dependent samples t-tests set at alpha 0.05 showed that Angry Faces paired with Angry Voices exhibited significantly less activity in the upper gamma 2 band in the posterior superior temporal sulcus of the left hemisphere when compared to Happy Faces paired with Happy Voices (t = -627.65, p < 0.05), see figure 4.3a. Brain structures were identified using coordinates generated in the Automated Anatomical Labelling (AAL; Tzourio-Mazoyer, et al., 2002) atlas in FieldTrip.

A significant increase in theta band activity appeared in the left ventrolateral prefrontal cortex (t = 403.39, p = 0.01), with another area of increased theta activity appearing over the right middle right superior temporal gyrus. see figure 4.3b. While the peak cluster did appear in the brainstem those results are not presented below as MEG cannot measure subcortical activity, and this activation is most likely an artifact of MEG source localization. One positive cluster appeared in the alpha band for the (Angry Face Angry Voice) – (Happy Face Happy Voice) comparison, but this difference did not research significance (p = 0.074). No other Face-Voice congruency condition comparisons reached significance for any frequency band. All results were cluster-corrected to control for multiple comparisons. No frequency band exhibited a significant main effect. Dependent t-tests between emotional congruency and emotion were also not significant for any frequency band.

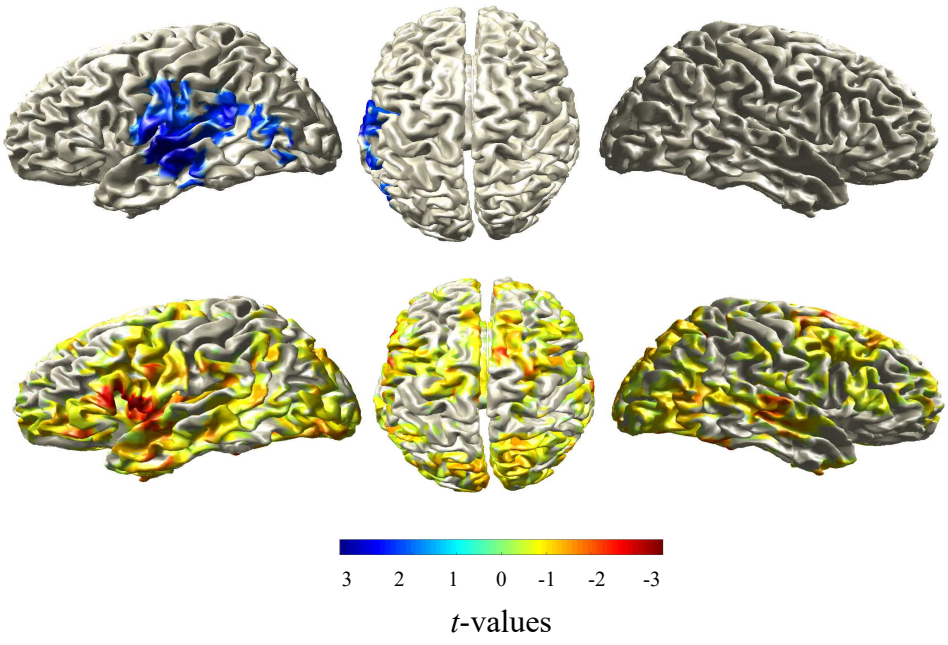

Figure 4.3: DICS beamformer source localization results for the congruent-congruent and incongruent-incongruent face-voice comparisons. Positive and negative clusters plotted across cortical surface maps for the Angry face Angry voice-Happy face Happy voice comparison within the gamma band (30-80 Hz) frequency (Top) and Angry face Happy voice-Happy face Angry voice comparison within the theta frequency band (8-12 Hz). Clusters significant at alpha = .05, cluster-corrected for multiple comparisons.

4.4 Discussion

The current study compared the neural activity underlying the integration of congruent and incongruent affective stimuli. The authors expected that the emotional congruency of the simultaneously presented face-voice pair would disrupt subjects' perception of the audiovisual stimuli and that this distortion would be evidenced by increased gamma activity in right pSTS for both the incongruent angry and happy face-voice conditions compared with the congruent face-voice pairings. This hypothesis was not supported by current findings, which only showed increased gamma band activity for the Happy Face Happy Voice (HH) over the Angry Face Angry Voice (AA) condition in the left pSTS. While significant activity did appear in the theta and gamma bands these patterns of activity were not spatially overlapping. Additionally, there were no significant differences in activity between the congruent and incongruent face voice pairs for any frequency bands. The differences that did appear came from comparisons that were within, rather than between, congruency conditions. These results suggest that emotionally congruent and incongruent stimuli may be differentially processed by spatially distinct brain areas within specific frequency bands.

This theory is partially supported by findings of supra-additivity to dynamic audiovisual stimuli in the pSTS for both congruent and incongruent emotional displays within 250 ms after stimulus presentation (Hagan et al. 2009; Hagan, Woods, Johnson, Green, & Young 2013). While these findings are not in complete agreement with those of the current study, it should be emphasized that the authors analyzed the entire stimulus window, rather than beamforming distinct periods of time during stimulus presentation. This methodological difference may have washed out temporally discrete differences between conditions, as one mismatch MEG study reported that analyzing short post-stimulus windows revealed increased theta power for mismatch conditions,

but these effects disappeared when larger time windows were analyzed (Garrido, Barnes, Kumaran, Maguire, & Dolan, 2015). The congruent conditions may have elicited activity in the pSTS as congruent audiovisual speech enhances speech comprehension (Crosse, Butler, & Lalor, 2015). Increased activity in the pSTS may represent the supra-additive response to bimodal affective inputs (Hagan et al. 2009; Hagan, Woods, Johnson, Green, & Young 2013). This sensitivity to multimodal stimuli may have been greater for the Happy Face Happy Voice condition due to the increased salience of happy faces relative to negatively valenced emotions leading to increased power in the gamma band (Calvo & Nummenmaa, 2008).

While only a subset of neuroimaging studies has directly examined the neural underpinnings of emotional congruence this study may have touched on a related aspect of emotional cognition known as emotional conflict. Emotional conflict refers to situations in which the emotional expression displayed by the face is not congruent with that expressed in the voice (Müller, Habel, Derntl, Schneider, Zilles, Turetsky, & Eickhoff, 2011). Few studies have focused on the effects of emotional conflict (Müller, Habel, Derntl, Schneider, Zilles, Turetsky, & Eickhoff, 2011), which have been associated with increased cognitive processing and longer reaction times for incongruent bimodal stimuli (de Gelder & Vroomen, 2000; Wittfoth, Schroder, Schardt, Dengler, Heinze, & Kotz, 2010). Emotional conflict may take many forms and can be studied using a variety of paradigms which examine emotional and cognitive control mechanisms (Xu, Xu, & Yang, 2016; Song, Zilverstand, Song, d'Oleire Uquillas, Wang, Xie, Cheng, & Zou, 2017). Meta-analyses examining the effect of strong emotional conflict during emotional Stroop tasks have consistently reported activity in the dorsolateral prefrontal cortex (DLPFC), inferior frontal gyrus, dorsal anterior cingulate cortex (dACC), and ventromedial prefrontal cortex (vmPFC) which has been associated with conflict detection (Xu, Xu, & Yang, 2016; Song,

Zilverstand, Song, d'Oleire Uquillas, Wang, Xie, Cheng, & Zou, 2017). Additionally, one fMRI study reported that incongruent affective face-voice stimuli were associated with increased activity in a network of cingulate-fronto-parietal areas, which appear to be involved in conflict monitoring and resolution (Müller, Habel, Derntl, Schneider, Zilles, Turetsky, & Eickhoff, 2011).

While the current study did not find activity in the vmPFC, effective connectivity analyses have shown that the vmPFC appears to drive theta band oscillations in the hippocampus to facilitate automatic mismatch detection (Garrido, Barnes, Kumaran, Maguire, & Dolan, 2015). The vmPFC has also been associated with reward and value-based decision-making (Liu, Hairston, Schrier, & Fan, 2011; Hiser & Koenigs, 2018), social conduct, and emotion processing (Tranel, Bechara, & Denburg, 2002; Hiser & Koenigs, 2018). These cognitive functions appear to be strongly right lateralized as subjects with lesions to the right vmPFC met criteria for "acquired sociopathy" (Tranel, Bechara, & Denburg, 2002). These results suggest that the vmPFC may be an essential component in emotion regulation with some suggesting that the vmPFC may be critical for the generation and regulation of negatively valenced emotions (Fullana, et al., 2016; Hiser & Koenigs, 2018). This specialization for negative emotions may indicate that Angry Faces paired with Happy Voices exhibited increased activity in the vmPFC than Happy Faces paired with Angry Voices due their negatively valenced visual content, as vision predominates perception during bimodal emotion perception (de Gelder & Vroomen, 2000; McGurk & McDonald, 1976).

Future studies should incorporate the use of functional connectivity methods to assess the potential relationships between these brain areas, which appear to be sensitive to both the integration of bimodal stimuli as well as mismatch detection. Communication between posterior sensory and frontal executive processing areas has been documented in MEG studies of cross frequency coupling, with cross frequency interactions in frontal and visual areas having been

reported in the theta and gamma bands during emotional processing (Luo, Cheng, Holroyd, Xu, Carver, & Blair, 2014). This dynamic has been equated to the differential involvement of each frequency in functionally connected processes underlying the same cognitive functions involved in affect perception (Luo, Cheng, Holroyd, Xu, Carver, & Blair, 2014). Collectively, these findings demonstrate that oscillations control a mosaic of attentional, cognitive, and perceptual processes, which support multimodal integration.

The current study had several limitations. While the visual stimuli used in this study were dynamic, they were created from two static images, which may have limited their ecological validity as they may not have accurately portrayed all of the articulatory configural changes that occur during a normal vocalization. Additionally, the voices and faces were not acquired from the same group of actors, which may further limit their ecological validity or unintentionally introduced timing delays creating asynchronous audiovisual stimuli. Asycnrhonous stimuli have been associated with increased activity in the left middle STS (Balk, Ojanen, Pekkola, Autti, Sams, & Jääskeläinen, 2010). The introduction of random or varied interstimulus intervals may have reduced an anticipatory effects (Gross, which may attenuate low frequency activity (Clementz, Barber, & Dzau, 2002). Lastly, although several studies have indicated that MEG can see deeper subcortical structures (Attel & Schwartz, 2013; Guitart-Masip, Barnes, Horner, Bauer, Dolan, & Duzel, 2013; Cornwell, Arkin, Overstreet, Carver, & Grillon, 2012), MEG is not sensitive to deep cortical structures and this may have limited its ability to image activity in deep brain structures which have been strongly associated with the processing of emotional stimuli (amygdala, fusiform face area).

REFERENCES

Adolphs, R. (2002). Neural systems for recognizing emotion. *Current Opinions in Neurobiology, 12*:169–177. PMID: 12015233

Adolphs, R., Tranel, D., Damasio, A. R. (2003). Dissociable neural systems for recognizing emotions. *Brain and Cognition, 52*:61-69

Attel, Y., Schwartz, D. (2013). Assessment of subcortical source localization using deep brain activity imaging model with minimum norm operators: a MEG study. *PLoS One, 8*(3):e59856. PMID: 23527277

Baart, M., Vroomen, J. (2018). Recalibration of vocal affect by a dynamic face. *Experimental Brain Research, 236*(7):1911-1918. PMID: 29696314

Baillet, S. (2017). Magnetoencephalography for brain electrophysiology and imaging. *Nature Neuroscience, 20*:327-339. PMID: 28230841

Beauchamp, M. S., Argall, B. D., Bodurka, J., Duyn, J. H., Martin, A. (2004). Unraveling multisensory integration: patchy organization within human STS multisensory cortex. *Nature Neuroscience*, *7*(11):1190-1192. PMID: 15475952

Calder, A. J., Young, A. W. (2005). Understanding the recognition of facial identity and facial expression. *Nature Reviews Neuroscience, 6*:641–651. PMID: 16062171

Calder, A. J., Young, A. W., Keane, J., Dean, M. (2000). Configural information in facial expression perception. *J Experimental Psychology Human Perception Performance, 26*:527–551. PMID: 10811161

Calvo, M. G., Nummenmaa, L. (2008). Detection of emotional face: silent physical features guide effective visual search. J Experimental Psychology General, 137:471–494. PMID: 18729711

Clementz, B. A., Barber, S. K., Dzau, J. R. (2002). Knowledge of stimulus repetition affects the magnitude and spatial distribution of low-frequency event-related brain potentials. *Audiology Neurootol, 7*:303–314. PMID: 12232500

Crosse, M. J., Butler, J. S., Lalor, E. C. (2015). Congruent visual speech enhances cortical entrainment to continuous auditory speech in noise-free conditions. *J Neuroscience, 35*(42):14195-14204. PMID: 26490860

Campanella, S., Belin, P. (2007). Integrating face and voice in person perception. *Trends in Cognitive Science*, 11:535–543. PMID: 17997124

Chen, Y. H., Edgar, J. C., Holroyd, T., Dammers, J., Thönneßen, H., Roberts, T. P. L., Mathiak, K. (2010). Neuromagnetic Oscillations to Emotional Faces and Prosody. *European J Neuroscience*, *31*(10):1818-27. PMID: 20584186

Cornwell, B.R., Arkin, N., Overstreet, C., Carver, F.W., Grillon, C. (2012). Distinct contributions of human hippocampal theta to spatial cognition and anxiety. *Hippocampus, 22*(9):1848-1859. PMID: 22467298

Debener, S., Herrmann, C. S., Kranczioch, C., Gembris, D., Engel, A. K. (2003). Top-down attentional processing enhances auditory evoked gamma band activity. *Neuroreport, 14*(5):683-686. PMID: 12692463

de Gelder, B., Vroomen, J. (2000). The Perception of Emotions by Ear and by Eye. Cognition and Emotion, 14(3): 289–311. doi:10.1080/026999300378824.

Fu, K. M., Foxe, J. J., Murray, M. M., Higgins, B. A., Javitt, D. C., Schroeder, C. E. (2001). Attention-dependent suppression of distracter visual input can be cross-modally cued as indexed by anticipatory parieto-occipital alpha-band oscillations. *Brain Res Cogn Brain Res, 12*(1):145-152. PMID: 11489617

Fullana, M. A., Harrison, B. J., Soriano-Mas, C., Vervliet, B., Cardoner, N., Avila-Parcet, A., et al. (2016). Neural signatures of human fear conditioning: an updated and extended meta-analysis of fMRI studies. *Molecular Psychiatry*, *21*(4):500–508. PMID: 26122585

Garrido, M. I., Barnes, G. R., Kumaran, D., Maguire, E. A., Dolan, R. J. (2015). Ventromedial prefrontal cortex drives hippocampal theta oscillations induced by mismatch computations.

Ghazanfar, A. A., Chandrasekaran, C., Logothetis, N. K. (2008). Interactions between the superior temporal sulcus and auditory cortex mediate dynamic face/voice integration in rhesus monkeys. *J Neuroscience, 28*:4457-4469. PMID: 18434524

Ghazanfar, A. A., Schroeder, C. E. (2006). Is neocortex essentially multisensory? *Trends in Cognitive Science, 10*:278-285. PMID: 16713325

Gianotti, G. (2019). The Role of the Right Hemisphere in Emotional and Behavioral Disorders of Patients With Frontotemporal Lobar Degeneration: An Updated Review. *Frontiers in Aging Neuroscience, 11*(55). PMID: 30941030

Gross, J., et al. (2013). Good practice for conducting and reporting MEG research. *Neuroimage, 65*(100):349-363. PMID: 23046981

Guitart-Masip, M., Barnes, G. R., Horner, A., Bauer, M., Dolan, R.J., Duzel, E. (2013). Synchronization of medial temporal lobe and prefrontal rhythms in human decision making. *J Neuroscience, 33*(2):442-451. PMID:23303925

Hagan, C. C., Woods, W., Johnson, S., Calder, A. J., Green, G. G. R., et al. (2009). MEG demonstrates a supra-additive response to facial and vocal emotion in the right superior temporal sulcus. *Proceedings of the National Academy of Sciences,* 106: 20010–20015. PMID: 19906999

Hagan, C. C., Woods, W., Johnson, S., Green, G. G. R., Young, A. W. (2013). Involvement of right STS in audio-visual integration for affective speech demonstrated using MEG. *PLoS One, 8*(8):e70648. PMID: 23950977

Haxby, J. V., Hoffman, E., Gobini, M. I. (2000). The distributed human neural system for face perception. *Trends in Cognitive Sciences, 4*:223-233. PMID: 10827445

Hiser, J., Koenigs, M. (2018). The multifaceted role of ventromedial prefrontal cortex in emotion, decision-making, social cognition, and psychopathology. *Biological Psychiatry, 83*(8):638-647. PMID: 29275839

Kanwisher, N., McDermott, J., Chun, M. M. (1997). The fusiform face area: a module in human extrastriate cortex specialized for face perception. *J Neuroscience*, *17*:4302–11. PMID: 9151747

Kaiser, J., Lutzenberger, W., Ackermann, H., Birbaumer, N. (2002). Dynamics of gamma-band activity induced by auditory pattern changes in humans. *Cerebral Cortex, 12*(2):212-221. PMID: 11739268

Kayser, C., Logothetis, N.K. (2007). Do early sensory cortices integrate cross- modal information? *Brain Structure & Function*, 212:121‑132. PMID: 17717687

Kreifelts, B., Ethofer, T., Grodd, W., Erb, M., Wildgruber, D. (2007). Audiovisual integration of emotional signals in voice and face: an event- related fMRI study. *Neuroimage*, *37*:1445–1456. PMID: 17659885

Leppänen, J. M., Nelson, C. (2008). Tuning the developing brain to social signals of emotion. *Nature Reviews Neuroscience, 10*(1):37-47. PMID: 19050711

Liu, X., Hairston, J., Schrier, M., Fan, J. (2011). Common and distinct networks underlying reward valence and processing stages: a meta-analysis of functional neuroimaging studies. *Neuroscience and biobehavioral reviews, 35*(5):1219-1236. PMID: 21185861

Luo, Q., Cheng, X., Holroyd, T., Xu, D., Carver, F., Blair, R. J. (2014). Theta band activity in response to emotional expressions and its relationship with gamma band activity as revealed by MEG and advanced beamformer source imaging. *Frontiers in Human Neuroscience, 7*:940. PMID: 24550804

McGurk, H., MacDonald, J. (1976). Hearing lips and seeing voices. Nature, 264(5588):746-8. PMID: 1012311.

Müller, V. I., Habel, U., Derntl, B., Schneider, F., Zilles, K., Turetsky, B. I., Eickhoff, S. B. (2011). Incongruence effects in crossmodal emotional integration. *Neuroimage, 54*(3):2257-2266. PMID: 20974266

Palva, S., Palva, J. M. (2007). New vistas for alpha-frequency band oscillations. *Trends in Neuroscience, 30*(4):150-158. PMID: 17307258

Pourtois, G., de Gelder, B., Vroomen, J., Rossion, B., Crommelinck, M. (2000). The time-course of intermodal binding between seeing and hearing affective information. *Neuroreport,11*(6):1329-1333. PMID: 10817616

Puce, A., Epling, J. A., Thompson, J. C., Carrick, O. K. (2007). Neural responses elicited to face emotion and vocalization pairings. *Neuropsychologia, 45*:93-106. PMID: 16766000

Roelfsema, P. R., Engel, A. K., König, P., Singer, W. (1997). Visuomotor integration is associated with zero time-lag synchronization among cortical areas. *Nature, 385*(6612):157-161. PMID: 8990118

Schirmer, A., Adolphs, R. (2017). Emotion Perception from Face, voice, and touch: Comparisons and convergence *Trends in Cognitive Neuroscience 21*(3):216-228. PMID:28173998Schneider, T. R., Debener, S., Oostenveld, R., Engel, A. K. (2008). Enhanced EEG gamma-band activity reflects multisensory semantic matching in visual-to-auditory object priming. *Neuroimage, 42*(3):1244-1254. PMID: 18617422

Schröger, E., Widmann, A. (1998). Speeded responses to audiovisual signal changes result from bimodal integration. *Psychophysiology*, 35:755-759. PMID: 9844437

Seltzer, B., Cola, M. G., Gutierrez, C., Massee, M., Weldon, C., Cusick, C. G. (1996). Overlapping and nonoverlapping cortical projections to cortex of the superior temporal sulcus in the rhesus monkey: double anterograde tracer studies. *J Computational Neurology, 370*(s):173-190. PMID: 8808729

Seltzer, B., Pandya, D. N. (1978). Afferent cortical connections and architectonics of the superior temporal sulcus and surrounding cortex in the rhesus monkey. *Brain Research, 149*(1):1-24. PMID: 418850

Senkowski, D., Schneider, T. R., Foxe, J. J., Engel, A. K. (2008). Crossmodal binding through neural coherence: implications for multisensory processing. *Trends in Neuroscience, 31*(8):401-409. PMID: 18602171

Song, S., Zilverstand, A., Song, H., d'Oleire Uquillas, F., Wang, Y., Xie, C., Cheng, L., Zou, Z. (2017). The influence of emotional interference on cognitive control: A meta-analysis of neuroimaging studies using the emotional Stroop task. *Scientific Reports, 7*(1):2088. PMID: 28522823

Tranel, D., Bechara, A., Denburg, N. L. (2002). Asymmetric functional role of right and left ventromedial prefrontal cortices in social conduct, decision-making, and emotional processing. *Cerebral Cortex, 38*(4):589-612. PMID: 12465670

Wittfoth, M., Schroder, C., Schardt, D.M., Dengler, R., Heinze, H.J., Kotz, S.A. (2010). On emotional conflict: interference resolution of happy and angry prosody reveals valence-specific effects. *Cerebral Cortex*, *20*:383-392. PMID: 19505993

Xu, M., Xu, G., Yang, Y. (2016). Neural systems underlying emotional and non-emotional interference processing: an ALE meta-analysis of functional neuroimaging studies. *Frontiers in Behavioral Neuroscience, 10*(220). PMCID: PMC5109402

CHAPTER 5 – GENERAL DISCUSSION

Emotion perception is the seemingly automatic integration of vocal and facial cues that together form a whole percept. While affective information can be gleaned from and identified in either modality independently (Ekman & Friesen, 1976; Schröder 2003; Belin, Fillion-Bilodeau, & Gosselin, 2008), the relative contribution and interaction of these channels is not fully understood. One of the most fundamental questions in cognitive neuroscience regards the functional and structural organization of multimodal emotion perception in the brain. While an abundant amount of research has focused on this topic, most of this work is predicated on the use of silent static face images (Johnson, 2011). These one-dimensional stimuli lack ecological validity (O'Toole, Roark, & Abdi, 2002; Jiang, Blanz, & O'Toole, 2009; Lander & Bruce, 2003) and are ineffective in accurately depicting normal social interactions (Roark, Barrett, Spence, Abdi, O'Toole, 2003), which typically involve more than one sensory modality whose activity continuously evolves over time (Schirmer & Adolphs, 2017). A similar perceptual constraint is exemplified by the transmission of vocal emotion, which unfolds over a relatively fixed time-course (Pell & Kotz, 2011) and is characterized by distinct acoustical changes in the speaker's voice (Banse & Scherer, 1996; Scherer, 2018). Sampling a single time point of a vocal utterance deprives the listener of the rich contextual information, which collectively conveys emotional meaning. These methods deprive subjects of the holistic representation of the intended emotion and inaccurately ascribe perceptual and neural processes to models of affect perception. Thus, the current work investigated the effects of visual spatial attention, stimulus modality and emotional valence, as well as, emotional congruency on differentially impacting multimodal affect perception. The present findings demonstrate that both stimulus type and emotional are central to

affect perception, and the activity associated with these components was localized to a distributed constellation of partially overlapping neural structures in the superior temporal sulcus (STS), middle superior temporal gyrus (mSTG), orbitofrontal cortex (OFC), somatosensory cortex, ventral occipitotemporal areas, and dorsolateral prefrontal cortex (DLPFC).

The effect of stimulus modality was first investigated using a two-alternative forced-choice task, which showed that the Happy Face+Voice condition and the Silent voice condition exhibited higher PSE values when compared to the Angry Face+Voice condition. The Silent voice condition exhibited a significantly higher, "happier", mean PSE value than the Happy Face+Voice condition. These results indicate that while happy voices may bias responses to be 'happier' than the Angry Face+Voice prosody conditions, the voices may not have been perceived to be as 'happy' as they were intended to be. These findings question whether the prosodic stimuli had equal arousal and intensity values and were oppositely valenced enough to equally bias multimodal stimuli in opposite directions. Interestingly, the Silent condition had the smallest just noticeable difference (JND) value when compared to the Angry and Happy prosody conditions and boasted the fastest reaction times for both the Eyes and Mouth fixation cues. These results indicate that unimodal presentation of dynamic affective stimuli may facilitate emotion recognition as the JND has acts as a measure of the level of confusion between choices, with smaller values indicating less confusion. These results partially replicate the findings of an identical study which used static emotionally ambiguous morphed face stimuli (Becker & Rokas, submittted), which showed that faces shown alone exhibited the highest JND values and fastest reaction times when compared to the bimodal face+voice conditions. Additionally, the mean PSE value for the face only condition was significantly 'happier' than the Angry or Neutral face+voice conditions, but this value was not significantly different than the Happy face+voice condition, which biased faces to be perceived

as ‘happier’ than their physical composition, indicating that emotional faces may exhibit an inherent perceptual bias for happy facial features (Calvo & Nummenmaa, 2008). Additionally, the Silent condition exhibited the fastest reaction times for both the Eyes and Mouth cue conditions, but reaction times between these fixation cues were not significant within the Silent condition. The authors interpreted these findings as indicating that judgments about ambiguous faces were facilitated through the presence of an affective voice. This discrepancy may reflect the significant difference in affect recognition between dynamic and static faces, which exhibit higher recognition rates over static faces (Lander & Bruce, 2003; Bassili, 1979; Johnson, 2011). Together with evidence that the visual channel predominates the perception of multimodal stimuli (McGurk & McDonald, 1976), these data suggest that the affective voices paired with the dynamic faces in the current study may have confused subjects, rather than facilitating response choices, as this supplementary information was both never completely congruent with the visual stimuli. This incongruency may also partially explain the lower mean PSE values for the Happy face+voice condition compared to the Silent, face only condition.

Conditions containing either a Happy or Angry prosodic voice took more processing time than silent face videos when subjects were directed to fixate on the eyes of speaking faces (Figure 2.6). Overall, reaction times for the Happy and Angry prosody conditions were not significantly different from one another for the Eyes cue condition (Figure 2.6). Conversely, subjects’ reaction times were significantly different between all three conditions for the majority of the steps across the morph continuum for the Mouth fixation cue (Figure 2.5). This effect appeared to be strongest for the Angry prosody condition as it showed more significant differences between the Mouth and Eyes cue conditions across the morph continuum (Figure 2.7b) when compared to Mouth and Eyes cues for the Happy (Figure 2.7a) and Silent (Figure 2.7c) conditions. These results indicate that

mouths and eyes may differ in their emotional saliency, with eyes selectively facilitating faster reaction times for negatively valenced emotions. Thus, some facial features may have a detection advantage which appears to be modulated by the emotional valence of a speaker's voice (Calvo & Nummenmaa, 2008). This visual saliency is particularly true for smiling mouths, which are associated with increased initial orienting and decreased detection times (Calvo & Nummenmaa, 2008). Collectively, these findings underscore the dynamic interplay of attentional, perceptual, and cognitive processes which may be differentially modulated by emotional valence and spatial cueing to different facial features.

The second experiment focused on parsing apart and localizing the sensory and perceptual processes underlying the perception of emotional faces, voices, and faces and voices paired together using independent component analysis and source localization techniques. Emotion is multifaceted and manipulation of one or more modalities can impact perceptual biases of bimodal stimuli, which can be quantified using psychophysical measures and neuroimaging techniques. The independent significance of voice (Hajcak, Weinberg, MacNamara, & Foti, 2011), face (Roisson et al., 2003; Hajcak, Weinberg, MacNamara, & Foti, 2011; Eimer & Holmes, 2007), and emotional stimulus (Cacioppo et al., 1993; Foti & Hajcak, 2008; Bernat, Bunce, & Shevrin, 2001) processing has been well studied in the EEG literature (Hajcak, Weinberg, MacNamara, & Foti, 2011). However, the neural substrates underpinning multimodal perception are poorly defined as multiple sensory and perceptual events occur in close temporal and spatial proximity in the brain (Hajcak, Weinberg, MacNamara, & Foti, 2011). Results showed that component activity was localized to a collection of brain areas including: the posterior STS (pSTS), occipitotemporal and inferior frontal areas of the right hemisphere, as well as, bilateral somatosensory areas, and fronto-parietal areas of the left hemisphere. These areas were significantly correlated with one or more

elements of the experiment (stimulus modality or emotional valence). These results underscore the multidimensional nature of emotion perception which draws upon cognitive, perceptual, and attentional processes as these components were independently localized to a diffuse constellation of brain areas. In particular, the three components localized to the right pSTS and occipitotemporal cortices most closely aligned with the authors' hypothesis that areas involved in the processing and integration of unimodal and multimodal stimuli would be correlated with unimodal (face, voice), bimodal (face+voice), and positively valenced stimuli. Two of the three components were significantly correlated with all stimulus types and emotional prosody conditions. These results were consistent with reports that the right pSTS possesses cells, which are sensitive to auditory, visual, and multimodal input (Beauchamp, Argall, Bodurka, Duyn, & Martin, 2004; Seltzer, Cola, Gutierrez, Massee, Weldon, & Cusick, 1996; Seltzer & Pandya, 1978). These findings indicate that this area appears to sensitive to emotional prosody, which complements research reporting a right lateralization for processing affective speech (Kotz, Meyer, & Paulmann, 2006; Ross & Monnot, 2008). This system exhibits a structural-functional organization homologous to propositional language areas in the left area with posterior areas being devoted to the receptive aspects of speech (comprehending, understanding) and anterior areas being associated with the expressive (articulatory) components of vocal emotion (Ross & Monnot, 2008). Thus, posterior activations may be a reflection of the task demands as subjects passively listened to and made judgments of affective voices. Similarly, occipitotemporal activity may have indicated the engagement of brain areas specialized in the detailed processing of changeable and invariant facial features (Haxby, Hoffman, & Gobbini, 2000; Pitcher, Dilks, Saxe, Triantaflyllou, & Kanwisher, 2011), which may have been crucial to making affective judgments about emotionally ambiguous visual stimuli.

Component activity was also localized to areas that were not hypothesized by the authors, which may reflect the concurrent engagement of several attentional and cognitive processes that were not directly related to the perceptual processes targeted by stimuli and task demands of the current study. Two components exhibited activity in left hemisphere areas including: the intraparietal sulcus, orbitofrontal cortex, superior frontal gyrus, and occipital lobe (Figure 3.6). These areas are interconnected and are thought to exert top-down attentional and emotional modulation on visual processing by evaluating the emotional value of incoming visual stimuli (Pessoa & Ungerleider, 2004; Vuilleumier & Driver, 2007). These components were significantly correlated with the Face Only and Face+Voice conditions, which may indicate that a top-down modulatory system may have been activated during visual processing of emotionally ambiguous stimuli as subjects were instructed to attend to and judge the emotional content of each stimulus. Additionally, multiple components exhibited unilateral or bilateral activity in somatosensory cortices. These areas have been associated with the subjective experience of emotion, which may occur as the result of local processing or connections between distributed brain regions involved in the discrimination of emotional face and voice stimuli (Kragel & LaBar, 2016; Sel, Forster, & Calvo-Merino, 2014). This connectivity may enable the somatosensory cortex to integrate affective faces and voices to create emergent internal representations of emotion, which facilitate an individual's subjective experience of emotion. Eleven of the 13 final components exhibited some activity that was localized to either unilateral or bilateral somatosensory areas. This persistent pattern of activity may reflect the continued self-reflection subjects experienced as they made affective judgments about the experimental stimuli. Variations in component activity may be attributed to the voice, face, or valence-related component that subjects' subjective experiences were based on. The behavioral results of this study may support this notion as happy and angry

prosodic voices were able to bias subjective judgments of emotion perception so that morphed faces would appear to be 'happier' or 'angrier' than their physical composition. This perceptual shift may indicate that affective voices were able to bias subjects' subjective experience of emotion and this may be evidenced by multiple spatially, and potentially functionally, overlapping components in the somatosensory cortices.

The emergence of an affective percept occurs via the instantaneous integration of an emotional facial expression with a concurrently presented affective vocalization. These channels are often complementary, conveying the same emotional message exhibiting supra-additive responses in the pSTS (Hagan, et al. 2009). The pSTS appears to be sensitive to both congruent and incongruent emotional stimuli (Hagan, et al. 2009). The current MEG results showed that Angry faces paired with Angry voices exhibited decreased activity in the gamma band (30-80 Hz) in the left pSTS when compared to the Happy face Happy voice condition. This result may be related to a timing delay between the presentation of the audio stimulus and the movement of the actor's mouth as asynchronous audiovisual speech stimuli have been shown to elicit increased activity in the left middle STS (Balk, Ojanen, Pekkola, Autti, Sams, & Jääskeläinen, 2010). Interestingly, the comparison of the two incongruent conditions voice elicited increased activity in the right middle superior temporal gyrus for the Angry face Happy voice condition over the Happy face Angry voice condition, an area which has been associated with the fine analysis of emotional prosody.

The current findings suggest that both faces and voices possess enough information to bias perception in different directions and these audiovisual inputs are integrated and mediated by higher order cognitive and attentional processes controlled by a distributed network of bilateral brain regions. Together, the EEG source localization results and behavioral findings from that

experiment indicate that the somatosensory cortex may play a crucial role in the subjective experience of emotion, which can be correlated with different elements of the experiment.

While the results of the MEG analysis were unexpected, future experiments may be able to further disentangle the effects of emotional congruency in multimodal processing by using videos of speaking actors to control for any delays between the movements of an actor's face and the presentation of the actor's voice. Future studies should employ simultaneous (EEG-fMRI) imaging methods to maximize both the spatial and temporal resolution of the experiment to better delineate the time-course and localize the neural activity associated with multimodal emotion perception. Similarly, simultaneous eye-tracking and neuroimaging experiments could provide further insights into the physical features that subjects fixate on to assess how spatial biases may influence prosodic biases when viewing dynamic faces.

Lastly, these results showed that emotion perception is closely linked to the prosody of a speaker's voice and that voices can influence emotional decisions and brain activity, but the impact of this bias may differ by the faces they are paired with as dynamic faces convey more info than static images. The point is tentatively supported by the juxtaposition of the just noticeable difference results from the first and second experiment. The first experiment showed that prosodic voices appeared to facilitate decision making for emotionally ambiguous static stimuli, but this effect was reversed when affective voices were paired with morphed dynamic stimuli. While it should be noted that these findings came from two separate experiments, it is striking that two identical experiments yielded such contrasting results. Moreover, these findings question how effective static images are in conveying authentic emotional experiences as emotional voices appear to confuse rather than facilitate emotional decisions when subjects are presented with information rich dynamic visual stimuli. This may have crucial implications for emotion

perception research in clinical populations, which has predicated itself on the use of static stimuli. In these paradigms, subjects are presented with silent static images of facial expressions made at one fixed point in time. These images deprive subjects of the essential simultaneous dynamic visual and vocal information that is necessary to make accurate judgments about another individual's emotional state. Despite this, thousands of studies have used these artificial stimuli to research emotion perception in numerous clinical populations. The results of the current study question the legitimacy of these findings and urge future research to use dynamic faces paired with emotional voices to more accurately replicate the emotional experiences that an individual encounters in the real world. Disregarding these essential components of emotion may predispose subjects to inaccurately identify emotional stimuli and these errors may be mistaken as pervasive deficits in emotion recognition, when in reality they only reflect deficits in distinguishing silent static artificial portrayals of emotion. Future studies should reassess these proposed deficits using more realistic stimuli and a freely available database including both static and dynamic images taken from the same actors should be created to facilitate this area of research. The inclusion of static and dynamic stimuli would allow for the direct comparison of the visual effect of movement on emotion perception when all other physical features and the identity of the model are kept constant.

REFERENCES

Balk, M. H., Ojanen, V., Pekkola, J., Autti, T., Sams, M., Jääskeläinen, I. P. (2010). Synchrony of audio-visual speech stimuli modulates left superior temporal sulcus. *Neuroreport, 21*(12):822-826. PMID: 20588202

Banse, R., Scherer, K. (1996). Acoustic profiles in vocal emotion expression. *J Personality and Social Psychology, 70*(3):614-636. PMID: 8851745

Bassili, J. N. (1979). Emotion recognition: the role of facial movement and the relative importance of upper and lower areas of the face. J Personality and Social Psychology, 37(11):2049-2058. PMID: 521902

Becker, K. M., Rojas, D. C. (Submitted). The role of prosody in influencing emotion perception: a near-infrared spectroscopy study.

Belin, P., Fillion-Bilodeau, S., Gosselin F. (2008). The Montreal Affective Voices: a validated set of nonverbal affect bursts for research on auditory affective processing. *Behavioral Research Methods, 40*(2):531-9. PMID: 18522064

Calvo, M. G., Nummenmaa, L. (2008). Detection of emotional face: silent physical features guide effective visual search. J Experimental Psychology General, 137:471–494. PMID: 18729711

Ekman, P., Friesen, W.V. (1976). *Pictures of Facial Affect*. Palo Alto, CA: Consulting Psychological Press.

Hajcak, G., Weinberg, A., MacNamara, A., Foti D. (2011). ERPs and the Study of Emotion. The Oxford Handbook of Event-Related Potential Components.

Haxby, J.V., Hoffman, E.A., Gobbini, M.I. (2000). The distributed human neural system for face perception. Trends Cognitive Science 4(6):223-233. PMID:10827445

Jiang, F., Blanz, V., O'Toole, A. J. (2009). Three-dimensional information in face representation revealed by identity aftereffects. *Psychological Science, 20*(3):318-325. PMID: 19207696

Johnson, A. (2011). Is dynamic face perception primary? In C. Curio, H. H. Bülthoff, & M. A. Giese (Eds.), *Dynamic faces: insights from experiments and computation* (pp. 3-13). The MIT Press.

Kessler, H., Doyen-Waldecker, C., Hofer, C., Hoffmann, H., Traue, H. C., Abler, B. (2011). Neural correlates of the perception of dynamic versus static facial expressions of emotion. *GMS Psycho-Social Medicine, 8*, 1-8. PMID: 21522486

Lander, K., Bruce, V. (2003). The role of motion in learning new faces. Visual Cognition, 10(8):897-912. DOI: https://doi.org/10.1080/13506280344000149

McGurk, H., MacDonald, J. (1976). Hearing lips and seeing voices. Nature, 264(5588):746-8. PMID: 1012311

O'Toole, A. J., Roark, D., Abdi, H. (2002). Recognition of moving faces: a psychological and neural framework. *Trends in Cognitive Sciences, 6*(6):261-266. PMID: 12039608

Pitcher, D., Dilks, D. D., Saxe, R. R., Triantaflyllou, C., & Kanwisher, N. (2011). Differential selectivity for dynamic versus static information in face-selective cortical regions. *Neuroimage 56*(4):2356-2363. PMID: 21473921

Pitcher, D., Garrido, L., Walsh, V., Duchaine, B. C. (2008). Transcranial magnetic stimulation disrupts the perception and embodiment of facial expressions. *J Neuroscience, 28*(36):8929 – 8933. PMID: 18768686

Pourtois, G., Sander, D., Andres, M., Grandjean, D., Reveret, L., Olivier, E., Vuilleumier, P. (2004). Dissociable roles of the human somatosensory and superior temporal cortices for processing social face signals. *European J Neuroscience*, *20*(12*)*:3507–3515. PMID: 15610183

Roark, D. A., Barrett, S. E., Spence, M. J., Abdi, H., O'Toole, A. J. (2003). Psychological and neural perspectives on the role of motion in face recognition. *Behav Cogn Neurosci Rev. 2*(1):15-46. PMID: 17715597

Ross, E. D., Monnot, M. (2008). Neurology of affective prosody and its functional-anatomic organization in right hemisphere. Brain and Language, 104(1):51-74. PMID: 17537499

Scherer, K. R. (2018). In Frühholz, S. & Belin, P. (Eds.), *Acoustic patterning of emotion vocalizations* (pp.. The Oxford Handbook of Voice Perception.

Schirmer, A., Adolphs, R. (2017). Emotion Perception from Face, voice, and touch: Comparisons and convergence Trends in Cognitive Neuroscience 21(3):216-228. PMID:28173998

Schröder, M. (2003). Experimental study of affect bursts. *Speech Communication,* 40:99-116. doi.org/10.1016/S0167-6393(02)00078-X

Sel, A., Forster, B., Calvo-Merino, B. (2014). The emotional homunculus: ERP evidence for independent somatosensory responses during facial emotional processing. *J Neuroscience, 34*(9):3263-3267. PMID: 24573285

APPENDIX A: ANALYSIS OF MTURKS OUTPUT MATLAB SCRIPT

```
% Extract data from MTurk csv files
% Written by Katherine M. Becker

clear

cd '/Users/katherinebecker/Documents/Dissertation/PsychophysicalData';
csv_list = dir('subject*.csv');
% Make empty matrices for table
% happy eyes
 hap_eyes_resp_1 = zeros(70,1);
 hap_eyes_resp_2 = zeros(70,1);
 hap_eyes_resp_3 = zeros(70,1);
 hap_eyes_resp_4 = zeros(70,1);
 hap_eyes_resp_5 = zeros(70,1);
 hap_eyes_resp_6 = zeros(70,1);
 hap_eyes_resp_7 = zeros(70,1);
 % break up reaction time by step
 hap_eyes_rt_1 = zeros(70,1);
 hap_eyes_rt_2 = zeros(70,1);
 hap_eyes_rt_3 = zeros(70,1);
 hap_eyes_rt_4 = zeros(70,1);
 hap_eyes_rt_5 = zeros(70,1);
 hap_eyes_rt_6 = zeros(70,1);
 hap_eyes_rt_7 = zeros(70,1);
 % angry eyes
 ang_eyes_resp_1 = zeros(70,1);
 ang_eyes_resp_2 = zeros(70,1);
 ang_eyes_resp_3 = zeros(70,1);
 ang_eyes_resp_4 = zeros(70,1);
 ang_eyes_resp_5 = zeros(70,1);
 ang_eyes_resp_6 = zeros(70,1);
 ang_eyes_resp_7 = zeros(70,1);
 % break up reaction time by step
 ang_eyes_rt_1 = zeros(70,1);
 ang_eyes_rt_2 = zeros(70,1);
 ang_eyes_rt_3 = zeros(70,1);
 ang_eyes_rt_4 = zeros(70,1);
 ang_eyes_rt_5 = zeros(70,1);
 ang_eyes_rt_6 = zeros(70,1);
 ang_eyes_rt_7 = zeros(70,1);
 % silent eyes
 silent_eyes_resp_1 = zeros(70,1);
 silent_eyes_resp_2 = zeros(70,1);
 silent_eyes_resp_3 = zeros(70,1);
 silent_eyes_resp_4 = zeros(70,1);
 silent_eyes_resp_5 = zeros(70,1);
 silent_eyes_resp_6 = zeros(70,1);
 silent_eyes_resp_7 = zeros(70,1);
 % break up reaction time by step
 silent_eyes_rt_1 = zeros(70,1);
```

```
51.  silent_eyes_rt_2 = zeros(70,1);
52.  silent_eyes_rt_3 = zeros(70,1);
53.  silent_eyes_rt_4 = zeros(70,1);
54.  silent_eyes_rt_5 = zeros(70,1);
55.  silent_eyes_rt_6 = zeros(70,1);
56.  silent_eyes_rt_7 = zeros(70,1);
57.  % happy mouth
58.  hap_mouth_resp_1 = zeros(70,1);
59.  hap_mouth_resp_2 = zeros(70,1);
60.  hap_mouth_resp_3 = zeros(70,1);
61.  hap_mouth_resp_4 = zeros(70,1);
62.  hap_mouth_resp_5 = zeros(70,1);
63.  hap_mouth_resp_6 = zeros(70,1);
64.  hap_mouth_resp_7 = zeros(70,1);
65.  % break up reaction time by step
66.  hap_mouth_rt_1 = zeros(70,1);
67.  hap_mouth_rt_2 = zeros(70,1);
68.  hap_mouth_rt_3 = zeros(70,1);
69.  hap_mouth_rt_4 = zeros(70,1);
70.  hap_mouth_rt_5 = zeros(70,1);
71.  hap_mouth_rt_6 = zeros(70,1);
72.  hap_mouth_rt_7 = zeros(70,1);
73.  % angry mouth
74.  ang_mouth_resp_1 = zeros(70,1);
75.  ang_mouth_resp_2 = zeros(70,1);
76.  ang_mouth_resp_3 = zeros(70,1);
77.  ang_mouth_resp_4 = zeros(70,1);
78.  ang_mouth_resp_5 = zeros(70,1);
79.  ang_mouth_resp_6 = zeros(70,1);
80.  ang_mouth_resp_7 = zeros(70,1);
81.  % break up reaction time by step
82.  ang_mouth_rt_1 = zeros(70,1);
83.  ang_mouth_rt_2 = zeros(70,1);
84.  ang_mouth_rt_3 = zeros(70,1);
85.  ang_mouth_rt_4 = zeros(70,1);
86.  ang_mouth_rt_5 = zeros(70,1);
87.  ang_mouth_rt_6 = zeros(70,1);
88.  ang_mouth_rt_7 = zeros(70,1);
89.  % silent mouth
90.  silent_mouth_resp_1 = zeros(70,1);
91.  silent_mouth_resp_2 = zeros(70,1);
92.  silent_mouth_resp_3 = zeros(70,1);
93.  silent_mouth_resp_4 = zeros(70,1);
94.  silent_mouth_resp_5 = zeros(70,1);
95.  silent_mouth_resp_6 = zeros(70,1);
96.  silent_mouth_resp_7 = zeros(70,1);
97.  % break up reaction time by step
98.  silent_mouth_rt_1 = zeros(70,1);
99.  silent_mouth_rt_2 = zeros(70,1);
100. silent_mouth_rt_3 = zeros(70,1);
101. silent_mouth_rt_4 = zeros(70,1);
102. silent_mouth_rt_5 = zeros(70,1);
103. silent_mouth_rt_6 = zeros(70,1);
104. silent_mouth_rt_7 = zeros(70,1);
105.
106. % Get average % happy responses and reaction times for each subject
     csv
```

```
107. for sub = 1:length(csv_list)
108.     file = readtable(csv_list(sub).name);
109.     % find & remove trials with negative reaction times & null
   responses
110.     idx_rt = find(file.subjectReactionTime<0);
111.     file(idx_rt,:) = [];
112.     % change string responses to numbers
113.
   file.subjectResponseValue(strcmpi(file.subjectResponseValue,'Digit1'))
   = {1};
114.
   file.subjectResponseValue(strcmpi(file.subjectResponseValue,'Digit2'))
   = {0};
115.
   file.subjectResponseValue(strcmpi(file.subjectResponseValue,'Inconsista
   nt Response')) = {[]};
116.     % if subjects used the number pad then...
117.
   file.subjectResponseValue(strcmpi(file.subjectResponseValue,'Numpad1'))
   = {1};
118.
   file.subjectResponseValue(strcmpi(file.subjectResponseValue,'Numpad2'))
   = {0};
119.     % remove inconsistent responses
120.     F = table2cell(file);
121.     idx = any(ismember(cellfun(@num2str,F,'un',0),''),2);
122.     file(idx,:) = [];
123.     % verbal cues to numbers
124.     file.VerbalCue(strcmpi(file.VerbalCue,'Eyes')) = {1};
125.     file.VerbalCue(strcmpi(file.VerbalCue,'Mouth')) = {2};
126.     VerbalCue = cell2mat(file.VerbalCue);
127.     BlockTrigg = [file.BlockTrigg];
128.     TrialTrigg = [file.TrialTrigg];
129.     Step = [file.Step];
130.     SubResp = cell2mat(file.subjectResponseValue);
131.     SubRT = [file.subjectReactionTime];
132.     file2 = [VerbalCue BlockTrigg TrialTrigg Step SubResp SubRT];
133.     file2 = sortrows(file2,[2,4]);
134.     % break up into conditions
135.     allBlockTrigg = file2(:,2);
136.     allStep = file2(:,4);
137.     allSubResp = file2(:,5);
138.     allSubRT = file2(:,6);
139.     M = [allBlockTrigg, allStep, allSubResp, allSubRT];
140.     hap_eyes = M(M(:,1) == 1,:);
141.     hap_mouth = M(M(:,1) == 3,:);
142.     ang_eyes = M(M(:,1) == 4,:);
143.     ang_mouth = M(M(:,1) == 9,:);
144.     silent_eyes = M(M(:,1) == 18,:);
145.     silent_mouth = M(M(:,1) == 24,:);
146.
147.     % ----------HAPPY_EYES----------%
148.     % break up into steps
149.     hap_eyes_1 = hap_eyes(hap_eyes(:,2) == 1,:);
150.     hap_eyes_2 = hap_eyes(hap_eyes(:,2) == 2,:);
151.     hap_eyes_3 = hap_eyes(hap_eyes(:,2) == 3,:);
152.     hap_eyes_4 = hap_eyes(hap_eyes(:,2) == 4,:);
```

```
153.     hap_eyes_5 = hap_eyes(hap_eyes(:,2) == 5,:);
154.     hap_eyes_6 = hap_eyes(hap_eyes(:,2) == 6,:);
155.     hap_eyes_7 = hap_eyes(hap_eyes(:,2) == 7,:);
156.     % break up responses by step & get average
157.     hap_eyes_resp_1(sub,1) = mean(hap_eyes_1(:,3));
158.     hap_eyes_resp_2(sub,1) = mean(hap_eyes_2(:,3));
159.     hap_eyes_resp_3(sub,1) = mean(hap_eyes_3(:,3));
160.     hap_eyes_resp_4(sub,1) = mean(hap_eyes_4(:,3));
161.     hap_eyes_resp_5(sub,1) = mean(hap_eyes_5(:,3));
162.     hap_eyes_resp_6(sub,1) = mean(hap_eyes_6(:,3));
163.     hap_eyes_resp_7(sub,1) = mean(hap_eyes_7(:,3));
164.     % break up reaction time by step
165.     hap_eyes_rt_1(sub,1) = mean(hap_eyes_1(:,4));
166.     hap_eyes_rt_2(sub,1) = mean(hap_eyes_2(:,4));
167.     hap_eyes_rt_3(sub,1) = mean(hap_eyes_3(:,4));
168.     hap_eyes_rt_4(sub,1) = mean(hap_eyes_4(:,4));
169.     hap_eyes_rt_5(sub,1) = mean(hap_eyes_5(:,4));
170.     hap_eyes_rt_6(sub,1) = mean(hap_eyes_6(:,4));
171.     hap_eyes_rt_7(sub,1) = mean(hap_eyes_7(:,4));
172.
173.     % ----------HAPPY_MOUTH----------%
174.     % break up into steps
175.     hap_mouth_1 = hap_mouth(hap_mouth(:,2) == 1,:);
176.     hap_mouth_2 = hap_mouth(hap_mouth(:,2) == 2,:);
177.     hap_mouth_3 = hap_mouth(hap_mouth(:,2) == 3,:);
178.     hap_mouth_4 = hap_mouth(hap_mouth(:,2) == 4,:);
179.     hap_mouth_5 = hap_mouth(hap_mouth(:,2) == 5,:);
180.     hap_mouth_6 = hap_mouth(hap_mouth(:,2) == 6,:);
181.     hap_mouth_7 = hap_mouth(hap_mouth(:,2) == 7,:);
182.     % break up responses by step & get average
183.     hap_mouth_resp_1(sub,1) = mean(hap_mouth_1(:,3));
184.     hap_mouth_resp_2(sub,1) = mean(hap_mouth_2(:,3));
185.     hap_mouth_resp_3(sub,1) = mean(hap_mouth_3(:,3));
186.     hap_mouth_resp_4(sub,1) = mean(hap_mouth_4(:,3));
187.     hap_mouth_resp_5(sub,1) = mean(hap_mouth_5(:,3));
188.     hap_mouth_resp_6(sub,1) = mean(hap_mouth_6(:,3));
189.     hap_mouth_resp_7(sub,1) = mean(hap_mouth_7(:,3));
190.     % break up reaction time by step
191.     hap_mouth_rt_1(sub,1) = mean(hap_mouth_1(:,4));
192.     hap_mouth_rt_2(sub,1) = mean(hap_mouth_2(:,4));
193.     hap_mouth_rt_3(sub,1) = mean(hap_mouth_3(:,4));
194.     hap_mouth_rt_4(sub,1) = mean(hap_mouth_4(:,4));
195.     hap_mouth_rt_5(sub,1) = mean(hap_mouth_5(:,4));
196.     hap_mouth_rt_6(sub,1) = mean(hap_mouth_6(:,4));
197.     hap_mouth_rt_7(sub,1) = mean(hap_mouth_7(:,4));
198.
199.     % ----------ANGRY_EYES----------%
200.     % break up into steps
201.     ang_eyes_1 = ang_eyes(ang_eyes(:,2) == 1,:);
202.     ang_eyes_2 = ang_eyes(ang_eyes(:,2) == 2,:);
203.     ang_eyes_3 = ang_eyes(ang_eyes(:,2) == 3,:);
204.     ang_eyes_4 = ang_eyes(ang_eyes(:,2) == 4,:);
205.     ang_eyes_5 = ang_eyes(ang_eyes(:,2) == 5,:);
206.     ang_eyes_6 = ang_eyes(ang_eyes(:,2) == 6,:);
207.     ang_eyes_7 = ang_eyes(ang_eyes(:,2) == 7,:);
208.     % break up responses by step & get average
209.     ang_eyes_resp_1(sub,1) = mean(ang_eyes_1(:,3));
```

```
    ang_eyes_resp_2(sub,1) = mean(ang_eyes_2(:,3));
    ang_eyes_resp_3(sub,1) = mean(ang_eyes_3(:,3));
    ang_eyes_resp_4(sub,1) = mean(ang_eyes_4(:,3));
    ang_eyes_resp_5(sub,1) = mean(ang_eyes_5(:,3));
    ang_eyes_resp_6(sub,1) = mean(ang_eyes_6(:,3));
    ang_eyes_resp_7(sub,1) = mean(ang_eyes_7(:,3));
    % break up reaction time by step
    ang_eyes_rt_1(sub,1) = mean(ang_eyes_1(:,4));
    ang_eyes_rt_2(sub,1) = mean(ang_eyes_2(:,4));
    ang_eyes_rt_3(sub,1) = mean(ang_eyes_3(:,4));
    ang_eyes_rt_4(sub,1) = mean(ang_eyes_4(:,4));
    ang_eyes_rt_5(sub,1) = mean(ang_eyes_5(:,4));
    ang_eyes_rt_6(sub,1) = mean(ang_eyes_6(:,4));
    ang_eyes_rt_7(sub,1) = mean(ang_eyes_7(:,4));

    % ----------ANGRY_MOUTH----------%
    % break up into steps
    ang_mouth_1 = ang_mouth(ang_mouth(:,2) == 1,:);
    ang_mouth_2 = ang_mouth(ang_mouth(:,2) == 2,:);
    ang_mouth_3 = ang_mouth(ang_mouth(:,2) == 3,:);
    ang_mouth_4 = ang_mouth(ang_mouth(:,2) == 4,:);
    ang_mouth_5 = ang_mouth(ang_mouth(:,2) == 5,:);
    ang_mouth_6 = ang_mouth(ang_mouth(:,2) == 6,:);
    ang_mouth_7 = ang_mouth(ang_mouth(:,2) == 7,:);
    % break up responses by step & get average
    ang_mouth_resp_1(sub,1) = mean(ang_mouth_1(:,3));
    ang_mouth_resp_2(sub,1) = mean(ang_mouth_2(:,3));
    ang_mouth_resp_3(sub,1) = mean(ang_mouth_3(:,3));
    ang_mouth_resp_4(sub,1) = mean(ang_mouth_4(:,3));
    ang_mouth_resp_5(sub,1) = mean(ang_mouth_5(:,3));
    ang_mouth_resp_6(sub,1) = mean(ang_mouth_6(:,3));
    ang_mouth_resp_7(sub,1) = mean(ang_mouth_7(:,3));
    % break up reaction time by step
    ang_mouth_rt_1(sub,1) = mean(ang_mouth_1(:,4));
    ang_mouth_rt_2(sub,1) = mean(ang_mouth_2(:,4));
    ang_mouth_rt_3(sub,1) = mean(ang_mouth_3(:,4));
    ang_mouth_rt_4(sub,1) = mean(ang_mouth_4(:,4));
    ang_mouth_rt_5(sub,1) = mean(ang_mouth_5(:,4));
    ang_mouth_rt_6(sub,1) = mean(ang_mouth_6(:,4));
    ang_mouth_rt_7(sub,1) = mean(ang_mouth_7(:,4));

    % ----------SILENT_EYES----------%
    % break up into steps
    silent_eyes_1 = silent_eyes(silent_eyes(:,2) == 1,:);
    silent_eyes_2 = silent_eyes(silent_eyes(:,2) == 2,:);
    silent_eyes_3 = silent_eyes(silent_eyes(:,2) == 3,:);
    silent_eyes_4 = silent_eyes(silent_eyes(:,2) == 4,:);
    silent_eyes_5 = silent_eyes(silent_eyes(:,2) == 5,:);
    silent_eyes_6 = silent_eyes(silent_eyes(:,2) == 6,:);
    silent_eyes_7 = silent_eyes(silent_eyes(:,2) == 7,:);
    % break up responses by step & get average
    silent_eyes_resp_1(sub,1) = mean(silent_eyes_1(:,3));
    silent_eyes_resp_2(sub,1) = mean(silent_eyes_2(:,3));
    silent_eyes_resp_3(sub,1) = mean(silent_eyes_3(:,3));
    silent_eyes_resp_4(sub,1) = mean(silent_eyes_4(:,3));
    silent_eyes_resp_5(sub,1) = mean(silent_eyes_5(:,3));
    silent_eyes_resp_6(sub,1) = mean(silent_eyes_6(:,3));
```

```
267.     silent_eyes_resp_7(sub,1) = mean(silent_eyes_7(:,3));
268.     % break up reaction time by step
269.     silent_eyes_rt_1(sub,1) = mean(silent_eyes_1(:,4));
270.     silent_eyes_rt_2(sub,1) = mean(silent_eyes_2(:,4));
271.     silent_eyes_rt_3(sub,1) = mean(silent_eyes_3(:,4));
272.     silent_eyes_rt_4(sub,1) = mean(silent_eyes_4(:,4));
273.     silent_eyes_rt_5(sub,1) = mean(silent_eyes_5(:,4));
274.     silent_eyes_rt_6(sub,1) = mean(silent_eyes_6(:,4));
275.     silent_eyes_rt_7(sub,1) = mean(silent_eyes_7(:,4));
276.
277.     % ----------SILENT_MOUTH----------%
278.     % break up into steps
279.     silent_mouth_1 = silent_mouth(silent_mouth(:,2) == 1,:);
280.     silent_mouth_2 = silent_mouth(silent_mouth(:,2) == 2,:);
281.     silent_mouth_3 = silent_mouth(silent_mouth(:,2) == 3,:);
282.     silent_mouth_4 = silent_mouth(silent_mouth(:,2) == 4,:);
283.     silent_mouth_5 = silent_mouth(silent_mouth(:,2) == 5,:);
284.     silent_mouth_6 = silent_mouth(silent_mouth(:,2) == 6,:);
285.     silent_mouth_7 = silent_mouth(silent_mouth(:,2) == 7,:);
286.     % break up responses by step & get average
287.     silent_mouth_resp_1(sub,1) = mean(silent_mouth_1(:,3));
288.     silent_mouth_resp_2(sub,1) = mean(silent_mouth_2(:,3));
289.     silent_mouth_resp_3(sub,1) = mean(silent_mouth_3(:,3));
290.     silent_mouth_resp_4(sub,1) = mean(silent_mouth_4(:,3));
291.     silent_mouth_resp_5(sub,1) = mean(silent_mouth_5(:,3));
292.     silent_mouth_resp_6(sub,1) = mean(silent_mouth_6(:,3));
293.     silent_mouth_resp_7(sub,1) = mean(silent_mouth_7(:,3));
294.     % break up reaction time by step
295.     silent_mouth_rt_1(sub,1) = mean(silent_mouth_1(:,4));
296.     silent_mouth_rt_2(sub,1) = mean(silent_mouth_2(:,4));
297.     silent_mouth_rt_3(sub,1) = mean(silent_mouth_3(:,4));
298.     silent_mouth_rt_4(sub,1) = mean(silent_mouth_4(:,4));
299.     silent_mouth_rt_5(sub,1) = mean(silent_mouth_5(:,4));
300.     silent_mouth_rt_6(sub,1) = mean(silent_mouth_6(:,4));
301.     silent_mouth_rt_7(sub,1) = mean(silent_mouth_7(:,4));
302. end
303. % create excel file
304. sub = [1:70]';
305. T =
   table(sub,hap_eyes_resp_7,hap_eyes_resp_6,hap_eyes_resp_5,hap_eyes_resp
   _4,hap_eyes_resp_3,hap_eyes_resp_2,hap_eyes_resp_1,hap_eyes_rt_7,hap_ey
   es_rt_6,hap_eyes_rt_5,hap_eyes_rt_4,hap_eyes_rt_3,hap_eyes_rt_2,hap_eye
   s_rt_1,hap_mouth_resp_7,hap_mouth_resp_6,hap_mouth_resp_5,hap_mouth_res
   p_4,hap_mouth_resp_3,hap_mouth_resp_2,hap_mouth_resp_1,hap_mouth_rt_7,h
   ap_mouth_rt_6,hap_mouth_rt_5,hap_mouth_rt_4,hap_mouth_rt_3,hap_mouth_rt
   _2,hap_mouth_rt_1,ang_eyes_resp_7,ang_eyes_resp_6,ang_eyes_resp_5,ang_e
   yes_resp_4,ang_eyes_resp_3,ang_eyes_resp_2,ang_eyes_resp_1,ang_eyes_rt_
   7,ang_eyes_rt_6,ang_eyes_rt_5,ang_eyes_rt_4,ang_eyes_rt_3,ang_eyes_rt_2
   ,ang_eyes_rt_1,ang_mouth_resp_7,ang_mouth_resp_6,ang_mouth_resp_5,ang_m
   outh_resp_4,ang_mouth_resp_3,ang_mouth_resp_2,ang_mouth_resp_1,ang_mouth
   h_rt_7,ang_mouth_rt_6,ang_mouth_rt_5,ang_mouth_rt_4,ang_mouth_rt_3,ang_
   mouth_rt_2,ang_mouth_rt_1,silent_eyes_resp_7,silent_eyes_resp_6,silent_
   eyes_resp_5,silent_eyes_resp_4,silent_eyes_resp_3,silent_eyes_resp_2,si
   lent_eyes_resp_1,silent_eyes_rt_7,silent_eyes_rt_6,silent_eyes_rt_5,sil
   ent_eyes_rt_4,silent_eyes_rt_3,silent_eyes_rt_2,silent_eyes_rt_1,silent
   _mouth_resp_7,silent_mouth_resp_6,silent_mouth_resp_5,silent_mouth_resp
   _4,silent_mouth_resp_3,silent_mouth_resp_2,silent_mouth_resp_1,silent_m
```

```
    outh_rt_7,silent_mouth_rt_6,silent_mouth_rt_5,silent_mouth_rt_4,silent_
    mouth_rt_3,silent_mouth_rt_2,silent_mouth_rt_1,
    'VariableNames',{'Subject','Hap_eyes_resp_7','Hap_eyes_resp_6','Hap_eye
    s_resp_5','Hap_eyes_resp_4','Hap_eyes_resp_3','Hap_eyes_resp_2','Hap_ey
    es_resp_1','Hap_eyes_rt_7','Hap_eyes_rt_6','Hap_eyes_rt_5','Hap_eyes_rt
    _4','Hap_eyes_rt_3','Hap_eyes_rt_2','Hap_eyes_rt_1','Hap_mouth_resp_7',
    'Hap_mouth_resp_6','Hap_mouth_resp_5','Hap_mouth_resp_4','Hap_mouth_res
    p_3','Hap_mouth_resp_2','Hap_mouth_resp_1','Hap_mouth_rt_7','Hap_mouth_
    rt_6','Hap_mouth_rt_5','Hap_mouth_rt_4','Hap_mouth_rt_3','Hap_mouth_rt_
    2','Hap_mouth_rt_1','Ang_eyes_resp_7','Ang_eyes_resp_6','Ang_eyes_resp_
    5','Ang_eyes_resp_4','Ang_eyes_resp_3','Ang_eyes_resp_2','Ang_eyes_resp
    _1','Ang_eyes_rt_7','Ang_eyes_rt_6','Ang_eyes_rt_5','Ang_eyes_rt_4','An
    g_eyes_rt_3','Ang_eyes_rt_2','Ang_eyes_rt_1','Ang_mouth_resp_7','Ang_mo
    uth_resp_6','Ang_mouth_resp_5','Ang_mouth_resp_4','Ang_mouth_resp_3','A
    ng_mouth_resp_2','Ang_mouth_resp_1','Ang_mouth_rt_7','Ang_mouth_rt_6','
    Ang_mouth_rt_5','Ang_mouth_rt_4','Ang_mouth_rt_3','Ang_mouth_rt_2','Ang
    _mouth_rt_1','Silent_eyes_resp_7','Silent_eyes_resp_6','Silent_eyes_res
    p_5','Silent_eyes_resp_4','Silent_eyes_resp_3','Silent_eyes_resp_2','Si
    lent_eyes_resp_1','Silent_eyes_rt_7','Silent_eyes_rt_6','Silent_eyes_rt
    _5','Silent_eyes_rt_4','Silent_eyes_rt_3','Silent_eyes_rt_2','Silent_ey
    es_rt_1','Silent_mouth_resp_7','Silent_mouth_resp_6','Silent_mouth_resp
    _5','Silent_mouth_resp_4','Silent_mouth_resp_3','Silent_mouth_resp_2','
    Silent_mouth_resp_1','Silent_mouth_rt_7','Silent_mouth_rt_6','Silent_mo
    uth_rt_5','Silent_mouth_rt_4','Silent_mouth_rt_3','Silent_mouth_rt_2','
    Silent_mouth_rt_1'});
306. writetable(T,'PsychophysicalData.xlsx');
```

APPENDIX B: FECHNER JND PSE CALCULATIONS MATLAB SCRIPT

```
% script to produce psychophysical output from 2AFC procedure. PSE and
% 25/75 thresholds are determined and a plot is made
% Based off of fechner script written by Dr. Donald C. Rojas, PhD
% Re-written by Katherine M. Becker

% NOTE: requires stats toolbox and logistic.m function
clear

cd '/Users/katherinebecker/Documents/Dissertation/PsychophysicalData'
 addpath '/Users/katherinebecker/Documents/MATLAB/stats'
 addpath '/Users/katherinebecker/Documents/MATLAB/boxplotGroup'

 id = xlsread('PsychophysicalData_NewSteps3.xlsx','A2:A71');
 age = xlsread('Demographics_Psychophysical.xlsx','B2:B71');
 gender = xlsread('Demographics_Psychophysical.xlsx','C2:C71');
 HE_data = xlsread('PsychophysicalData_NewSteps3.xlsx','B2:H71');
 HM_data = xlsread('PsychophysicalData_NewSteps3.xlsx','P2:V71');
 AE_data = xlsread('PsychophysicalData_NewSteps3.xlsx','AD2:AJ71');
 AM_data = xlsread('PsychophysicalData_NewSteps3.xlsx','AR2:AX71');
 SE_data = xlsread('PsychophysicalData_NewSteps3.xlsx','BF2:BL71');
 SM_data = xlsread('PsychophysicalData_NewSteps3.xlsx','BT2:BZ71');
 HE_rt_data = xlsread('PsychophysicalData_NewSteps3.xlsx','I2:O71');
 HM_rt_data = xlsread('PsychophysicalData_NewSteps3.xlsx','W2:AC71');
 AE_rt_data = xlsread('PsychophysicalData_NewSteps3.xlsx','AK2:AQ71');
 AM_rt_data = xlsread('PsychophysicalData_NewSteps3.xlsx','AY2:BE71');
 SE_rt_data = xlsread('PsychophysicalData_NewSteps3.xlsx','BM2:BS71');
 SM_rt_data = xlsread('PsychophysicalData_NewSteps3.xlsx','CA2:CG71');

 % matrices to fill
 PSE_HE = zeros(70,1);
 PSE_HM = zeros(70,1);
 PSE_AE = zeros(70,1);
 PSE_AM = zeros(70,1);
 PSE_SE = zeros(70,1);
 PSE_SM = zeros(70,1);
 JND_HE = zeros(70,1);
 JND_HM = zeros(70,1);
 JND_AE = zeros(70,1);
 JND_AM = zeros(70,1);
 JND_SE = zeros(70,1);
 JND_SM = zeros(70,1);
 Zp_HE = zeros(70,601);
 Zp_AE = zeros(70,601);
 Zp_SE = zeros(70,601);
 Zp_HM = zeros(70,601);
 Zp_AM = zeros(70,601);
 Zp_SM = zeros(70,601);
 Op_HE = zeros(70,601);
 Op_AE = zeros(70,601);
 Op_SE = zeros(70,601);
```

```
51.  Op_HM = zeros(70,601);
52.  Op_AM = zeros(70,601);
53.  Op_SM = zeros(70,601);
54.
55.  % defaults
56.  Np = .01; % steps for prettier figure output
57.  start = 1;
58.  stop = 7;
59.
60.  % Happy Eyes
61.  for sub = 1:length(HE_data)
62.      % define column vectors for X and Y here...
63.      Y = HE_data(sub,:)';
64.      X = [1:7];
65.
66.      % calculate the fit
67.      [B,Dev,Stat] = glmfit(X,[Y
   ones(length(X),1)],'binomial','link','logit');
68.      Z = B(1) + X * (B(2));
69.      O = logistic(Z);
70.
71.      % finer res output
72.      Xp = start:Np:stop;
73.      Zp = B(1) + Xp * (B(2));
74.      Zp_HE(sub,:) = Zp;
75.      Op = logistic(Zp);
76.      Op_HE(sub,:) = Op;
77.
78.      % PSE, JND
79.      [~,ind] = min(abs(Op - .5));
80.      PSE = Xp(ind);
81.      PSE_HE(sub,:) = PSE;
82.      [~,ind] = min(abs(Op - .25));
83.      JND25 = Xp(ind);
84.      [~,ind] = min(abs(Op - .75));
85.      JND75 = Xp(ind);
86.      JND = JND75-JND25;
87.      JND_HE(sub,:) = JND;
88.  end
89.
90.  % Happy Mouth
91.  for sub = 1:length(HM_data)
92.      % define column vectors for X and Y here...
93.      Y = HM_data(sub,:)';
94.      X = [1:7];
95.
96.      % calculate the fit
97.      [B,Dev,Stat] = glmfit(X,[Y
   ones(length(X),1)],'binomial','link','logit');
98.      Z = B(1) + X * (B(2));
99.      O = logistic(Z);
100.
101.     % finer res output
102.     Xp = start:Np:stop;
103.     Zp = B(1) + Xp * (B(2));
104.     Zp_HM(sub,:) = Zp;
105.     Op = logistic(Zp);
```

```
106.     Op_HM(sub,:) = Op;
107.
108.     % PSE, JND
109.     [~,ind] = min(abs(Op - .5));
110.     PSE = Xp(ind);
111.     PSE_HM(sub,:) = PSE;
112.     [~,ind] = min(abs(Op - .25));
113.     JND25 = Xp(ind);
114.     [~,ind] = min(abs(Op - .75));
115.     JND75 = Xp(ind);
116.     JND = JND75-JND25;
117.     JND_HM(sub,:) = JND;
118. end
119.
120. % Angry Eyes
121. for sub = 1:length(AE_data)
122.     % define column vectors for X and Y here...
123.     Y = AE_data(sub,:)';
124.     X = [1:7];
125.
126.     % calculate the fit
127.     [B,Dev,Stat] = glmfit(X,[Y
   ones(length(X),1)],'binomial','link','logit');
128.     Z = B(1) + X * (B(2));
129.     O = logistic(Z);
130.
131.     % finer res output
132.     Xp = start:Np:stop;
133.     Zp = B(1) + Xp * (B(2));
134.     Zp_AE(sub,:) = Zp;
135.     Op = logistic(Zp);
136.     Op_AE(sub,:) = Op;
137.
138.     % PSE, JND
139.     [~,ind] = min(abs(Op - .5));
140.     PSE = Xp(ind);
141.     PSE_AE(sub,:) = PSE;
142.     [~,ind] = min(abs(Op - .25));
143.     JND25 = Xp(ind);
144.     [~,ind] = min(abs(Op - .75));
145.     JND75 = Xp(ind);
146.     JND = JND75-JND25;
147.     JND_AE(sub,:) = JND;
148. end
149.
150. % Angry Mouth
151. for sub = 1:length(AM_data)
152.     % define column vectors for X and Y here...
153.     Y = AM_data(sub,:)';
154.     X = [1:7];
155.
156.     % calculate the fit
157.     [B,Dev,Stat] = glmfit(X,[Y
   ones(length(X),1)],'binomial','link','logit');
158.     Z = B(1) + X * (B(2));
159.     O = logistic(Z);
160.
```

```
161.     % finer res output
162.     Xp = start:Np:stop;
163.     Zp = B(1) + Xp * (B(2));
164.     Zp_AM(sub,:) = Zp;
165.     Op = logistic(Zp);
166.     Op_AM(sub,:) = Op;
167.
168.     % PSE, JND
169.     [~,ind] = min(abs(Op - .5));
170.     PSE = Xp(ind);
171.     PSE_AM(sub,:) = PSE;
172.     [~,ind] = min(abs(Op - .25));
173.     JND25 = Xp(ind);
174.     [~,ind] = min(abs(Op - .75));
175.     JND75 = Xp(ind);
176.     JND = JND75-JND25;
177.     JND_AM(sub,:) = JND;
178. end
179.
180. % Silent Eyes
181. for sub = 1:length(SE_data)
182.     % define column vectors for X and Y here...
183.     Y = SE_data(sub,:)';
184.     X = [1:7];
185.
186.     % calculate the fit
187.     [B,Dev,Stat] = glmfit(X,[Y
   ones(length(X),1)],'binomial','link','logit');
188.     Z = B(1) + X * (B(2));
189.     O = logistic(Z);
190.
191.     % finer res output
192.     Xp = start:Np:stop;
193.     Zp = B(1) + Xp * (B(2));
194.     Zp_SE(sub,:) = Zp;
195.     Op = logistic(Zp);
196.     Op_SE(sub,:) = Op;
197.
198.     % PSE, JND
199.     [~,ind] = min(abs(Op - .5));
200.     PSE = Xp(ind);
201.     PSE_SE(sub,:) = PSE;
202.     [~,ind] = min(abs(Op - .25));
203.     JND25 = Xp(ind);
204.     [~,ind] = min(abs(Op - .75));
205.     JND75 = Xp(ind);
206.     JND = JND75-JND25;
207.     JND_SE(sub,:) = JND;
208. end
209.
210. % Silent Mouth
211. for sub = 1:length(SM_data)
212.     % define column vectors for X and Y here...
213.     Y = SM_data(sub,:)';
214.     X = [1:7];
215.
216.     % calculate the fit
```

```
217.     [B,Dev,Stat] = glmfit(X,[Y
   ones(length(X),1)],'binomial','link','logit');
218.     Z = B(1) + X * (B(2));
219.     O = logistic(Z);
220.
221.     % finer res output
222.     Xp = start:Np:stop;
223.     Zp = B(1) + Xp * (B(2));
224.     Zp_SM(sub,:) = Zp;
225.     Op = logistic(Zp);
226.     Op_SM(sub,:) = Op;
227.
228.     % PSE, JND
229.     [~,ind] = min(abs(Op - .5));
230.     PSE = Xp(ind);
231.     PSE_SM(sub,:) = PSE;
232.     [~,ind] = min(abs(Op - .25));
233.     JND25 = Xp(ind);
234.     [~,ind] = min(abs(Op - .75));
235.     JND75 = Xp(ind);
236.     JND = JND75-JND25;
237.     JND_SM(sub,:) = JND;
238. end
239.
240. % Mean PSE and JND for each condition
241. HappyEyes_PSE = mean(PSE_HE);
242. HappyMouth_PSE = mean(PSE_HM);
243. AngryEyes_PSE = mean(PSE_AE);
244. AngryMouth_PSE = mean(PSE_AM);
245. SilentEyes_PSE = mean(PSE_SE);
246. SilentMouth_PSE = mean(PSE_SM);
247. HappyEyes_JND = mean(JND_HE);
248. HappyMouth_JND = mean(JND_HM);
249. AngryEyes_JND = mean(JND_AE);
250. AngryMouth_JND = mean(JND_AM);
251. SilentEyes_JND = mean(JND_SE);
252. SilentMouth_JND = mean(JND_SM);
253.
254. % Reaction time data
255. %happy-eyes
256. HE_rt1 = HE_rt_data(:,1);
257. HE_rt2 = HE_rt_data(:,2);
258. HE_rt3 = HE_rt_data(:,3);
259. HE_rt4 = HE_rt_data(:,4);
260. HE_rt5 = HE_rt_data(:,5);
261. HE_rt6 = HE_rt_data(:,6);
262. HE_rt7 = HE_rt_data(:,7);
263. %happy-mouth
264. HM_rt1 = HM_rt_data(:,1);
265. HM_rt2 = HM_rt_data(:,2);
266. HM_rt3 = HM_rt_data(:,3);
267. HM_rt4 = HM_rt_data(:,4);
268. HM_rt5 = HM_rt_data(:,5);
269. HM_rt6 = HM_rt_data(:,6);
270. HM_rt7 = HM_rt_data(:,7);
271. %angry-eyes
272. AE_rt1 = AE_rt_data(:,1);
```

```
AE_rt2 = AE_rt_data(:,2);
AE_rt3 = AE_rt_data(:,3);
AE_rt4 = AE_rt_data(:,4);
AE_rt5 = AE_rt_data(:,5);
AE_rt6 = AE_rt_data(:,6);
AE_rt7 = AE_rt_data(:,7);
%angry-mouth
AM_rt1 = AM_rt_data(:,1);
AM_rt2 = AM_rt_data(:,2);
AM_rt3 = AM_rt_data(:,3);
AM_rt4 = AM_rt_data(:,4);
AM_rt5 = AM_rt_data(:,5);
AM_rt6 = AM_rt_data(:,6);
AM_rt7 = AM_rt_data(:,7);
%silent-eyes
SE_rt1 = SE_rt_data(:,1);
SE_rt2 = SE_rt_data(:,2);
SE_rt3 = SE_rt_data(:,3);
SE_rt4 = SE_rt_data(:,4);
SE_rt5 = SE_rt_data(:,5);
SE_rt6 = SE_rt_data(:,6);
SE_rt7 = SE_rt_data(:,7);
%silent-mouth
SM_rt1 = mean(SM_rt_data(:,1));
SM_rt2 = mean(SM_rt_data(:,2));
SM_rt3 = mean(SM_rt_data(:,3));
SM_rt4 = mean(SM_rt_data(:,4));
SM_rt5 = mean(SM_rt_data(:,5));
SM_rt6 = mean(SM_rt_data(:,6));
SM_rt7 = mean(SM_rt_data(:,7));

% save results
T =
   table(id,age,gender,PSE_HE,PSE_HM,PSE_AE,PSE_AM,PSE_SE,PSE_SM,JND_HE,JN
   D_HM,JND_AE,JND_AM,JND_SE,JND_SM,
   'VariableNames',{'id','age','gender','HappyEyes_PSE','HappyMouth_PSE','
   AngryEyes_PSE','AngryMouth_PSE','SilentEyes_PSE','SilentMouth_PSE','Hap
   pyEyes_JND','HappyMouth_JND','AngryEyes_JND','AngryMouth_JND','SilentEy
   es_JND','SilentMouth_JND'});
writetable(T,'PSE_JND_DataValues_R4.xlsx');

T2 =
   table(id,age,gender,HE_rt1,HE_rt2,HE_rt3,HE_rt4,HE_rt5,HE_rt6,HE_rt7,HM
   _rt1,HM_rt2,HM_rt3,HM_rt4,HM_rt5,HM_rt6,HM_rt7,AE_rt1,AE_rt2,AE_rt3,AE_
   rt4,AE_rt5,AE_rt6,AE_rt7,AM_rt1,AM_rt2,AM_rt3,AM_rt4,AM_rt5,AM_rt6,AM_r
   t7,SE_rt1,SE_rt2,SE_rt3,SE_rt4,SE_rt5,SE_rt6,SE_rt7,SM_rt1,SM_rt2,SM_rt
   3,SM_rt4,SM_rt5,SM_rt6,SM_rt7,'VariableNames',{'id','age','gender','Hap
   E_rt1','HapE_rt2','HapE_rt3','HapE_rt4','HapE_rt5','HapE_rt6','HapE_rt7
   ','HapM_rt1','HapM_rt2','HapM_rt3','HapM_rt4','HapM_rt5','HapM_rt6','Ha
   pM_rt7','AngE_rt1','AngE_rt2','AngE_rt3','AngE_rt4','AngE_rt5','AngE_rt
   6','AngE_rt7','AngM_rt1','AngM_rt2','AngM_rt3','AngM_rt4','AngM_rt5','A
   ngM_rt6','AngM_rt7','SilE_rt1','SilE_rt2','SilE_rt3','SilE_rt4','SilE_r
   t5','SilE_rt6','SilE_rt7','SilM_rt1','SilM_rt2','SilM_rt3','SilM_rt4','
   SilM_rt5','SilM_rt6','SilM_rt7'});
writetable(T2,'RT_DataValues_R4.xlsx');
```

APPENDIX C: LINEAR MIXED MODELS PSE JND VALUES R SCRIPT

```
# Originally written by Dr. Donald C. Rojas, PhD, adapated by Katherine M. Becker

library(readr) # csv reading
library(nlme) # mixed effects
library(multcomp) # multiple comparisons
library(tidyr) # reformatting from wide to long
library(plyr) # for renaming variables
library(dplyr) # easy subsetting
library(reshape) # for wide to long
library(ggplot2) # fancier plotting
library(Rmisc) # some summary stuff - summarySE and multiplot
 library(ggsignif) # for indicating significance on ggplots
 library(tidyverse) # box plots
 library(gapminder) # box plots

 # read csv file
 setwd('/Users/katherinebecker/Documents/Dissertation/PsychophysicalData')
 dat <-
read_csv("/Users/katherinebecker/Documents/Dissertation/PsychophysicalData/PSE_JND_DataValues_R4.csv")

 # reformat data to long rather than wide, creating separate pselong and jndlong datasets for PSE and JND values
 pse <-
select(dat,id,age,gender,cFCzdiffA.1:cFCzdiffA.3,lFCzdiffA.1:lFCzdiffA.3)
 pse <- as.data.frame(pse)
 pse$id <- factor(pse$id)
 pse$age <- factor(pse$age)
 pse$gender <- factor(pse$gender)
 pselong <- pse %>%
   gather(key, value, -id, -age, -gender) %>%
   separate(key, into = c("FixCue","Prosody"), sep="\\.")
 colnames(pselong)[6] <- "PSE"
 pselong$Prosody<-revalue(pselong$Prosody,c("1"="Happy"))
 pselong$Prosody<-revalue(pselong$Prosody,c("2"="Angry"))
 pselong$Prosody<-revalue(pselong$Prosody,c("3"="Silent"))
 pselong$FixCue<-revalue(pselong$FixCue,c("cFCzdiffA"="Eyes"))
 pselong$FixCue<-revalue(pselong$FixCue,c("lFCzdiffA"="Mouth"))
 # descriptives PSE
 summary(pselong)

 jnd <-
select(dat,id,age,gender,cFCzdiffL.1:cFCzdiffL.3,lFCzdiffL.1:lFCzdiffL.3)
 jnd <- as.data.frame(jnd)
 jnd$id <- factor(jnd$id)
 jnd$age <- factor(jnd$age)
```

```
jnd$gender <- factor(jnd$gender)
jndlong <- jnd %>%
  gather(key, value, -id, -age, -gender) %>%
  separate(key, into = c("FixCue","Prosody"), sep="\\.")
colnames(jndlong)[6] <- "JND"
jndlong$Prosody<-revalue(jndlong$Prosody,c("1"="Happy"))
jndlong$Prosody<-revalue(jndlong$Prosody,c("2"="Angry"))
jndlong$Prosody<-revalue(jndlong$Prosody,c("3"="Silent"))
jndlong$FixCue<-revalue(jndlong$FixCue,c("cFCzdiffL"="Eyes"))
jndlong$FixCue<-revalue(jndlong$FixCue,c("lFCzdiffL"="Mouth"))
# descriptives JND
summary(jndlong)

# mixed effects - nlme package, anova call is for conventional anova table
pselong.lme1<-lme(PSE~FixCue*Prosody,
                  random=list(id=pdBlocked(list(~1, pdIdent(~Prosody-1), pdIdent(~FixCue-1)))),

correlation=corCompSymm(form=~1|id),method="ML",data=pselong,na.action = na.exclude)
      summary(pselong.lme1)
jndlong.lme1<-lme(JND~FixCue*Prosody,
                  random=list(id=pdBlocked(list(~1, pdIdent(~FixCue-1), pdIdent(~Prosody-1)))),

correlation=corCompSymm(form=~1|id),method="ML",data=jndlong,na.action = na.exclude)
      summary(jndlong.lme1)

# compute an interaction term manually for next steps
pselong$FxbyCue <- interaction(pselong$FixCue,pselong$Prosody)
jndlong$FxbyCue <- interaction(jndlong$FixCue,jndlong$Prosody)

# next models are formatted better for multiple comparisons
pselong.lme2 <- lme(PSE~FxbyCue,
                    random=list(id=pdBlocked(list(~1, pdIdent(~FixCue-1), pdIdent(~Prosody-1)))),

correlation=corCompSymm(form=~1|id),method="ML",data=pselong,na.action = na.exclude)
jndlong.lme2 <- lme(JND~FxbyCue,
                    random=list(id=pdBlocked(list(~1, pdIdent(~FixCue-1), pdIdent(~Prosody-1)))),

correlation=corCompSymm(form=~1|id),method="ML",data=jndlong,na.action = na.exclude)

# only way to get Tukey for lme/RM ANOVA
summary(glht(pselong.lme2, linfct=mcp(FxbyCue="Tukey")), test = adjusted(type = "fdr"))
summary(glht(jndlong.lme2, linfct=mcp(FxbyCue="Tukey")), test = adjusted(type = "fdr"))

# multiple comparisons with paired T (tukey is better, see above)

# summary variables for reporting
```

```
82.  sumpse <- summarySE(pselong, measurevar="PSE",
83.    groupvars=c("FixCue","Prosody"),na.rm = TRUE)
84.  sumjnd <- summarySE(jndlong, measurevar="JND",
85.    groupvars=c("FixCue","Prosody"),na.rm = TRUE)
```

APPENDIX D: LINEAR MIXED MODEL REACTION TIME R SCRIPT

```
1. # code originally written by Dr. Donald C. Rojas, modified by Katherine
   M. Becker to perform linear mixed models on the reaction time data from
   the psychophysical data acquired on MTurks for her dissertation.
2. library(readr) # csv reading
3. #library(nlme) # mixed effects
4. library(multcomp) # multiple comparisons
5. library(tidyr) # reformatting from wide to long
6. library(plyr) # for renaming variables
7. library(dplyr) # easy subsetting
8. library(reshape) # for wide to long
9. library(lme4) # alternative to lme, but no significance testing - have
   to compare models
10.  library(ggplot2) # fancier plotting
11.  library(Rmisc) # some summary stuff - summarySE and multiplot
12.  library(ggsignif) # for indicating significance on ggplots
13.
14.  # read csv file
15.  setwd('/Users/katherinebecker/Documents/Dissertation/PsychophysicalDat
   a')
16.  dat <-
   read_csv("/Users/katherinebecker/Documents/Dissertation/PsychophysicalD
   ata/RT_DataValues_R4.csv")
17.
18.  # reformat data to long rather than wide, creating a rtlong dataset
   for reaction time values
19.  rt <-
   select(dat,id,age,gender,Hap.E.1:Hap.E.7,Hap.M.1:Hap.M.7,Ang.E.1:Ang.E.
   7,Ang.M.1:Ang.M.7,Sil.E.1:Sil.E.7,Sil.M.1:Sil.M.7)
20.  rt <- as.data.frame(rt)
21.  rt$id <- factor(rt$id)
22.  rt$age <- factor(rt$age)
23.  rt$gender <- factor(rt$gender)
24.  rtlong <- rt %>%
25.    gather(key, value, -id, -age, -gender) %>%
26.    separate(key, into = c("Prosody","FixCue","Step"), sep="\\.")
27.  colnames(rtlong)[7] <- "ReactionTime"
28.  rtlong$Prosody<-revalue(rtlong$Prosody,c("Hap"="Happy"))
29.  rtlong$Prosody<-revalue(rtlong$Prosody,c("Ang"="Angry"))
30.  rtlong$Prosody<-revalue(rtlong$Prosody,c("Sil"="Silent"))
31.  rtlong$FixCue<-revalue(rtlong$FixCue,c("E"="Eyes"))
32.  rtlong$FixCue<-revalue(rtlong$FixCue,c("M"="Mouth"))
33.  rtlong$Step<-revalue(rtlong$Step,c("1"="Step1"))
34.  rtlong$Step<-revalue(rtlong$Step,c("2"="Step2"))
35.  rtlong$Step<-revalue(rtlong$Step,c("3"="Step3"))
36.  rtlong$Step<-revalue(rtlong$Step,c("4"="Step4"))
37.  rtlong$Step<-revalue(rtlong$Step,c("5"="Step5"))
38.  rtlong$Step<-revalue(rtlong$Step,c("6"="Step6"))
39.  rtlong$Step<-revalue(rtlong$Step,c("7"="Step7"))
40.
41.
```

```
42.  # mixed effects - nlme package, anova call is for conventional anova
   table
43.  rtlong.lme1<-lme(ReactionTime~FixCue*Prosody*Step,
44.                 random=list(id=pdBlocked(list(~1, pdIdent(~Prosody-1),
   pdIdent(~FixCue-1)))),
45.
   correlation=corCompSymm(form=~1|id),method="ML",data=rtlong,na.action =
   na.exclude)
46.       summary(rtlong.lme1)
47.  anova(rtlong.lme1)
48.
49.  # compute an interaction term manually for next steps
50.  rtlong$FxbyCuebyStep <-
   interaction(rtlong$FixCue,rtlong$Prosody,rtlong$Step)
51.
52.  # next models are formatted better for multiple comparisons
53.  rtlong.lme2 <- lme(ReactionTime~FxbyCuebyStep,
54.                  random=list(id=pdBlocked(list(~1, pdIdent(~FixCue-1),
   pdIdent(~Prosody-1), pdIdent(~Step-1)))),
55.
   correlation=corCompSymm(form=~1|id),method="ML",data=rtlong,na.action =
   na.exclude)
56.
57.  # only way to get Tukey for lme/RM ANOVA
58.  summary(glht(rtlong.lme2, linfct=mcp(FxbyCuebyStep="Tukey")), test =
   adjusted(type = "fdr"))
59.
60.  # summary variables for reporting
61.  sumrt <- summarySE(rtlong, measurevar="ReactionTime",
62.    groupvars=c("FixCue","Prosody","Step"),na.rm = TRUE)
```

APPENDIX E: EEG PREPROCESSING MATLAB SCRIPT

```
1. % eeglab script to preprocess prosody dataset
2. % Based on a script written by Dr. Donald C. Rojas
3. % Written by Katherine M. Becker
4.
5. clear;
6.
7. addpath('/Users/katherinebecker/Documents/MATLAB/structfind'); % need function
8. addpath('/Users/katherinebecker/Documents/MATLAB/insertrows'); % need function
9. addpath('/Users/katherinebecker/Documents/MATLAB/eeglab13_6_5b');
10. cd
    '/Users/katherinebecker/Documents/MATLAB/eeglab13_6_5b/EEG_OrigFiles_Check_lp'
    ; % main directory
11. cwd = pwd;
12.
13. art_thresh = 75; % +/- amplitude (mV) for trial rejection
14. passband = [0.1 35]; % band pass filter cutoffs (Hz)
15. notch = 60; % notch filter
16. twin = [-0.2 1.5]; % trial window (s)
17. script_report = 'script_report_preproc_final.txt';
18. master = load('masterFile_type_EEG_FILE.txt');
19.
20. % output directory
21. outpath = fullfile(cwd,'averages');
22.
23. % open a file for reporting
24. fp = fopen(fullfile(outpath,script_report),'a');
25. fprintf(fp,'File\tBad-Chans\tICA-
    rej\tdup_count\tduplicate_ind\tmissing_missingtrials\tmissingtrial_conditions\
    tBad-Trials\tTotal-Trials\n');
26.
27. % run eeglab first to set path, then close
28. eeglab;
29. close gcf;
30.
31. % find EEGLAB path for files
32. [pth,~,~] = fileparts(which('eeglab'));
33. ten_five_positions = 'plugins/dipfit2.3/standard_BESA/standard-10-5-
    cap385.elp';
34. eeg_path = fullfile(pth,ten_five_positions);
35.
36. % list of files to be processed
37. subFiles = dir('0*_AD_Cz.set');
38.
39. for nsub=1:length(subFiles)
40.       file = subFiles(nsub).name;
41.       path = char({subFiles(nsub).folder});
42.
43.       EEG = pop_loadset('filename',file,'filepath',cwd);
44.       [~,nam,ext] = fileparts(file);
```

```
45.       fprintf(fp,'%s\t',nam);
46.
47.        % events to average separately
48.        events = {EEG.event.type};
49.        events = string(events);
50.        unique_events = unique(events);
51.        counts = zeros(1,length(unique_events));
52.        for ii=1:length(unique_events)
53.            counts(ii) = length(find(ismember(events,unique_events{ii})));
54.        end
55.        [Y,I]=sort(counts);
56.
57.        % Set chanloc.type labels
58.        EEG=pop_chanedit(EEG, 'settype',{'1:37 40:41' 'EEG'});
59.        EEG=pop_chanedit(EEG, 'settype',{'38:39' 'POL'});
60.
61.        % find all the EEG type electrodes
62.         allind = find(ismember({EEG.chanlocs.type},'EEG'));
63.
64.        % put channel positions in file from standard locations
65.        EEG = pop_chanedit(EEG, 'lookup',eeg_path);
66.
67.        % find bad channels based on 3 * SD of max/min rms amplitude
68.        EEG = pop_rmbase(EEG,[],[]);
69.        rmsdata = sqrt(EEG.data(allind,:).^2);
70.        averms  = mean(rmsdata,2);
71.        grandaverms = mean(averms);
72.        stdrms = std(averms);
73.        max_ind = find(averms > grandaverms + (3*stdrms));
74.        min_ind = find(averms < grandaverms - (3*stdrms));
75.        badch_ind = unique([max_ind;min_ind]);
76.
77.        % interpolate bad channels
78.        if ~isempty(badch_ind)
79.            if find(ismember({EEG.chanlocs(badch_ind).labels},'VEOG'));
80.                % remove instead of interpolate in this case
81.                vind = find(ismember({EEG.chanlocs.labels},'HEOG'));
82.                EEG.data(vind,:)=[];
83.                EEG.chanlocs(vind)=[];
84.            else
85.                EEG = pop_interp(EEG,badch_ind,'spherical');
86.            end
87.            for chn = 1:length(badch_ind)
88.                if chn == length(badch_ind)
89.                    fprintf(fp,'%s',EEG.chanlocs(badch_ind(chn)).labels);
90.                else
91.                    fprintf(fp,'%s,',EEG.chanlocs(badch_ind(chn)).labels);
92.                end
93.            end
94.        end
95.
96.        % run ica
97.        EEG = pop_runica(EEG,'icatype','runica','chanind',allind);
98.
99.        % compare and remove top EOG components
```

```
100.        if isempty(find(ismember({EEG.chanlocs.labels},'HEOG')));
101.            heog_ind = [];
102.        else
103.            heog_ind = find(ismember({EEG.chanlocs.labels},'HEOG'));
104.        end
105.        heog = EEG.data(heog_ind,:);
106.        icdata = eeg_getdatact(EEG);
107.        icdata = (EEG.icaweights*EEG.icasphere)*icdata(EEG.icachansind,:);
108.        for ii=1:size(icdata,1)
109.            [tmp,~] = corrcoef(heog,icdata(ii,:));
110.            r(ii) = tmp(2);
111.        end
112.        [~,comp_ind1] = sort(abs(r),'descend');
113.        top_comp1 = comp_ind1(1); % need top component out of ordered
    components based on corrcoeff val
114.
115.        % now VEOG
116.        if isempty(find(ismember({EEG.chanlocs.labels},'VEOG')));
117.            veog_ind = [];
118.        else
119.            veog_ind = find(ismember({EEG.chanlocs.labels},'VEOG'));
120.        end
121.        veog = EEG.data(veog_ind,:);
122.        icdata = eeg_getdatact(EEG);
123.        icdata = (EEG.icaweights*EEG.icasphere)*icdata(EEG.icachansind,:);
124.        for ii=1:size(icdata,1)
125.            [tmp,~] = corrcoef(veog,icdata(ii,:));
126.            rr(ii) = tmp(2);
127.        end
128.        [~,comp_ind2] = sort(abs(rr),'descend');
129.        top_comp2 = comp_ind2(1);
130.
131.        % subtract top components
132.        ic_eye = [top_comp1 top_comp2];
133.        clear icdata veog* r;
134.
135.        % plot and save before subtracting
136.        M = [EEG.icawinv];
137.        [~,col] = size(M);
138.
139.        % view components
140.        pop_topoplot(EEG,0, [1:col] ,'CNT file pruned with ICA pruned with
    ICA epochs',[6 7] ,0,'electrodes','on');
141.       % savefig([nam '_ica_topoplots_pre.fig']);
142.
143.        % report ica result
144.        fprintf(fp,'\t%d', ic_eye);
145.
146.        % remove top eye component
147.        EEG = pop_subcomp(EEG,ic_eye,0);
148.
149.        % re-reference
150.        eog_ind = [find(ismember({EEG.chanlocs.labels},'HEOG'))
    find(ismember({EEG.chanlocs.labels},'VEOG'))];
151.        EEG = pop_reref(EEG, [],'exclude',eog_ind); % average is default
```

```
152.
153.        % custom notch filter out 60 Hz, avoiding potential bug in eegfilt
   with narrow passbands
154.        fn      = EEG.srate/2; % Niquist
155.        fR      = notch/fn; % ratio of notch to Niquist
156.        nW      = .1 * 6; % 6th order width
157.        n0      = [exp(sqrt(-1)*pi*fR), exp(-sqrt(-1)*pi*fR)];
158.        poles   = (1-nW)*n0;
159.        B       = double(poly(n0));
160.        A       = double(poly(poles));
161.        data    = EEG.data;
162.        for chn = 1:EEG.nbchan
163.            % non-causal filter
164.            data(chn,:) = filtfilt(B, A, double(data(chn,:)));
165.        end
166.        EEG.data = data;
167.        clear data;
168.
169.        % band pass filter EEG
170.        EEG = pop_eegfilt(EEG, passband(1), passband(2), ...
171.             [24], [0], 0, 0, 'fir1', 0);
172.
173.        % remove last row for subject025
174.        subject = nam(1:end-14);
175.        subname = str2num(subject);
176.        if subname == 25
177.            [~,col] = size([EEG.event.type]);
178.            EEG.event(col) = [];
179.        end
180.
181.        % remove duplicates
182.        [EEG,duplicate_count,duplicate_idx] = rm_duplicates(EEG);
183.        fprintf(fp,'\t%d',duplicate_count);
184.        fprintf(fp,'\t%d',duplicate_idx);
185.
186.        % extract epochs
187.        EEG = pop_epoch(EEG,{'16'  '32'  '48'  '128'  '144'  '160'  '240'},
   twin);
188.        EEG = pop_saveset(EEG,'filename',[nam '_dup.set']);
189.
190.        % remove baseline
191.        EEG = pop_rmbase( EEG, [-200    0]);
192.
193.        % check if first three trials are 160 and remove
194.        [yn_row_answer] = check_first_type_three_for_160(EEG);
195.        if yn_row_answer == 1
196.            [EEG,missingtri_ind,missingtri_con,~] =
   find_rm_missingtrials_160_final2(EEG,nam);
197.            fprintf(fp,'\t%d',missingtri_ind);
198.            fprintf(fp,'\t%d',missingtri_con);
199.        else
200.        %    [EEG] = check_first_type_miss_160(EEG,nam);
201.            [EEG,missingtri_ind,missingtri_con,~] =
   find_rm_missingtrials_final2(EEG,nam);
202.            fprintf(fp,'\t%d',missingtri_ind);
```

```
203.             fprintf(fp,'\t%d',missingtri_con);
204.         end
205.
206.         % trim out bad trials exceeding +/- 75 uV and average surrounding
   trials to restore bad trial
207.         [~,badtri] = pop_eegthresh(EEG,1,allind,-art_thresh,art_thresh,-
   0.2,1.499,0,1); % stops bad trials from being removed
208.         fprintf(fp,'\t%d',badtri);
209.         [EEG] = average_badtrials_final(EEG,badtri);
210.
211.         % total trials
212.         ttrials = [EEG.event.type];
213.         fprintf(fp,'\t%d\n',length(ttrials));
214.
215.         % relabel EEG.event.urevent and remove EOG electrodes
216.         [EEG] = relabel_eeg2(EEG);
217.         [EEG] = rm_eog2(EEG);
218.         EEG = pop_saveset(EEG,'filename',[nam '_preprocessed.set']);
219. end
220. fclose(fp);
```

APPENDIX F: EEG COMPONENT CORRELATION MATLAB SCRIPT

```
% Graphs showing correlations between each component and each
experimental
% element (emotion or stimulus type)
% Written by Katherine M. Becker

load('PROSODY_FINAL_mean_component_ica_s_all_.mat');
corrvectors=load('component_correlation_vectors.mat');
% rearrange order of fieldnames
corrvectors=struct('AN',corrvectors.AN,'HA',corrvectors.HA,'NU',corrvec
tors.NU,'FACE',corrvectors.FACE,'FV',corrvectors.FV,'VO',corrvectors.VO
);
fnames=fieldnames(corrvectors);
 npoints=1700;

 for c=1:37
     for vec=1:length(fnames)
         onsets=1:1700:length(timecourse);
         comp1=timecourse(c,:);
         for ii=1:length(onsets)
             trials(ii,:)=comp1(onsets(ii):onsets(ii)+npoints-1);
         end

         r=zeros(1,npoints);
         for ii=1:npoints

[tmpr,tmpp]=corrcoef(trials(:,ii),corrvectors.(fnames{vec}));
             r(ii)=tmpr(2);
             p(ii)=tmpp(2);
         end
         if vec==1
            r1=r;
         end
         if vec==2
            r2=r;
         end
         if vec==3
            r3=r;
         end
         if vec==4
            r4=r;
         end
         if vec==5
            r5=r;
         end
         if vec==6
            r6=r;
         end

         % FDR correction
         [FDR,~,~,~]=mafdr(p,'Method','polynomial');
```

```
47.          if vec==1
48.              FDR1=FDR;
49.          end
50.          if vec==2
51.              FDR2=FDR;
52.          end
53.          if vec==3
54.              FDR3=FDR;
55.          end
56.          if vec==4
57.              FDR4=FDR;
58.          end
59.          if vec==5
60.              FDR5=FDR;
61.          end
62.          if vec==6
63.              FDR6=FDR;
64.          end
65.
66.          % plot the results accross all subcomponents
67.          % level for color/style change
68.          lev=0.05;
69.          % points below level, find where p < .05 to highlight areas on
     plots, use FDR
70.          aboveline=(FDR<=.05);
71.          % create two copies of y
72.          bottomline=r;
73.          topline=r;
74.          % set unwanted values to get drawn to nan
75.          bottomline(aboveline)=NaN;
76.          topline(~aboveline)=NaN;
77.
     plot1=plot(1:npoints,bottomline,'k',1:npoints,topline,'r:','LineWidth',
     1,'MarkerSize',4);
78.          xlim([0 1700]);
79.          saveas(gcf,[num2str(c) '_all_corr.png']);
80.      end
81.
82.          % Emotion components
83.          % points below level
84.          aboveline1=(FDR1<=.05);
85.          aboveline2=(FDR2<=.05);
86.          aboveline3=(FDR3<=.05);
87.          % create two copies of y
88.          bottomline1=r1;
89.          topline1=r1;
90.          bottomline2=r2;
91.          topline2=r2;
92.          bottomline3=r3;
93.          topline3=r3;
94.          % set unwanted values to get drawn to nan
95.          bottomline1(aboveline1)=NaN;
96.          topline1(~aboveline1)=NaN;
97.          bottomline2(aboveline2)=NaN;
98.          topline2(~aboveline2)=NaN;
99.          bottomline3(aboveline3)=NaN;
100.         topline3(~aboveline3)=NaN;
```

```
101.
   plot1=plot(1:npoints,bottomline1,1:npoints,topline1,'*',1:npoints,botto
   mline2,1:npoints,topline2,'*',1:npoints,bottomline3,1:npoints,topline3,
   '*','LineWidth',2,'MarkerSize',4);
102.         set(plot1(1),'DisplayName','Anger','LineWidth',1,...
103.             'Color',[0.980392156862745 0.027450980392157
   0.027450980392157]);
104.
   set(plot1(2),'DisplayName','','Marker','*','LineWidth',2,'LineStyle','n
   one',...
105.             'Color',[0.980392156862745 0.027450980392157
   0.027450980392157]);
106.         set(plot1(3),'DisplayName','Happy','LineWidth',1,...
107.             'Color',[0.780392156862745 0.780392156862745
   0.780392156862745]);
108.
   set(plot1(4),'DisplayName','','Marker','*','LineWidth',2,'LineStyle','n
   one',...
109.             'Color',[0.780392156862745 0.780392156862745
   0.780392156862745]);
110.         set(plot1(5),'DisplayName','Neutral','LineWidth',1,...
111.             'Color',[0.286274509803922 0.819607843137255
   0.741176470588235]);
112.
   set(plot1(6),'DisplayName','','Marker','*','LineWidth',2,'LineStyle','n
   one',...
113.             'Color',[0.250980392156863 0.811764705882353
   0.670588235294118]);
114.         legend1=legend;
115.         set(legend1,'Location','northeast');
116.         xlim([0 1700]);
117.         saveas(gcf,[num2str(c) '_emo_corr.fig']);
118.
119.         % Condition Components
120.         % points below level
121.         aboveline4=(FDR4<=.05);
122.         aboveline5=(FDR5<=.05);
123.         aboveline6=(FDR6<=.05);
124.         % create two copies of y
125.         bottomline4=r4;
126.         topline4=r4;
127.         bottomline5=r5;
128.         topline5=r5;
129.         bottomline6=r6;
130.         topline6=r6;
131.         % set unwanted values to get drawn to nan
132.         bottomline4(aboveline4)=NaN;
133.         topline4(~aboveline4)=NaN;
134.         bottomline5(aboveline5)=NaN;
135.         topline5(~aboveline5)=NaN;
136.         bottomline6(aboveline6)=NaN;
137.         topline6(~aboveline6)=NaN;
138.
   plot1=plot(1:npoints,bottomline4,1:npoints,topline4,'r*',1:npoints,bott
   omline5,1:npoints,topline5,'b*',1:npoints,bottomline6,1:npoints,topline
   6,'k*','LineWidth',1,'MarkerSize',4);
139.         set(plot1(1),'DisplayName','Face Only',...
```

```
140.             'Color',[0.603921568627451 0.92156862745098
   0.470588235294118]);
141.
   set(plot1(2),'DisplayName','','Marker','*','LineStyle','none',...
142.             'Color',[0.603921568627451 0.92156862745098
   0.470588235294118]);
143.         set(plot1(3),'DisplayName','Face+Voice',...
144.             'Color',[0.929411764705882 0.196078431372549
   0.490196078431373]);
145.
   set(plot1(4),'DisplayName','','Marker','*','LineStyle','none',...
146.             'Color',[0.909803921568627 0.101960784313725
   0.505882352941176]);
147.         set(plot1(5),'DisplayName','Voice Only',...
148.             'Color',[0.690196078431373 0.690196078431373
   0.690196078431373]);
149.
   set(plot1(6),'DisplayName','','Marker','*','LineStyle','none',...
150.             'Color',[0.690196078431373 0.690196078431373
   0.690196078431373]);
151.         legend1=legend;
152.         set(legend1,'Location','northeast');
153.         xlim([0 1700]);
154.         saveas(gcf,[num2str(c) '_cond_corr.fig']);
155. end
156.
```

APPENDIX G: EEG COMPONENT COMPARISON TO BASELINE MATLAB SCRIPT

```
% compare component time-course to baseline for top 26 significant components
cd '/Users/katherinebecker/Documents/MATLAB'
addpath '/Users/katherinebecker/Documents/MATLAB/bonf_holm'
load('PROSODY_FINAL_mean_component_ica_s_all_.mat');

% make new component matrix
M = reshape(timecourse,[37,1700,944]);
A = mean(M,3);
top_comps = [1 5 6 7 8 9 10 12 13 15 16 18 19 20 21 22 23 25 27 28 29 30 31 35 36 37];
 A = A(top_comps,:); % select comps with sig corr
 Pvals = zeros(1,1500);
 sigtime_list = zeros(26,450);
 FW_alpha = 0.01;

 for c = 1
     baseline = A(c,1:200);
     active = A(c,201:1700);
     for time = 1:1500
         [~,p,~,~] = ttest2(baseline,active(time),'Alpha',.001);
         Pvals(1,time) = p;
     end
     [BON,~] = bonf_holm(Pvals,(FW_alpha/length(active)));
     % points below level, find where p < .01 to highlight areas on plots,
     % use Bonferroni
     aboveline = (BON <= (FW_alpha/length(active)));
     % create two copies of y
     bottomline = A(c,201:1700);
     topline = A(c,201:1700);
     % set unwanted values to get drawn to nan
     bottomline(aboveline) = NaN;
     topline(~aboveline) = NaN;
     figure
     plot(1:1500,topline,'r:','LineWidth',4,'MarkerSize',4);
     hold on
     plot(1:1500,bottomline,'k','LineWidth',1,'MarkerSize',4)
     xlim([0 1500]);
     saveas(gcf,[num2str(top_comps(c)) '_compare2baseline.png']);
     BON_sub = BON(101:600);
     X = find(BON_sub <= (FW_alpha/length(active)));
     ind = X+101;
     sigtime_list(c,1:length(X)) = ind;
     miss_ind = setxor(ind,101:600); % if you want to see which ind are missing
 end

```

```
45.  % find final list of all significant components w/ activity btwn 151-
   600 ms
46.  sigtime_comps = [top_comps' sigtime_list];
47.  nonsig_list = zeros(25,1);
48.  for s = 1:length(top_comps)
49.      if isempty(find(sigtime_list(s,2:end)>0) == 0) == 1
50.         nonsig_list(s,:) = s
51.      end
52.  end
53.  nonsig_list(nonsig_list==0) = [];
54.  sigtime_comps(nonsig_list,:) = [];
55.  sigtimes_comp_list = sigtime_comps(:,1);
```

APPENDIX H: MEG PREPROCESSING MATLAB SCRIPT

```
% clean data and do fft analysis in sensor space on EMOP MEG data
% Used in FieldTrip version: 20171231.zip
% Originally written by Dr. Donald C. Rojas, PhD
% Adapted by Katherine M. Becker

clear all;

% default settings to edit
ft_defaults;
 chans_all_selection = {'all', '-A139', '-A156',...
     '-A141', '-A195', '-A229'}; % chans deleted
 ampthresh = 3; % threshold in +/- SD for bad channels - was 2
 nbadchanthresh = 25;
 singletrialthresh =  3000/1e15; % +/- artifact threshold in fT
 bpcutoffs = [0.1 80]; % band pass filter
 interactive = 0;
 layoutfile = '4D248.lay';
 datafile = 'c,rfhp0.1Hz,clean';
 qa_suffix = 'qa.jpg';
 [ftver,ftdir] = ft_version;
 fttemplatedir = fullfile(ftdir,'template');
 subsinfile = 0;

 ftdir = '/Users/katherinebecker/Documents/MATLAB/fieldtrip-master';

 % select directories
 cwd             = spm_select(1,'dir','Select root directory for
studies',...
                   '',pwd);
 cd(cwd);
 if ~subsinfile
     pth_subjdirs    = spm_select([1,Inf],'dir',...
         'Select subject directories to process','',pwd);
 else % select subjects from a file
     pthfile = spm_select(1,'mat','Select a subjects file to process');
     load(pthfile);
 end
 nsub = size(pth_subjdirs,1);
 fprintf('The following %d subject(s) will be examined:\n',nsub);
 disp(pth_subjdirs);
 save(fullfile(cwd,['emop_meg_EMOP_preproc_script_' date
'.mat']),'pth_subjdirs','ftver');

 % load artifact weight file for spatial correlation of ica components
 load(fullfile(cwd,'megtools-master/templates/artweights.mat')); % in
megtools

 % load channel neighbors from file
 load(fullfile(ftdir,'template/neighbours','bti248grad_neighb.mat'));

```

```
% main loop
for sub=1:nsub
    % change working directory
    cd(strtrim(pth_subjdirs(sub,1:end)));
    [~, nam, ~] = fileparts(pwd);
    outfile = [nam '_ft.mat'];
    list=dir('**/*.*');
    cd(list(10).folder);

    % get subject id from path
    tmp            = deblank(pth_subjdirs(sub,:));
    [~, meg_id, ~] = fileparts(tmp);
    fprintf('\nWorking on %s\n', meg_id);

    % read continuous data for bad channel identification
    cfg = [];
    cfg.channel = chans_all_selection;
    cfg.continuous = 'yes';
    cfg.demean = 'yes';
    cfg.bpfilter = 'yes';
    cfg.bpfreq = bpcutoffs;
    cfg.bporder = 4;
    cfg.dataset = datafile;
    cfg.dftfreq = [60 120 180];
    cfg.trialdef.prestim = .25;
    cfg.trialdef.poststim  = 1;
    cfg.trialdef.eventtype = 'TRIGGER';
    cfg.trialdef.eventvalue = [2 4 6 8];
    cfg = ft_definetrial(cfg);
    trl = cfg.trl; % use later
    % preprocessing
    ft_bad = ft_preprocessing(cfg);

    % identify bad channels
    cfg = [];
%    cfg.toilim = [.25 1];
    cfg.offset = .034;
    ft_bad  = ft_redefinetrial(cfg, ft_bad);

    badfft = findbadfft(ft_bad,neighbours);
    cfg = [];
    cfg.channel = ['all';badfft];
    ft_bad = ft_preprocessing(cfg,ft_bad);
    badamp = findbadamp(ft_bad,ampthresh);
    cfg.channel = ['all';badamp];
    cfg.dftfreq = [60,120,180]; % added
    ft_bad = ft_preprocessing(cfg,ft_bad);
    badchans = sort([badfft;badamp]);
    fprintf('%d bad channels:\n',length(badchans));
    for ii=1:length(badchans)
        fprintf('%s\t',char(badchans{ii}));
    end
    fprintf('\n');
    goodmeg = find(ft_chantype(ft_bad.label,'meg'));
    goodchans = ft_bad.label(goodmeg);
    if length(badchans) > nbadchanthresh
        fp = fopen(['Error_' meg_id '.txt'],'w');
```

```
105.         fprintf(fp,'Possibly too many bad channels!');
106.         fclose(fp);
107.         save(outfile,'ft_bad','goodchans','badchans');
108.         continue; % skip to next subject
109.     end
110.
111.     % order weights appropriately for correlation in case channels are
112.     % ordered differently from subject to subject from the artifact
    template
113.     megindeleted = find(ft_chantype(ft_bad.label,'meg'));
114.     labelsindeleted = ft_bad.label(megindeleted);
115.     wasdeleted = [];
116.     for ii=1:length(meglabels)
117.         tmp = find(ismember(labelsindeleted,meglabels{ii}));
118.         if isempty(tmp)
119.             wasdeleted = [wasdeleted ii];
120.         end
121.     end
122.     nW = W;
123.     nW(:,wasdeleted) = [];
124.
125.     % define 1.25-sec trials in continuous data for jump artifacts
126.     cfg = [];
127.     cfg.channel = chans_all_selection;
128.     cfg.dataset = datafile;
129.     cfg.trialdef.prestim = .25;
130.     cfg.trialdef.poststim  = 1;
131.     cfg.trialdef.eventtype = 'TRIGGER';
132.     cfg.trialdef.eventvalue = [2 4 6 8];
133.     cfg = ft_definetrial(cfg);
134.
135.     % reject jump trials
136.     cfg.artfctdef.channel = goodchans; % use good chans for artifact
    detection
137.     cfg.artfctdef.reject = 'complete';
138.     [cfg,ar] = ft_artifact_jump(cfg);
139.     cfg = ft_rejectartifact(cfg);
140.
141.     % read data and filter without artifact trials
142.     cfg.demean = 'yes';
143.     cfg.bpfilter = 'yes';
144.     cfg.bpfreq = bpcutoffs;
145.     cfg.bpfiltord = 4;
146.     cfg.channel = [goodchans; 'EKG'];
147.     ft_orig  = ft_preprocessing(cfg);
148.
149.     % view data
150.     if interactive
151.         cfg = [];
152.         cfg.continuous = 'no';
153.         cfg.channel = 'MEG';
154.         cfg.viewmode = 'vertical';
155.         ft_databrowser(cfg,ft_orig);
156.     end
157.
158.     % for convenient correlations after ica, concatenate trials into
    continuous single trial
```

```
159.     trial = [];
160.     time = [];
161.     for ii=1:length(ft_orig.trial)
162.         trialtmp = ft_orig.trial{ii};
163.         timetmp = ft_orig.time{ii};
164.         trial = [trial trialtmp];
165.         time = [time timetmp];
166.     end
167.     ft_tmp = ft_orig;
168.     ft_tmp.trial = {trial};
169.     ft_tmp.time = {time};
170.
171.     % downsample for ica
172.     cfg = [];
173.     cfg.resamplefs = 150;
174.     cfg.detrend    = 'no';
175.     ft_ds          = ft_resampledata(cfg, ft_tmp);
176.
177.     % do ica
178.     cfg = [];
179.     cfg.method = 'runica';
180.     cfg.channel = 'MEG';
181.     cfg.runica.pca = 50;
182.     comp = ft_componentanalysis(cfg,ft_ds);
183.
184.     % identify eye artifact components by temporal correlation, using
    rms of sensitive channels
185.     % for eog signal to correlate with components
186.     clear r p;
187.     heog_ind =
    find(ismember(ft_ds.label,{'A176','A228','A177','A123','A89','A90'}));
188.     heog = sqrt(mean(ft_ds.trial{1}(heog_ind,:).^2));
189.     heog_ic = [];
190.     for ii=1:size(comp.label,1)
191.         rmscomp = sqrt(comp.trial{1}(ii,:).^2);
192.         [tmpr,tmpp] = corrcoef(heog,rmscomp);
193.         r(ii) = tmpr(2);
194.         p(ii) = tmpp(2);
195.         heog_ic = [heog_ic find(r > .35)];
196.     end
197.     heog_ic = unique(heog_ic);
198.
199.     % find the ekg indices, if ekg channel exists, by correlation with
    EKG
200.     % channel
201.     ekg_ind = find(ismember(ft_tmp.label,'EKG'));
202.     if ~isempty(ekg_ind)
203.         ekg = ft_ds.trial{1}(ekg_ind,:);
204.         for ii=1:size(comp.label,1)
205.             rmscomp = comp.trial{1}(ii,:);
206.             [tmpr,tmpp] = corrcoef(ekg,rmscomp);
207.             r(ii) = tmpr(2);
208.             p(ii) = tmpp(2);
209.         end
210.     end
211.     ekg_ic = find(r > .35);
212.
```

```
    % idenfity artifacts based on topographic, or spatial correlation
    topo_ic = [];
    max_corr = [];
    min_pval = [];
    for ii=1:size(nW,1)
        topo = nW(ii,:); % topo = topo - mean(topo);
        for jj=1:length(comp.label)
            normcomp = comp.topo(:,jj)'; % normalize component amplitudes
            maxc=max(normcomp);
            minc=min(normcomp);
            normcomp = (normcomp - minc).*((1- -1)/(maxc - minc)) - 1.0;
            [tmpr,tmpp] = corrcoef(topo,normcomp);
            r(ii,jj) = tmpr(2);
            p(ii,jj) = tmpp(2);
        end
        [val,ind] = max(abs(r(ii,:)));
        topo_ic = [topo_ic ind];
        max_corr = [max_corr val];
        pval = p(ii,ind);
        min_pval = [min_pval pval];
    end
    topo_ic = unique(topo_ic);
    max_corr = unique(max_corr);
    badtopo = find(min_pval>1e3); % components that aren't good enough to use by p-val
    badtopo = [badtopo find(max_corr<.5)]; % components that aren't good enough to use by correlation
    topo_ic = setxor(badtopo,topo_ic);

    % plot ica noise components
    ic_to_remove = unique([heog_ic ekg_ic topo_ic]);
    if ~isempty(ic_to_remove)
        h = figure('color','w');
        pos = get(h,'position');
        set(h,'position',[pos(1) pos(2) 768 768]);
        cfg           = [];
        cfg.component = ic_to_remove;
        cfg.layout    = layoutfile;
        cfg.comment   = 'no';
        cfg.marker = 'on';
        ft_topoplotIC(cfg, comp);
        print(h, '-djpeg', [meg_id '_ica_' qa_suffix]); close(h);
    end

    % remove eye and ekg artifacts, if present
    if ~isempty(ic_to_remove)
        % decompose the original data as it was prior to downsampling to 150Hz
        cfg           = [];
        cfg.unmixing  = comp.unmixing;
        cfg.topolabel = comp.topolabel;
        comp_orig     = ft_componentanalysis(cfg, ft_tmp);

        % the original data can now be reconstructed, excluding those components
```

```
264.         cfg           = [];
265.         cfg.component = ic_to_remove;
266.         ft_clean      = ft_rejectcomponent(cfg, comp_orig,ft_tmp);
267.     else
268.         ft_clean      = ft_tmp;
269.     end
270.
271.     % reform 1.25-sec trials with 0.0 s overlap from clean data
272.     cfg = [];
273.     cfg.length = 1.25; % 2
274.     cfg.overlap = 0.0; % 0.5
275. %    cfg.trl = ft_orig.cfg.trl;
276.     ft_clean = ft_redefinetrial(cfg,ft_clean);
277.
278.     % one more pass to threshold remaining artifact trials
279.     cfg = [];
280. %    cfg.trl = [ft_clean.sampleinfo
   zeros(length(ft_clean.sampleinfo),1)]; % could I just change this to
   trials - Do I want zeros?
281.     cfg.trl = [ft_clean.sampleinfo ft_orig.cfg.trl(:,3:4)];
282.     cfg.continuous = 'no';
283.     cfg.artfctdef.threshold.channel = 'MEG';
284.     cfg.artfctdef.threshold.max = singletrialthresh;
285.     cfg.artfctdef.threshold.min = -singletrialthresh;
286.     cfg.artfctdef.reject = 'complete';
287.     [cfg, artifacts] = ft_artifact_threshold(cfg,ft_clean);
288.     ft_clean.trialinfo = [cfg.trl zeros(size(cfg.trl,1),1)];
289.     try
290.         ft_clean = ft_rejectartifact(cfg,ft_clean);
291.     catch
292.         fp = fopen(['Error_' meg_id '.txt'],'w');
293.         fprintf(fp,'Possibly no good trials left after artifact
   rejection!');
294.         fclose(fp);
295.
   save(outfile,'ft_clean','comp','heog_ic','ekg_ic','topo_ic','goodchans'
   ,'badchans');
296.         clear r p ekg_ic heog_ic ic_to_remove;
297.         continue; % skip to next subject
298.     end
299.     ntrials = length(ft_clean.trial);
300.     if ntrials < 100
301.         fp = fopen(['Error_' meg_id '.txt'],'w');
302.         fprintf(fp,'Only %d good trials left after artifact
   rejection!',ntrials);
303.         fclose(fp);
304.
   save(outfile,'ft_clean','comp','heog_ic','ekg_ic','topo_ic','ic_to_remo
   ve','goodchans','badchans');
305.         clear r p ekg_ic heog_ic ic_to_remove;
306.         continue; % skip to next subject
307.     end
308.
309.     % plot headshape and COH result
310.     sens = ft_clean.grad;
311.     sens = rmfield(sens,'balance'); % this field causes problems with
   ft_sens_plot
```

```
312.     hs = ft_read_headshape('hs_file');
313.     h = figure('color','w');
314.     subplot(2,2,1);
315.     ft_plot_headshape(hs); hold on;
316.     ft_plot_sens(sens,'chantype','meg'); view(0,0); % left
317.     subplot(2,2,2);
318.     ft_plot_headshape(hs); hold on;
319.     ft_plot_sens(sens,'chantype','meg'); view(180,0); % right
320.     subplot(2,2,3);
321.     ft_plot_headshape(hs); hold on;
322.     ft_plot_sens(sens,'chantype','meg'); view(0,90); % top
323.     subplot(2,2,4);
324.     ft_plot_headshape(hs); hold on;
325.     ft_plot_sens(sens,'chantype','meg'); view(45,0); % right
326.     print(h, '-djpeg', [meg_id '_coh_' qa_suffix]);
327.     close(h);
328.
329.     % save results
330. save(outfile,'ft_clean','comp','heog_ic','ekg_ic','goodchans','badchan
   s'); % need to change trials
331.
332.     % clean up a bit before next dataset
333.     clear r p ekg_ic heog_ic ic_to_remove data comp ft_orig ft_clean
   ft_bad;
334.
335. end % end main loop
```

APPENDIX I: MEG SPECTRAL PROCESSING MATLAB SCRIPT

```
% script frequency analysis across emotion MEG dataset
% Used with FieldTrip Version: 20171231.zip
% Originally written by Dr. Donald C. Rojas, PhD
% Modified by Katherine M. Becker

% clear workspace
clear;

% default settings
 ft_defaults;
 megsuffix   = '_ft.mat';
 outsuffix   = '_spec.mat';
 spmdir      = spm('dir');
 [~,ftdir]   = ft_version;
 fttemplatedir = fullfile(ftdir,'template');
 qa_suffix   = 'qa.jpg';
 subsinfile  = 0;

 % spectral defaults
 bandnames = {'alpha','beta','theta','delta','gamma1','gamma2'};
 bandlimits = [ 8  12;
               13  30;
                4   7;
              0.1 3.5;
               31  55;
               56  80];

 % select directories
 cwd             = spm_select(1,'dir','Select root directory for
studies',...
                   '',pwd);
 cd(cwd);
 fidtemplatedir = fullfile(cwd,'templates');
 if ~subsinfile
     pth_subjdirs    = spm_select([1,Inf],'dir',...
         'Select subject directories to process','',pwd);
 else
     pthfile = spm_select(1,'mat','Select a subjects file to process');
     load(pthfile);
 end
 nsub = size(pth_subjdirs,1);
 fprintf('The following %d subject(s) will be examined:\n',nsub);
 disp(pth_subjdirs);

 % loop throuh subjects
 for sub=1:nsub
     tic;
     % change working directory
     cd(deblank(pth_subjdirs(sub,1:end)));

```

```
50.      % get subject id from path
51.      tmp              = deblank(pth_subjdirs(sub,:));
52.      [pth, meg_id, ext] = fileparts(tmp);
53.      fprintf('\nWorking on %s\n', meg_id);
54.      list=dir('**/*.*');
55.      cd(list(10).folder);
56.
57.      % if file has error, skip this subject
58.      err_files = dir('Error*');
59.      if ~isempty(err_files)
60.          continue;
61.      end
62.
63.      % load preprocessed data
64.      megfile = [meg_id megsuffix];
65.      load(megfile,'ft_clean','goodchans');
66.
67.      % overall power spectra
68.      cfg              = [];
69.      cfg.output       = 'pow';
70.      cfg.method       = 'mtmfft';
71.      cfg.taper        = 'dpss';
72.      cfg.pad          = 'nextpow2';
73.      cfg.foilim       = [0.1 80];  % was [1 50]
74.      cfg.tapsmofrq    = 1;
75.      cfg.keeptrials   = 'yes';
76.      datapow          = ft_freqanalysis(cfg, ft_clean);
77.
78.      % get indices of high/low power from median split
79.      for ii = 1:length(bandnames)
80.          mfreq =  round(mean(bandlimits(ii,:)));
81.          ind = nearest(datapow.freq,mfreq);
82.          tmp = datapow.powspctrm(:,:,ind); % do mean power?
83.          chanind = find(mean(tmp,1) == max(mean(tmp,1)));
84.          eval([bandnames{ii} 'low =
   find(tmp(:,chanind)<=median(tmp(:,chanind)))']);
85.          eval([bandnames{ii} 'high =
   find(tmp(:,chanind)>=median(tmp(:,chanind)))']);
86.      end
87.
88.      % complex Fourier spectra for cross spectral density
89.      % start with delta
90.      cfg            = [];
91.      cfg.method     = 'mtmfft';
92.      cfg.output     = 'fourier';
93.      cfg.keeptrials = 'yes';
94.      cfg.pad        = 'nextpow2';
95.      cfg.tapsmofrq  = 1.75;
96.      cfg.foi        = 2.25;
97.      cfg.trials     = 'all';
98.      delta_all      = ft_freqanalysis(cfg, ft_clean);
99.      cfg.trials     = deltalow;
100.     delta_low      = ft_freqanalysis(cfg, ft_clean);
101.     cfg.trials     = deltahigh;
102.     delta_high     = ft_freqanalysis(cfg, ft_clean);
103.     % alpha - do two ways, one using high/low split
104.     cfg.tapsmofrq  = 2;
```

```
105.     cfg.foi         = 10;
106.     cfg.trials      = 'all';
107.     alpha_all       = ft_freqanalysis(cfg, ft_clean);
108.     cfg.trials      = alphalow;
109.     alpha_low       = ft_freqanalysis(cfg, ft_clean);
110.     cfg.trials      = alphahigh;
111.     alpha_high      = ft_freqanalysis(cfg, ft_clean);
112.     % theta
113.     cfg.tapsmofrq   = 2;
114.     cfg.foi         = 6;
115.     cfg.trials      = 'all';
116.     theta_all       = ft_freqanalysis(cfg, ft_clean);
117.     cfg.trials      = thetalow;
118.     theta_low       = ft_freqanalysis(cfg, ft_clean);
119.     cfg.trials      = thetahigh;
120.     theta_high      = ft_freqanalysis(cfg, ft_clean);
121.     % beta
122.     cfg.tapsmofrq   = 8;
123.     cfg.foi         = 21.5;
124.     cfg.trials      = 'all';
125.     beta_all        = ft_freqanalysis(cfg, ft_clean);
126.     cfg.trials      = betalow;
127.     beta_low        = ft_freqanalysis(cfg, ft_clean);
128.     cfg.trials      = betahigh;
129.     beta_high       = ft_freqanalysis(cfg, ft_clean);
130.     % gamma1
131.     cfg.tapsmofrq   = 10;
132.     cfg.foi         = 40;
133.     cfg.trials      = 'all';
134.     gamma1_all      = ft_freqanalysis(cfg, ft_clean);
135.     cfg.trials      = gamma1low;
136.     gamma1_low      = ft_freqanalysis(cfg, ft_clean);
137.     cfg.trials      = gamma1high;
138.     gamma1_high     = ft_freqanalysis(cfg, ft_clean);
139.     % gamma2
140.     cfg.tapsmofrq   = 12;
141.     cfg.foi         = 68;
142.     cfg.trials      = 'all';
143.     gamma2_all      = ft_freqanalysis(cfg, ft_clean);
144.     cfg.trials      = gamma2low;
145.     gamma2_low      = ft_freqanalysis(cfg, ft_clean);
146.     cfg.trials      = gamma2high;
147.     gamma2_high     = ft_freqanalysis(cfg, ft_clean);
148.
149.     % plot results
150.     h = figure('color','w');
151.     pos = get(h,'position');
152.     set(h,'position',[pos(1) pos(2) 256 256]);
153.     megchans = find(ft_chantype(datapow.label,'meg'));
154.     avgpow = mean(squeeze(mean(datapow.powspctrm(:,megchans,:),1)));
155.     plot(datapow.freq,avgpow,'b','linewidth',1.5);
156.     title('Mean channel power'); xlabel('Freq'); ylabel('Power');
157.     print(h, '-djpeg', [meg_id '_pow_' qa_suffix]); close(h);
158.
159.     % save results
160.     save([meg_id
   outsuffix],'datapow','alpha_all','alpha_low','alpha_high',...
```

```
161.         'beta_all','beta_low','beta_high','theta_all',...
162.
   'theta_low','theta_high','delta_all','delta_low','delta_high',...
163.
   'gamma1_all','gamma1_low','gamma1_high','gamma2_all','gamma2_low','gamm
   a2_high');
164.
165.     % report time
166.     tlapse = toc; esttime = tlapse * (nsub - sub);
167.     fprintf('Time elapsed: %.2f s...Est. time remaining: %.2f
   s\n',tlapse, esttime);
168. end
169.
```

APPENDIX J: MEG COMMON FILTER MATLAB SCRIPT

```
% beamformer common filter script for emotion MEG data
% Used in FieldTrip Version: 20171231.zip
% Based off of an example script written by Dr. Donald C. Rojas, PhD
% Modified by Katherine M. Becker

% --- CONDITIONS --- %
% HH = 2
% AA = 4
% AH = 6
 % HA = 8

 clear;
 ft_defaults;

 % directories
 ftdir = '/Users/katherinebecker/Documents/MATLAB/fieldtrip-master'
 fttemplatedir = fullfile(ftdir,'template');
 fidtemplatedir = '/Users/katherinebecker/Documents/MATLAB/fieldtrip-
master/MEG scripts/templates';
 fftsuffix = '_ft.mat';
 subsinfile  = 0;

 % load source and head model info, make sure units same
 load(fullfile(fttemplatedir,'headmodel','standard_singleshell.mat'));
 vol = ft_convert_units(vol,'mm');
 load(fullfile(fttemplatedir,'sourcemodel','standard_sourcemodel3d8mm.m
at'));
 sourcemodel = ft_convert_units(sourcemodel,'mm');

 % read template coregistration information
 load(fullfile(fidtemplatedir,'ch2_fiducials.xfm'), '-mat');

 % select directories
 cwd             = spm_select(1,'dir','Select root directory for
studies',...
                   '',pwd);
 cd(cwd);
 fidtemplatedir = fullfile(cwd,'megtools-master');
 if ~subsinfile
     pth_subjdirs    = spm_select([1,Inf],'dir',...
         'Select subject directories to process','',pwd);
 else
     pthfile = spm_select(1,'mat','Select a subjects file to process');
     load(pthfile);
 end
 nsub = size(pth_subjdirs,1);
 fprintf('The following %d subject(s) will be examined:\n',nsub);
 disp(pth_subjdirs);

 for sub=1:nsub
```

```
48.
49.      % change working directory
50.      cd(deblank(pth_subjdirs(sub,1:end)));
51.
52.      % get subject id from path
53.      tmp            = deblank(pth_subjdirs(sub,:));
54.      [pth, id, ext] = fileparts(tmp);
55.      fprintf('\nWorking on %s\n', id);
56.      list=dir('**/*.*');
57.      cd(list(10).folder);
58.
59.      % load spectral data
60.      fftfile = [id fftsuffix];
61.      load(fftfile,'ft_clean');
62.
63.      % coregister the MEG sensors and headshape to the MNI template
64.      sensors = ft_clean.grad;
65.      hshape  = ft_read_headshape('hs_file');
66.      sensors = ft_convert_units(sensors,'mm');
67.      hshape  = ft_convert_units(hshape,'mm');
68.      megfids = hshape.fid.pos(1:3,:);
69.      mrifids = [transform.mri.nas;transform.mri.lpa;transform.mri.rpa];
70.      sform   = spm_eeg_inv_rigidreg(mrifids',megfids');
71.      sensors = ft_transform_sens(sform,sensors);
72.      hshape  = ft_transform_headshape(sform,hshape);
73.
74.      % compute leadfields
75.      cfg             = [];
76.      cfg.grid        = sourcemodel;
77.      cfg.headmodel   = vol;
78.      cfg.channel     = {'MEG'};
79.      cfg.grad        = sensors;
80.      cfg.reducerank  = 2;
81.      grid            = ft_prepare_leadfield(cfg);
82.
83.      % trials
84.      [HH,~] = find(ft_clean.trialinfo(:,4)==2);
85.      [HA,~] = find(ft_clean.trialinfo(:,4)==8);
86.      [AA,~] = find(ft_clean.trialinfo(:,4)==4);
87.      [AH,~] = find(ft_clean.trialinfo(:,4)==6);
88.
89.      % --- DELTA --- %
90.      % spectral analysis
91.      cfg = [];
92.      cfg.channel      = {'MEG'};
93.      cfg.method       = 'mtmfft';
94.      cfg.taper        = 'dpss';
95.      cfg.output       = 'powandcsd';
96.      cfg.keeptrials   = 'no';
97.      cfg.foi          = 2.25;
98.      cfg.tapsmofrq    = 1.75;
99.      delta_all         = ft_freqanalysis(cfg, ft_clean);
100.
101.     cfg.trials = HH;
102.     delta_HH = ft_freqanalysis(cfg, ft_clean);
103.     cfg.trials = HA;
104.     delta_HA = ft_freqanalysis(cfg, ft_clean);
```

```
105.     cfg.trials = AA;
106.     delta_AA = ft_freqanalysis(cfg, ft_clean);
107.     cfg.trials = AH;
108.     delta_AH = ft_freqanalysis(cfg, ft_clean);
109.
110.     % source analysis
111.     cfg                 = [];
112.     cfg.frequency       = delta_all.freq;
113.     cfg.headmodel       = vol;
114.     cfg.grid            = grid;
115.     cfg.keeptrials      = 'yes';
116.     cfg.method          = 'dics';
117.     cfg.dics.keepfilter = 'yes';
118.     cfg.dics.projectnoise = 'yes';
119.     cfg.dics.lambda     = '5%';
120.     cfg.channel         = 'MEG';
121.     cfg.trials          = 'all';
122.     delta_source         = ft_sourceanalysis(cfg, delta_all);
123.
124.     % common filter application to individual trials
125.     cfg              = [];
126.     cfg.channel      = {'MEG'};
127.     cfg.method       = 'dics';
128.     cfg.frequency    = delta_all.freq;
129.     cfg.grid         = grid;
130.     cfg.sourcemodel.filter  = delta_source.avg.filter;
131.     cfg.headmodel    = vol;
132.     cfg.senstype     ='MEG';
133.     delta_source_HH  = ft_sourceanalysis(cfg, delta_HH);
134.     delta_source_HA  = ft_sourceanalysis(cfg, delta_HA);
135.     delta_source_AA  = ft_sourceanalysis(cfg, delta_AA);
136.     delta_source_AH  = ft_sourceanalysis(cfg, delta_AH);
137.
138.     % --- THETA --- %
139.     % spectral analysis
140.     cfg = [];
141.     cfg.channel      = {'MEG'};
142.     cfg.method       = 'mtmfft';
143.     cfg.taper        = 'dpss';
144.     cfg.output       = 'powandcsd';
145.     cfg.keeptrials   = 'no';
146.     cfg.foi          = 6;
147.     cfg.tapsmofrq    = 2;
148.     theta_all        = ft_freqanalysis(cfg, ft_clean);
149.
150.     % spectrum for trials
151.     cfg.trials = HH;
152.     theta_HH = ft_freqanalysis(cfg, ft_clean);
153.     cfg.trials = HA;
154.     theta_HA = ft_freqanalysis(cfg, ft_clean);
155.     cfg.trials = AA;
156.     theta_AA = ft_freqanalysis(cfg, ft_clean);
157.     cfg.trials = AH;
158.     theta_AH = ft_freqanalysis(cfg, ft_clean);
159.
160.     % source analysis for theta
161.     cfg                 = [];
```

```
    cfg.frequency       = theta_all.freq;
    cfg.headmodel       = vol;
    cfg.grid            = grid;
    cfg.keeptrials      = 'yes';
    cfg.method          = 'dics';
    cfg.dics.keepfilter = 'yes';
    cfg.dics.projectnoise = 'yes';
    cfg.dics.lambda     = '5%';
    cfg.channel         = 'MEG';
    cfg.trials          = 'all';
    theta_source        = ft_sourceanalysis(cfg, theta_all);

    % common filter application to individual trials
    cfg              = [];
    cfg.channel      = {'MEG'};
    cfg.method       = 'dics';
    cfg.frequency    = theta_all.freq;
    cfg.grid         = grid;
    cfg.sourcemodel.filter  = theta_source.avg.filter;
    cfg.headmodel    = vol;
    cfg.senstype     ='MEG';
    theta_source_HH  = ft_sourceanalysis(cfg, theta_HH);
    theta_source_HA  = ft_sourceanalysis(cfg, theta_HA);
    theta_source_AA  = ft_sourceanalysis(cfg, theta_AA);
    theta_source_AH  = ft_sourceanalysis(cfg, theta_AH);

    % --- ALPHA --- %
    % spectral analysis
    cfg = [];
    cfg.channel      = {'MEG'};
    cfg.method       = 'mtmfft';
    cfg.taper        = 'dpss';
    cfg.output       = 'powandcsd';
    cfg.keeptrials   = 'no';
    cfg.foi          = 10;
    cfg.tapsmofrq    = 2;
    alpha_all        = ft_freqanalysis(cfg, ft_clean);

    % spectrum for trials
    cfg.trials = HH;
    alpha_HH = ft_freqanalysis(cfg, ft_clean);
    cfg.trials = HA;
    alpha_HA = ft_freqanalysis(cfg, ft_clean);
    cfg.trials = AA;
    alpha_AA = ft_freqanalysis(cfg, ft_clean);
    cfg.trials = AH;
    alpha_AH = ft_freqanalysis(cfg, ft_clean);

    % source analysis for alpha
    cfg                 = [];
    cfg.frequency       = alpha_all.freq;
    cfg.headmodel       = vol;
    cfg.grid            = grid;
    cfg.keeptrials      = 'yes';
    cfg.method          = 'dics';
    cfg.dics.keepfilter = 'yes';
    cfg.dics.projectnoise = 'yes';
```

```
219.     cfg.dics.lambda     = '5%';
220.     cfg.channel         = 'MEG';
221.     cfg.trials          = 'all';
222.     alpha_source        = ft_sourceanalysis(cfg, alpha_all);
223.
224.     % common filter application to individual trials
225.     cfg                 = [];
226.     cfg.channel         = {'MEG'};
227.     cfg.method          = 'dics';
228.     cfg.frequency       = alpha_all.freq;
229.     cfg.grid            = grid;
230.     cfg.sourcemodel.filter  = alpha_source.avg.filter;
231.     cfg.headmodel       = vol;
232.     cfg.senstype        ='MEG';
233.     alpha_source_HH     = ft_sourceanalysis(cfg, alpha_HH);
234.     alpha_source_HA     = ft_sourceanalysis(cfg, alpha_HA);
235.     alpha_source_AA     = ft_sourceanalysis(cfg, alpha_AA);
236.     alpha_source_AH     = ft_sourceanalysis(cfg, alpha_AH);
237.
238.     % --- BETA --- %
239.     % spectral analysis
240.     cfg = [];
241.     cfg.channel         = {'MEG'};
242.     cfg.method          = 'mtmfft';
243.     cfg.taper           = 'dpss';
244.     cfg.output          = 'powandcsd';
245.     cfg.keeptrials      = 'no';
246.     cfg.foi             = 21;
247.     cfg.tapsmofrq       = 8;
248.     beta_all            = ft_freqanalysis(cfg, ft_clean);
249.
250.     cfg.trials = HH;
251.     beta_HH = ft_freqanalysis(cfg, ft_clean);
252.     cfg.trials = HA;
253.     beta_HA = ft_freqanalysis(cfg, ft_clean);
254.     cfg.trials = AA;
255.     beta_AA = ft_freqanalysis(cfg, ft_clean);
256.     cfg.trials = AH;
257.     beta_AH = ft_freqanalysis(cfg, ft_clean);
258.
259.     % source analysis
260.     cfg                 = [];
261.     cfg.frequency       = beta_all.freq;
262.     cfg.headmodel       = vol;
263.     cfg.grid            = grid;
264.     cfg.keeptrials      = 'yes';
265.     cfg.method          = 'dics';
266.     cfg.dics.keepfilter = 'yes';
267.     cfg.dics.projectnoise = 'yes';
268.     cfg.dics.lambda     = '5%';
269.     cfg.channel         = 'MEG';
270.     cfg.trials          = 'all';
271.     beta_source         = ft_sourceanalysis(cfg, beta_all);
272.
273.     % common filter application to individual trials
274.     cfg                 = [];
275.     cfg.channel         = {'MEG'};
```

```
276.     cfg.method       = 'dics';
277.     cfg.frequency    = beta_all.freq;
278.     cfg.grid         = grid;
279.     cfg.sourcemodel.filter  = beta_source.avg.filter;
280.     cfg.headmodel    = vol;
281.     cfg.senstype     ='MEG';
282.     beta_source_HH  = ft_sourceanalysis(cfg, beta_HH);
283.     beta_source_HA  = ft_sourceanalysis(cfg, beta_HA);
284.     beta_source_AA  = ft_sourceanalysis(cfg, beta_AA);
285.     beta_source_AH  = ft_sourceanalysis(cfg, beta_AH);
286.
287.     % --- GAMMA 1 --- %
288.     % spectral analysis
289.     cfg = [];
290.     cfg.channel      = {'MEG'};
291.     cfg.method       = 'mtmfft';
292.     cfg.taper        = 'dpss';
293.     cfg.output       = 'powandcsd';
294.     cfg.keeptrials   = 'no';
295.     cfg.foi          = 40;
296.     cfg.tapsmofrq    = 10;
297.     gamma1_all       = ft_freqanalysis(cfg, ft_clean);
298.
299.     % spectrum for trials
300.     cfg.trials = HH;
301.     gamma1_HH = ft_freqanalysis(cfg, ft_clean);
302.     cfg.trials = HA;
303.     gamma1_HA = ft_freqanalysis(cfg, ft_clean);
304.     cfg.trials = AA;
305.     gamma1_AA = ft_freqanalysis(cfg, ft_clean);
306.     cfg.trials = AH;
307.     gamma1_AH = ft_freqanalysis(cfg, ft_clean);
308.
309.     % source analysis for gamma1
310.     cfg                 = [];
311.     cfg.frequency       = gamma1_all.freq;
312.     cfg.headmodel       = vol;
313.     cfg.grid            = grid;
314.     cfg.keeptrials      = 'yes';
315.     cfg.method          = 'dics';
316.     cfg.dics.keepfilter = 'yes';
317.     cfg.dics.projectnoise = 'yes';
318.     cfg.dics.lambda     = '5%';
319.     cfg.channel         = 'MEG';
320.     cfg.trials          = 'all';
321.     gamma1_source       = ft_sourceanalysis(cfg, gamma1_all);
322.
323.     % common filter application to individual trials
324.     cfg              = [];
325.     cfg.channel      = {'MEG'};
326.     cfg.method       = 'dics';
327.     cfg.frequency    = gamma1_all.freq;
328.     cfg.grid         = grid;
329.     cfg.sourcemodel.filter  = gamma1_source.avg.filter;
330.     cfg.headmodel    = vol;
331.     cfg.senstype     ='MEG';
332.     gamma1_source_HH  = ft_sourceanalysis(cfg, gamma1_HH);
```

```
333.     gamma1_source_HA  = ft_sourceanalysis(cfg, gamma1_HA);
334.     gamma1_source_AA  = ft_sourceanalysis(cfg, gamma1_AA);
335.     gamma1_source_AH  = ft_sourceanalysis(cfg, gamma1_AH);
336.
337.     % --- GAMMA 2 --- %
338.     % spectral analysis
339.     cfg = [];
340.     cfg.channel      = {'MEG'};
341.     cfg.method       = 'mtmfft';
342.     cfg.taper        = 'dpss';
343.     cfg.output       = 'powandcsd';
344.     cfg.keeptrials   = 'no';
345.     cfg.foi          = 68;
346.     cfg.tapsmofrq    = 12;
347.     gamma2_all       = ft_freqanalysis(cfg, ft_clean);
348.
349.     % spectrum for trials
350.     cfg.trials = HH;
351.     gamma2_HH = ft_freqanalysis(cfg, ft_clean);
352.     cfg.trials = HA;
353.     gamma2_HA = ft_freqanalysis(cfg, ft_clean);
354.     cfg.trials = AA;
355.     gamma2_AA = ft_freqanalysis(cfg, ft_clean);
356.     cfg.trials = AH;
357.     gamma2_AH = ft_freqanalysis(cfg, ft_clean);
358.
359.     % source analysis for gamma2
360.     cfg                 = [];
361.     cfg.frequency       = gamma2_all.freq;
362.     cfg.headmodel       = vol;
363.     cfg.grid            = grid;
364.     cfg.keeptrials      = 'yes';
365.     cfg.method          = 'dics';
366.     cfg.dics.keepfilter = 'yes';
367.     cfg.dics.projectnoise = 'yes';
368.     cfg.dics.lambda     = '5%';
369.     cfg.channel         = 'MEG';
370.     cfg.trials          = 'all';
371.     gamma2_source       = ft_sourceanalysis(cfg, gamma2_all);
372.
373.     % common filter application to individual trials
374.     cfg              = [];
375.     cfg.channel      = {'MEG'};
376.     cfg.method       = 'dics';
377.     cfg.frequency    = gamma2_all.freq;
378.     cfg.grid         = grid;
379.     cfg.sourcemodel.filter  = gamma2_source.avg.filter;
380.     cfg.headmodel    = vol;
381.     cfg.senstype     ='MEG';
382.     gamma2_source_HH  = ft_sourceanalysis(cfg, gamma2_HH);
383.     gamma2_source_HA  = ft_sourceanalysis(cfg, gamma2_HA);
384.     gamma2_source_AA  = ft_sourceanalysis(cfg, gamma2_AA);
385.     gamma2_source_AH  = ft_sourceanalysis(cfg, gamma2_AH);
386. end
387.
```

APPENDIX K: MEG SOURCE AVERAGING MATLAB SCRIPT

```
% script to gather sources of same condition to do group comparisons
% Used in FieldTrip Version: 20171231.zip
% Written by Katherine M. Becker

clear;
ft_defaults;

% GET ROOT DIRECTORY
cwd             = spm_select(1,'dir','Select root directory for studies',...
                    '',pwd);
 cd(cwd);
 % GET SUBJECTS DIRECTORIES
 pth_subjdirs    = spm_select([1,Inf],'dir','Select subject directories to process',...
                    '',pwd);
 nsub = size(pth_subjdirs,1);
 fprintf('The following %d subject(s) will be examined:\n',nsub);
 disp(pth_subjdirs);

 for sub=1:nsub
     % change working directory
     cd(strtrim(pth_subjdirs(sub,1:end)));
     [~, nam, ~] = fileparts(pwd);
     outfile = [nam '_ft.mat'];
     list=dir('**/*.*');
     cd(list(10).folder);
     fprintf('\nWorking on %s\n', nam);

     % --- DELTA --- %
     DeltaHH(sub,:) = load('deltasource_HH.mat','delta_source_HH');
     DeltaAA(sub,:) = load('deltasource_AA.mat','delta_source_AA');
     DeltaAH(sub,:) = load('deltasource_AH.mat','delta_source_AH');
     DeltaHA(sub,:) = load('deltasource_HA.mat','delta_source_HA');

     % --- THETA --- %
     thetaHH(sub,:) = load('thetasource_HH.mat','theta_source_HH');
     thetaAA(sub,:) = load('thetasource_AA.mat','theta_source_AA');
     thetaAH(sub,:) = load('thetasource_AH.mat','theta_source_AH');
     thetaHA(sub,:) = load('thetasource_HA.mat','theta_source_HA');

     % --- ALPHA --- %
     alphaHH(sub,:) = load('alphasource_HH.mat','alpha_source_HH');
     alphaAA(sub,:) = load('alphasource_AA.mat','alpha_source_AA');
     alphaAH(sub,:) = load('alphasource_AH.mat','alpha_source_AH');
     alphaHA(sub,:) = load('alphasource_HA.mat','alpha_source_HA');

     % --- BETA --- %
     betaHH(sub,:) = load('betasource_HH.mat','beta_source_HH');
     betaAA(sub,:) = load('betasource_AA.mat','beta_source_AA');
```

```
49.       betaAH(sub,:) = load('betasource_AH.mat','beta_source_AH');
50.       betaHA(sub,:) = load('betasource_HA.mat','beta_source_HA');
51.
52.       % --- GAMMA1 --- %
53.       gamma1HH(sub,:) = load('gamma1source_HH.mat','gamma1_source_HH');
54.       gamma1AA(sub,:) = load('gamma1source_AA.mat','gamma1_source_AA');
55.       gamma1AH(sub,:) = load('gamma1source_AH.mat','gamma1_source_AH');
56.       gamma1HA(sub,:) = load('gamma1source_HA.mat','gamma1_source_HA');
57.
58.       % --- GAMMA2 --- %
59.       gamma2HH(sub,:) = load('gamma2source_HH.mat','gamma2_source_HH');
60.       gamma2AA(sub,:) = load('gamma2source_AA.mat','gamma2_source_AA');
61.       gamma2AH(sub,:) = load('gamma2source_AH.mat','gamma2_source_AH');
62.       gamma2HA(sub,:) = load('gamma2source_HA.mat','gamma2_source_HA');
63.   end
64.
65.   % GRAND AVERAGE SOURCES
66.   cfg = [];
67.   cfg.parameter       = 'pow';
68.   cfg.keepindividual  = 'yes';
69.
70.   % --- Delta --- %
71.   deltaAAavg =
     ft_sourcegrandaverage(cfg,DeltaAA(1).delta_source_AA,DeltaAA(2).delta_s
     ource_AA,DeltaAA(3).delta_source_AA,DeltaAA(4).delta_source_AA,DeltaAA(
     5).delta_source_AA,DeltaAA(6).delta_source_AA,DeltaAA(7).delta_source_A
     A,DeltaAA(8).delta_source_AA,DeltaAA(9).delta_source_AA,DeltaAA(10).del
     ta_source_AA,DeltaAA(11).delta_source_AA,DeltaAA(12).delta_source_AA,De
     ltaAA(13).delta_source_AA,DeltaAA(14).delta_source_AA,DeltaAA(15).delta
     _source_AA,DeltaAA(16).delta_source_AA,DeltaAA(17).delta_source_AA,Delt
     aAA(18).delta_source_AA,DeltaAA(19).delta_source_AA,DeltaAA(20).delta_s
     ource_AA,DeltaAA(21).delta_source_AA,DeltaAA(22).delta_source_AA,DeltaA
     A(23).delta_source_AA,DeltaAA(24).delta_source_AA);
72.   deltaAHavg =
     ft_sourcegrandaverage(cfg,DeltaAH(1).delta_source_AH,DeltaAH(2).delta_s
     ource_AH,DeltaAH(3).delta_source_AH,DeltaAH(4).delta_source_AH,DeltaAH(
     5).delta_source_AH,DeltaAH(6).delta_source_AH,DeltaAH(7).delta_source_A
     H,DeltaAH(8).delta_source_AH,DeltaAH(9).delta_source_AH,DeltaAH(10).del
     ta_source_AH,DeltaAH(11).delta_source_AH,DeltaAH(12).delta_source_AH,De
     ltaAH(13).delta_source_AH,DeltaAH(14).delta_source_AH,DeltaAH(15).delta
     _source_AH,DeltaAH(16).delta_source_AH,DeltaAH(17).delta_source_AH,Delt
     aAH(18).delta_source_AH,DeltaAH(19).delta_source_AH,DeltaAH(20).delta_s
     ource_AH,DeltaAH(21).delta_source_AH,DeltaAH(22).delta_source_AH,DeltaA
     H(23).delta_source_AH,DeltaAH(24).delta_source_AH);
73.   deltaHHavg =
     ft_sourcegrandaverage(cfg,DeltaHH(1).delta_source_HH,DeltaHH(2).delta_s
     ource_HH,DeltaHH(3).delta_source_HH,DeltaHH(4).delta_source_HH,DeltaHH(
     5).delta_source_HH,DeltaHH(6).delta_source_HH,DeltaHH(7).delta_source_H
     H,DeltaHH(8).delta_source_HH,DeltaHH(9).delta_source_HH,DeltaHH(10).del
     ta_source_HH,DeltaHH(11).delta_source_HH,DeltaHH(12).delta_source_HH,De
     ltaHH(13).delta_source_HH,DeltaHH(14).delta_source_HH,DeltaHH(15).delta
     _source_HH,DeltaHH(16).delta_source_HH,DeltaHH(17).delta_source_HH,Delt
     aHH(18).delta_source_HH,DeltaHH(19).delta_source_HH,DeltaHH(20).delta_s
     ource_HH,DeltaHH(21).delta_source_HH,DeltaHH(22).delta_source_HH,DeltaH
     H(23).delta_source_HH,DeltaHH(24).delta_source_HH);
74.   deltaHAavg =
     ft_sourcegrandaverage(cfg,DeltaHA(1).delta_source_HA,DeltaHA(2).delta_s
```

```
   ource_HA,DeltaHA(3).delta_source_HA,DeltaHA(4).delta_source_HA,DeltaHA(
   5).delta_source_HA,DeltaHA(6).delta_source_HA,DeltaHA(7).delta_source_H
   A,DeltaHA(8).delta_source_HA,DeltaHA(9).delta_source_HA,DeltaHA(10).del
   ta_source_HA,DeltaHA(11).delta_source_HA,DeltaHA(12).delta_source_HA,De
   ltaHA(13).delta_source_HA,DeltaHA(14).delta_source_HA,DeltaHA(15).delta
   _source_HA,DeltaHA(16).delta_source_HA,DeltaHA(17).delta_source_HA,Delt
   aHA(18).delta_source_HA,DeltaHA(19).delta_source_HA,DeltaHA(20).delta_s
   ource_HA,DeltaHA(21).delta_source_HA,DeltaHA(22).delta_source_HA,DeltaH
   A(23).delta_source_HA,DeltaHA(24).delta_source_HA);
75.  save('deltaAAavg.mat','deltaAAavg','-v7.3');
76.  save('deltaAHavg.mat','deltaAHavg','-v7.3');
77.  save('deltaHHavg.mat','deltaHHavg','-v7.3');
78.  save('deltaHAavg.mat','deltaHAavg','-v7.3');
79.  % --- Theta --- %
80.  thetaAAavg =
   ft_sourcegrandaverage(cfg,thetaAA(1).theta_source_AA,thetaAA(2).theta_s
   ource_AA,thetaAA(3).theta_source_AA,thetaAA(4).theta_source_AA,thetaAA(
   5).theta_source_AA,thetaAA(6).theta_source_AA,thetaAA(7).theta_source_A
   A,thetaAA(8).theta_source_AA,thetaAA(9).theta_source_AA,thetaAA(10).the
   ta_source_AA,thetaAA(11).theta_source_AA,thetaAA(12).theta_source_AA,th
   etaAA(13).theta_source_AA,thetaAA(14).theta_source_AA,thetaAA(15).theta
   _source_AA,thetaAA(16).theta_source_AA,thetaAA(17).theta_source_AA,thet
   aAA(18).theta_source_AA,thetaAA(19).theta_source_AA,thetaAA(20).theta_s
   ource_AA,thetaAA(21).theta_source_AA,thetaAA(22).theta_source_AA,thetaA
   A(23).theta_source_AA,thetaAA(24).theta_source_AA);
81.  thetaAHavg =
   ft_sourcegrandaverage(cfg,thetaAH(1).theta_source_AH,thetaAH(2).theta_s
   ource_AH,thetaAH(3).theta_source_AH,thetaAH(4).theta_source_AH,thetaAH(
   5).theta_source_AH,thetaAH(6).theta_source_AH,thetaAH(7).theta_source_A
   H,thetaAH(8).theta_source_AH,thetaAH(9).theta_source_AH,thetaAH(10).the
   ta_source_AH,thetaAH(11).theta_source_AH,thetaAH(12).theta_source_AH,th
   etaAH(13).theta_source_AH,thetaAH(14).theta_source_AH,thetaAH(15).theta
   _source_AH,thetaAH(16).theta_source_AH,thetaAH(17).theta_source_AH,thet
   aAH(18).theta_source_AH,thetaAH(19).theta_source_AH,thetaAH(20).theta_s
   ource_AH,thetaAH(21).theta_source_AH,thetaAH(22).theta_source_AH,thetaA
   H(23).theta_source_AH,thetaAH(24).theta_source_AH);
82.  thetaHHavg =
   ft_sourcegrandaverage(cfg,thetaHH(1).theta_source_HH,thetaHH(2).theta_s
   ource_HH,thetaHH(3).theta_source_HH,thetaHH(4).theta_source_HH,thetaHH(
   5).theta_source_HH,thetaHH(6).theta_source_HH,thetaHH(7).theta_source_H
   H,thetaHH(8).theta_source_HH,thetaHH(9).theta_source_HH,thetaHH(10).the
   ta_source_HH,thetaHH(11).theta_source_HH,thetaHH(12).theta_source_HH,th
   etaHH(13).theta_source_HH,thetaHH(14).theta_source_HH,thetaHH(15).theta
   _source_HH,thetaHH(16).theta_source_HH,thetaHH(17).theta_source_HH,thet
   aHH(18).theta_source_HH,thetaHH(19).theta_source_HH,thetaHH(20).theta_s
   ource_HH,thetaHH(21).theta_source_HH,thetaHH(22).theta_source_HH,thetaH
   H(23).theta_source_HH,thetaHH(24).theta_source_HH);
83.  thetaHAavg =
   ft_sourcegrandaverage(cfg,thetaHA(1).theta_source_HA,thetaHA(2).theta_s
   ource_HA,thetaHA(3).theta_source_HA,thetaHA(4).theta_source_HA,thetaHA(
   5).theta_source_HA,thetaHA(6).theta_source_HA,thetaHA(7).theta_source_H
   A,thetaHA(8).theta_source_HA,thetaHA(9).theta_source_HA,thetaHA(10).the
   ta_source_HA,thetaHA(11).theta_source_HA,thetaHA(12).theta_source_HA,th
   etaHA(13).theta_source_HA,thetaHA(14).theta_source_HA,thetaHA(15).theta
   _source_HA,thetaHA(16).theta_source_HA,thetaHA(17).theta_source_HA,thet
   aHA(18).theta_source_HA,thetaHA(19).theta_source_HA,thetaHA(20).theta_s
```

```
   ource_HA,thetaHA(21).theta_source_HA,thetaHA(22).theta_source_HA,thetaH
   A(23).theta_source_HA,thetaHA(24).theta_source_HA);
84.  save('thetaAAavg.mat','thetaAAavg','-v7.3');
85.  save('thetaAHavg.mat','thetaAHavg','-v7.3');
86.  save('thetaHHavg.mat','thetaHHavg','-v7.3');
87.  save('thetaHAavg.mat','thetaHAavg','-v7.3');
88.  % --- ALPHA --- %
89.  alphaAAavg =
   ft_sourcegrandaverage(cfg,alphaAA(1).alpha_source_AA,alphaAA(2).alpha_s
   ource_AA,alphaAA(3).alpha_source_AA,alphaAA(4).alpha_source_AA,alphaAA(
   5).alpha_source_AA,alphaAA(6).alpha_source_AA,alphaAA(7).alpha_source_A
   A,alphaAA(8).alpha_source_AA,alphaAA(9).alpha_source_AA,alphaAA(10).alp
   ha_source_AA,alphaAA(11).alpha_source_AA,alphaAA(12).alpha_source_AA,al
   phaAA(13).alpha_source_AA,alphaAA(14).alpha_source_AA,alphaAA(15).alpha
   _source_AA,alphaAA(16).alpha_source_AA,alphaAA(17).alpha_source_AA,alph
   aAA(18).alpha_source_AA,alphaAA(19).alpha_source_AA,alphaAA(20).alpha_s
   ource_AA,alphaAA(21).alpha_source_AA,alphaAA(22).alpha_source_AA,alphaA
   A(23).alpha_source_AA,alphaAA(24).alpha_source_AA);
90.  alphaAHavg =
   ft_sourcegrandaverage(cfg,alphaAH(1).alpha_source_AH,alphaAH(2).alpha_s
   ource_AH,alphaAH(3).alpha_source_AH,alphaAH(4).alpha_source_AH,alphaAH(
   5).alpha_source_AH,alphaAH(6).alpha_source_AH,alphaAH(7).alpha_source_A
   H,alphaAH(8).alpha_source_AH,alphaAH(9).alpha_source_AH,alphaAH(10).alp
   ha_source_AH,alphaAH(11).alpha_source_AH,alphaAH(12).alpha_source_AH,al
   phaAH(13).alpha_source_AH,alphaAH(14).alpha_source_AH,alphaAH(15).alpha
   _source_AH,alphaAH(16).alpha_source_AH,alphaAH(17).alpha_source_AH,alph
   aAH(18).alpha_source_AH,alphaAH(19).alpha_source_AH,alphaAH(20).alpha_s
   ource_AH,alphaAH(21).alpha_source_AH,alphaAH(22).alpha_source_AH,alphaA
   H(23).alpha_source_AH,alphaAH(24).alpha_source_AH);
91.  alphaHHavg =
   ft_sourcegrandaverage(cfg,alphaHH(1).alpha_source_HH,alphaHH(2).alpha_s
   ource_HH,alphaHH(3).alpha_source_HH,alphaHH(4).alpha_source_HH,alphaHH(
   5).alpha_source_HH,alphaHH(6).alpha_source_HH,alphaHH(7).alpha_source_H
   H,alphaHH(8).alpha_source_HH,alphaHH(9).alpha_source_HH,alphaHH(10).alp
   ha_source_HH,alphaHH(11).alpha_source_HH,alphaHH(12).alpha_source_HH,al
   phaHH(13).alpha_source_HH,alphaHH(14).alpha_source_HH,alphaHH(15).alpha
   _source_HH,alphaHH(16).alpha_source_HH,alphaHH(17).alpha_source_HH,alph
   aHH(18).alpha_source_HH,alphaHH(19).alpha_source_HH,alphaHH(20).alpha_s
   ource_HH,alphaHH(21).alpha_source_HH,alphaHH(22).alpha_source_HH,alphaH
   H(23).alpha_source_HH,alphaHH(24).alpha_source_HH);
92.  alphaHAavg =
   ft_sourcegrandaverage(cfg,alphaHA(1).alpha_source_HA,alphaHA(2).alpha_s
   ource_HA,alphaHA(3).alpha_source_HA,alphaHA(4).alpha_source_HA,alphaHA(
   5).alpha_source_HA,alphaHA(6).alpha_source_HA,alphaHA(7).alpha_source_H
   A,alphaHA(8).alpha_source_HA,alphaHA(9).alpha_source_HA,alphaHA(10).alp
   ha_source_HA,alphaHA(11).alpha_source_HA,alphaHA(12).alpha_source_HA,al
   phaHA(13).alpha_source_HA,alphaHA(14).alpha_source_HA,alphaHA(15).alpha
   _source_HA,alphaHA(16).alpha_source_HA,alphaHA(17).alpha_source_HA,alph
   aHA(18).alpha_source_HA,alphaHA(19).alpha_source_HA,alphaHA(20).alpha_s
   ource_HA,alphaHA(21).alpha_source_HA,alphaHA(22).alpha_source_HA,alphaH
   A(23).alpha_source_HA,alphaHA(24).alpha_source_HA);
93.  save('alphaAAavg.mat','alphaAAavg','-v7.3');
94.  save('alphaAHavg.mat','alphaAHavg','-v7.3');
95.  save('alphaHHavg.mat','alphaHHavg','-v7.3');
96.  save('alphaHAavg.mat','alphaHAavg','-v7.3');
97.  % --- BETA --- %
```

```
98.  betaAAavg =
   ft_sourcegrandaverage(cfg,betaAA(1).beta_source_AA,betaAA(2).beta_sourc
   e_AA,betaAA(3).beta_source_AA,betaAA(4).beta_source_AA,betaAA(5).beta_s
   ource_AA,betaAA(6).beta_source_AA,betaAA(7).beta_source_AA,betaAA(8).be
   ta_source_AA,betaAA(9).beta_source_AA,betaAA(10).beta_source_AA,betaAA(
   11).beta_source_AA,betaAA(12).beta_source_AA,betaAA(13).beta_source_AA,
   betaAA(14).beta_source_AA,betaAA(15).beta_source_AA,betaAA(16).beta_sou
   rce_AA,betaAA(17).beta_source_AA,betaAA(18).beta_source_AA,betaAA(19).b
   eta_source_AA,betaAA(20).beta_source_AA,betaAA(21).beta_source_AA,betaA
   A(22).beta_source_AA,betaAA(23).beta_source_AA,betaAA(24).beta_source_A
   A);
99.  betaAHavg =
   ft_sourcegrandaverage(cfg,betaAH(1).beta_source_AH,betaAH(2).beta_sourc
   e_AH,betaAH(3).beta_source_AH,betaAH(4).beta_source_AH,betaAH(5).beta_s
   ource_AH,betaAH(6).beta_source_AH,betaAH(7).beta_source_AH,betaAH(8).be
   ta_source_AH,betaAH(9).beta_source_AH,betaAH(10).beta_source_AH,betaAH(
   11).beta_source_AH,betaAH(12).beta_source_AH,betaAH(13).beta_source_AH,
   betaAH(14).beta_source_AH,betaAH(15).beta_source_AH,betaAH(16).beta_sou
   rce_AH,betaAH(17).beta_source_AH,betaAH(18).beta_source_AH,betaAH(19).b
   eta_source_AH,betaAH(20).beta_source_AH,betaAH(21).beta_source_AH,betaA
   H(22).beta_source_AH,betaAH(23).beta_source_AH,betaAH(24).beta_source_A
   H);
100. betaHHavg =
   ft_sourcegrandaverage(cfg,betaHH(1).beta_source_HH,betaHH(2).beta_sourc
   e_HH,betaHH(3).beta_source_HH,betaHH(4).beta_source_HH,betaHH(5).beta_s
   ource_HH,betaHH(6).beta_source_HH,betaHH(7).beta_source_HH,betaHH(8).be
   ta_source_HH,betaHH(9).beta_source_HH,betaHH(10).beta_source_HH,betaHH(
   11).beta_source_HH,betaHH(12).beta_source_HH,betaHH(13).beta_source_HH,
   betaHH(14).beta_source_HH,betaHH(15).beta_source_HH,betaHH(16).beta_sou
   rce_HH,betaHH(17).beta_source_HH,betaHH(18).beta_source_HH,betaHH(19).b
   eta_source_HH,betaHH(20).beta_source_HH,betaHH(21).beta_source_HH,betaH
   H(22).beta_source_HH,betaHH(23).beta_source_HH,betaHH(24).beta_source_H
   H);
101. betaHAavg =
   ft_sourcegrandaverage(cfg,betaHA(1).beta_source_HA,betaHA(2).beta_sourc
   e_HA,betaHA(3).beta_source_HA,betaHA(4).beta_source_HA,betaHA(5).beta_s
   ource_HA,betaHA(6).beta_source_HA,betaHA(7).beta_source_HA,betaHA(8).be
   ta_source_HA,betaHA(9).beta_source_HA,betaHA(10).beta_source_HA,betaHA(
   11).beta_source_HA,betaHA(12).beta_source_HA,betaHA(13).beta_source_HA,
   betaHA(14).beta_source_HA,betaHA(15).beta_source_HA,betaHA(16).beta_sou
   rce_HA,betaHA(17).beta_source_HA,betaHA(18).beta_source_HA,betaHA(19).b
   eta_source_HA,betaHA(20).beta_source_HA,betaHA(21).beta_source_HA,betaH
   A(22).beta_source_HA,betaHA(23).beta_source_HA,betaHA(24).beta_source_H
   A);
102. save('betaAAavg.mat','betaAAavg','-v7.3');
103. save('betaAHavg.mat','betaAHavg','-v7.3');
104. save('betaHHavg.mat','betaHHavg','-v7.3');
105. save('betaHAavg.mat','betaHAavg','-v7.3');
106. % --- GAMMA1 --- %
107. gamma1AAavg =
   ft_sourcegrandaverage(cfg,gamma1AA(1).gamma1_source_AA,gamma1AA(2).gamm
   a1_source_AA,gamma1AA(3).gamma1_source_AA,gamma1AA(4).gamma1_source_AA,
   gamma1AA(5).gamma1_source_AA,gamma1AA(6).gamma1_source_AA,gamma1AA(7).g
   amma1_source_AA,gamma1AA(8).gamma1_source_AA,gamma1AA(9).gamma1_source_
   AA,gamma1AA(10).gamma1_source_AA,gamma1AA(11).gamma1_source_AA,gamma1AA
   (12).gamma1_source_AA,gamma1AA(13).gamma1_source_AA,gamma1AA(14).gamma1
   _source_AA,gamma1AA(15).gamma1_source_AA,gamma1AA(16).gamma1_source_AA,
```

```
   gamma1AA(17).gamma1_source_AA,gamma1AA(18).gamma1_source_AA,gamma1AA(19
   ).gamma1_source_AA,gamma1AA(20).gamma1_source_AA,gamma1AA(21).gamma1_so
   urce_AA,gamma1AA(22).gamma1_source_AA,gamma1AA(23).gamma1_source_AA,gam
   ma1AA(24).gamma1_source_AA);
108. gamma1AHavg =
   ft_sourcegrandaverage(cfg,gamma1AH(1).gamma1_source_AH,gamma1AH(2).gamm
   a1_source_AH,gamma1AH(3).gamma1_source_AH,gamma1AH(4).gamma1_source_AH,
   gamma1AH(5).gamma1_source_AH,gamma1AH(6).gamma1_source_AH,gamma1AH(7).g
   amma1_source_AH,gamma1AH(8).gamma1_source_AH,gamma1AH(9).gamma1_source_
   AH,gamma1AH(10).gamma1_source_AH,gamma1AH(11).gamma1_source_AH,gamma1AH
   (12).gamma1_source_AH,gamma1AH(13).gamma1_source_AH,gamma1AH(14).gamma1
   _source_AH,gamma1AH(15).gamma1_source_AH,gamma1AH(16).gamma1_source_AH,
   gamma1AH(17).gamma1_source_AH,gamma1AH(18).gamma1_source_AH,gamma1AH(19
   ).gamma1_source_AH,gamma1AH(20).gamma1_source_AH,gamma1AH(21).gamma1_so
   urce_AH,gamma1AH(22).gamma1_source_AH,gamma1AH(23).gamma1_source_AH,gam
   ma1AH(24).gamma1_source_AH);
109. gamma1HHavg =
   ft_sourcegrandaverage(cfg,gamma1HH(1).gamma1_source_HH,gamma1HH(2).gamm
   a1_source_HH,gamma1HH(3).gamma1_source_HH,gamma1HH(4).gamma1_source_HH,
   gamma1HH(5).gamma1_source_HH,gamma1HH(6).gamma1_source_HH,gamma1HH(7).g
   amma1_source_HH,gamma1HH(8).gamma1_source_HH,gamma1HH(9).gamma1_source_
   HH,gamma1HH(10).gamma1_source_HH,gamma1HH(11).gamma1_source_HH,gamma1HH
   (12).gamma1_source_HH,gamma1HH(13).gamma1_source_HH,gamma1HH(14).gamma1
   _source_HH,gamma1HH(15).gamma1_source_HH,gamma1HH(16).gamma1_source_HH,
   gamma1HH(17).gamma1_source_HH,gamma1HH(18).gamma1_source_HH,gamma1HH(19
   ).gamma1_source_HH,gamma1HH(20).gamma1_source_HH,gamma1HH(21).gamma1_so
   urce_HH,gamma1HH(22).gamma1_source_HH,gamma1HH(23).gamma1_source_HH,gam
   ma1HH(24).gamma1_source_HH);
110. gamma1HAavg =
   ft_sourcegrandaverage(cfg,gamma1HA(1).gamma1_source_HA,gamma1HA(2).gamm
   a1_source_HA,gamma1HA(3).gamma1_source_HA,gamma1HA(4).gamma1_source_HA,
   gamma1HA(5).gamma1_source_HA,gamma1HA(6).gamma1_source_HA,gamma1HA(7).g
   amma1_source_HA,gamma1HA(8).gamma1_source_HA,gamma1HA(9).gamma1_source_
   HA,gamma1HA(10).gamma1_source_HA,gamma1HA(11).gamma1_source_HA,gamma1HA
   (12).gamma1_source_HA,gamma1HA(13).gamma1_source_HA,gamma1HA(14).gamma1
   _source_HA,gamma1HA(15).gamma1_source_HA,gamma1HA(16).gamma1_source_HA,
   gamma1HA(17).gamma1_source_HA,gamma1HA(18).gamma1_source_HA,gamma1HA(19
   ).gamma1_source_HA,gamma1HA(20).gamma1_source_HA,gamma1HA(21).gamma1_so
   urce_HA,gamma1HA(22).gamma1_source_HA,gamma1HA(23).gamma1_source_HA,gam
   ma1HA(24).gamma1_source_HA);
111. save('gamma1AAavg.mat','gamma1AAavg','-v7.3');
112. save('gamma1AHavg.mat','gamma1AHavg','-v7.3');
113. save('gamma1HHavg.mat','gamma1HHavg','-v7.3');
114. save('gamma1HAavg.mat','gamma1HAavg','-v7.3');
115. % --- GAMMA2 --- %
116. gamma2AAavg =
   ft_sourcegrandaverage(cfg,gamma2AA(1).gamma2_source_AA,gamma2AA(2).gamm
   a2_source_AA,gamma2AA(3).gamma2_source_AA,gamma2AA(4).gamma2_source_AA,
   gamma2AA(5).gamma2_source_AA,gamma2AA(6).gamma2_source_AA,gamma2AA(7).g
   amma2_source_AA,gamma2AA(8).gamma2_source_AA,gamma2AA(9).gamma2_source_
   AA,gamma2AA(10).gamma2_source_AA,gamma2AA(11).gamma2_source_AA,gamma2AA
   (12).gamma2_source_AA,gamma2AA(13).gamma2_source_AA,gamma2AA(14).gamma2
   _source_AA,gamma2AA(15).gamma2_source_AA,gamma2AA(16).gamma2_source_AA,
   gamma2AA(17).gamma2_source_AA,gamma2AA(18).gamma2_source_AA,gamma2AA(19
   ).gamma2_source_AA,gamma2AA(20).gamma2_source_AA,gamma2AA(21).gamma2_so
   urce_AA,gamma2AA(22).gamma2_source_AA,gamma2AA(23).gamma2_source_AA,gam
   ma2AA(24).gamma2_source_AA); gamma2AHavg =
```

```
   ft_sourcegrandaverage(cfg,gamma2AH(1).gamma2_source_AH,gamma2AH(2).gamm
   a2_source_AH,gamma2AH(3).gamma2_source_AH,gamma2AH(4).gamma2_source_AH,
   gamma2AH(5).gamma2_source_AH,gamma2AH(6).gamma2_source_AH,gamma2AH(7).g
   amma2_source_AH,gamma2AH(8).gamma2_source_AH,gamma2AH(9).gamma2_source_
   AH,gamma2AH(10).gamma2_source_AH,gamma2AH(11).gamma2_source_AH,gamma2AH
   (12).gamma2_source_AH,gamma2AH(13).gamma2_source_AH,gamma2AH(14).gamma2
   _source_AH,gamma2AH(15).gamma2_source_AH,gamma2AH(16).gamma2_source_AH,
   gamma2AH(17).gamma2_source_AH,gamma2AH(18).gamma2_source_AH,gamma2AH(19
   ).gamma2_source_AH,gamma2AH(20).gamma2_source_AH,gamma2AH(21).gamma2_so
   urce_AH,gamma2AH(22).gamma2_source_AH,gamma2AH(23).gamma2_source_AH,gam
   ma2AH(24).gamma2_source_AH);
117. gamma2HHavg =
   ft_sourcegrandaverage(cfg,gamma2HH(1).gamma2_source_HH,gamma2HH(2).gamm
   a2_source_HH,gamma2HH(3).gamma2_source_HH,gamma2HH(4).gamma2_source_HH,
   gamma2HH(5).gamma2_source_HH,gamma2HH(6).gamma2_source_HH,gamma2HH(7).g
   amma2_source_HH,gamma2HH(8).gamma2_source_HH,gamma2HH(9).gamma2_source_
   HH,gamma2HH(10).gamma2_source_HH,gamma2HH(11).gamma2_source_HH,gamma2HH
   (12).gamma2_source_HH,gamma2HH(13).gamma2_source_HH,gamma2HH(14).gamma2
   _source_HH,gamma2HH(15).gamma2_source_HH,gamma2HH(16).gamma2_source_HH,
   gamma2HH(17).gamma2_source_HH,gamma2HH(18).gamma2_source_HH,gamma2HH(19
   ).gamma2_source_HH,gamma2HH(20).gamma2_source_HH,gamma2HH(21).gamma2_so
   urce_HH,gamma2HH(22).gamma2_source_HH,gamma2HH(23).gamma2_source_HH,gam
   ma2HH(24).gamma2_source_HH);
118. gamma2HAavg =
   ft_sourcegrandaverage(cfg,gamma2HA(1).gamma2_source_HA,gamma2HA(2).gamm
   a2_source_HA,gamma2HA(3).gamma2_source_HA,gamma2HA(4).gamma2_source_HA,
   gamma2HA(5).gamma2_source_HA,gamma2HA(6).gamma2_source_HA,gamma2HA(7).g
   amma2_source_HA,gamma2HA(8).gamma2_source_HA,gamma2HA(9).gamma2_source_
   HA,gamma2HA(10).gamma2_source_HA,gamma2HA(11).gamma2_source_HA,gamma2HA
   (12).gamma2_source_HA,gamma2HA(13).gamma2_source_HA,gamma2HA(14).gamma2
   _source_HA,gamma2HA(15).gamma2_source_HA,gamma2HA(16).gamma2_source_HA,
   gamma2HA(17).gamma2_source_HA,gamma2HA(18).gamma2_source_HA,gamma2HA(19
   ).gamma2_source_HA,gamma2HA(20).gamma2_source_HA,gamma2HA(21).gamma2_so
   urce_HA,gamma2HA(22).gamma2_source_HA,gamma2HA(23).gamma2_source_HA,gam
   ma2HA(24).gamma2_source_HA);
119. save('gamma2AAavg.mat','gamma2AAavg','-v7.3');
120. save('gamma2AHavg.mat','gamma2AHavg','-v7.3');
121. save('gamma2HHavg.mat','gamma2HHavg','-v7.3');
122. save('gamma2HAavg.mat','gamma2HAavg','-v7.3');
```

APPENDIX L: MEG SOURCE INTERPOLATION MATLAB SCRIPT

```
% script to do group comparisons and source localize results
% Used with FieldTrip Version: 20171231.zip
% Written by Katherine M. Becker

clear;
ft_defaults;

ftdir = fileparts(which('ft_defaults'));

 % load mri and interpolate for visualization
 template_mri = ft_read_mri(fullfile(ftdir,'external','spm8',...
     'templates','T1.nii'));

 cfg = [];
 mri = ft_volumereslice(cfg, template_mri);

 cfg            = [];
 cfg.downsample = 2;
 cfg.parameter  = 'stat';

 deltaHH_HA_int  = ft_sourceinterpolate(cfg, deltaHH_HA, mri);
 deltaAA_HH_int  = ft_sourceinterpolate(cfg, deltaAA_HH, mri);
 deltaAH_HA_int  = ft_sourceinterpolate(cfg, deltaAH_HA, mri);

 thetaAA_AH_int  = ft_sourceinterpolate(cfg, thetaAA_AH, mri);
 thetaHH_HA_int  = ft_sourceinterpolate(cfg, thetaHH_HA, mri);
 thetaAA_HH_int  = ft_sourceinterpolate(cfg, thetaAA_HH, mri);
 thetaAH_HA_int  = ft_sourceinterpolate(cfg, thetaAH_HA, mri);

 alphaAA_AH_int  = ft_sourceinterpolate(cfg, alphaAA_AH, mri);
 alphaHH_HA_int  = ft_sourceinterpolate(cfg, alphaHH_HA, mri);
 alphaAA_HH_int  = ft_sourceinterpolate(cfg, alphaAA_HH, mri);
 alphaAH_HA_int  = ft_sourceinterpolate(cfg, alphaAH_HA, mri);

 betaAA_AH_int  = ft_sourceinterpolate(cfg, betaAA_AH, mri);
 betaHH_HA_int  = ft_sourceinterpolate(cfg, betaHH_HA, mri);
 betaAA_HH_int  = ft_sourceinterpolate(cfg, betaAA_HH, mri);
 betaAH_HA_int  = ft_sourceinterpolate(cfg, betaAH_HA, mri);

 gamma1AA_AH_int  = ft_sourceinterpolate(cfg, gamma1AA_AH, mri);
 gamma1HH_HA_int  = ft_sourceinterpolate(cfg, gamma1HH_HA, mri);
 gamma1AA_HH_int  = ft_sourceinterpolate(cfg, gamma1AA_HH, mri);
 gamma1AH_HA_int  = ft_sourceinterpolate(cfg, gamma1AH_HA, mri);

 gamma2AA_AH_int  = ft_sourceinterpolate(cfg, gamma2AA_AH, mri);
 gamma2HH_HA_int  = ft_sourceinterpolate(cfg, gamma2HH_HA, mri);
 gamma2AA_HH_int  = ft_sourceinterpolate(cfg, gamma2AA_HH, mri);
 gamma2AH_HA_int  = ft_sourceinterpolate(cfg, gamma2AH_HA, mri);

 % --- INTERACTIONS --- %
```

```
Add
cfg = [];
cfg.parameter = 'pow';
cfg.operation = 'add';

% --- CONGRUENCY --- %
deltaAAHH = ft_math(cfg,deltaAAavg,deltaHHavg);
deltaAHHA = ft_math(cfg,deltaAHavg,deltaHAavg);

thetaAAHH = ft_math(cfg,thetaAAavg,thetaHHavg);
thetaAHHA = ft_math(cfg,thetaAHavg,thetaHAavg);

alphaAAHH = ft_math(cfg,alphaAAavg,alphaHHavg);
alphaAHHA = ft_math(cfg,alphaAHavg,alphaHAavg);

betaAAHH = ft_math(cfg,betaAAavg,betaHHavg);
betaAHHA = ft_math(cfg,betaAHavg,betaHAavg);

gamma1AAHH = ft_math(cfg,gamma1AAavg,gamma1HHavg);
gamma1AHHA = ft_math(cfg,gamma1AHavg,gamma1HAavg);

gamma2AAHH = ft_math(cfg,gamma2AAavg,gamma2HHavg);
gamma2AHHA = ft_math(cfg,gamma2AHavg,gamma2HAavg);

Subtract
cfg = [];
cfg.parameter = 'pow';
cfg.operation = 'subtract';

% --- CONGRUENCY --- %
delta_con = ft_math(cfg,deltaAAHH,deltaAHHA);
theta_con = ft_math(cfg,thetaAAHH,thetaAHHA);
alpha_con = ft_math(cfg,alphaAAHH,alphaAHHA);
beta_con = ft_math(cfg,betaAAHH,betaAHHA);
gamma1_con = ft_math(cfg,gamma1AAHH,gamma1AHHA);
gamma2_con = ft_math(cfg,gamma2AAHH,gamma2AHHA);

% --- EMOTION --- %
delta_emo = ft_math(cfg,deltaHHavg,deltaAAavg);
theta_emo = ft_math(cfg,thetaHHavg,thetaAAavg);
alpha_emo = ft_math(cfg,alphaHHavg,alphaAAavg);
beta_emo = ft_math(cfg,betaHHavg,betaAAavg);
gamma1_emo = ft_math(cfg,gamma1HHavg,gamma1AAavg);
gamma2_emo = ft_math(cfg,gamma2HHavg,gamma2AAavg);

% MAIN EFFECTS
cfg = [];
cfg.method           = 'montecarlo';
cfg.statistic        = 'ft_statfun_depsamplesT';
cfg.parameter        = 'pow';
cfg.correctm         = 'cluster';
cfg.numrandomization = 1000;
cfg.alpha            = 0.05;
cfg.tail             = 0;

nsubj=numel(alphaAAavg);
cfg.design(1,:) = [1:24 1:24];
```

```
cfg.design(2,:) = [ones(1,24)*1 ones(1,24)*2];
cfg.uvar        = 1; % row of design matrix that contains unit
   variable (in this case: subjects)
cfg.ivar        = 2; % row of design matrix that contains independent
   variable (the conditions)

delta_main = ft_sourcestatistics(cfg,deltaAAHH,deltaAHHA);
theta_main = ft_sourcestatistics(cfg,thetaAAHH,thetaAHHA);
alpha_main = ft_sourcestatistics(cfg,alphaAAHH,alphaAHHA);
beta_main = ft_sourcestatistics(cfg,betaAAHH,betaAHHA);
gamma1_main = ft_sourcestatistics(cfg,gamma1AAHH,gamma1AHHA);
gamma2_main = ft_sourcestatistics(cfg,gamma1AAHH,gamma1AHHA);

% interpolate
cfg            = [];
cfg.downsample = 2;
cfg.parameter  = 'stat';

delta_main_int  = ft_sourceinterpolate(cfg, delta_main, mri);
theta_main_int  = ft_sourceinterpolate(cfg, theta_main, mri);
alpha_main_int  = ft_sourceinterpolate(cfg, alpha_main, mri);
beta_main_int  = ft_sourceinterpolate(cfg, beta_main, mri);
gamma1_main_int  = ft_sourceinterpolate(cfg, gamma1_main, mri);
gamma2_main_int  = ft_sourceinterpolate(cfg, gamma2_main, mri);

% INTERACTIONS
cfg = [];
cfg.parameter = 'pow';
cfg.operation = 'multiply';

delta_conxemo = ft_math(cfg,delta_con,delta_emo);
theta_conxemo = ft_math(cfg,theta_con,theta_emo);
alpha_conxemo = ft_math(cfg,alpha_con,alpha_emo);
beta_conxemo = ft_math(cfg,beta_con,beta_emo);
gamma1_conxemo = ft_math(cfg,gamma1_con,gamma1_emo);
gamma2_conxemo = ft_math(cfg,gamma2_con,gamma2_emo);

% interpolate
cfg            = [];
cfg.downsample = 2;
cfg.parameter  = 'pow';

delta_conxemo_int  = ft_sourceinterpolate(cfg, delta_conxemo, mri);
theta_conxemo_int  = ft_sourceinterpolate(cfg, theta_conxemo, mri);
alpha_conxemo_int  = ft_sourceinterpolate(cfg, alpha_conxemo, mri);
beta_conxemo_int  = ft_sourceinterpolate(cfg, beta_conxemo, mri);
gamma1_conxemo_int  = ft_sourceinterpolate(cfg, gamma1_conxemo, mri);
gamma2_conxemo_int  = ft_sourceinterpolate(cfg, gamma2_conxemo, mri);

% SOURCE COMPARISONS
cfg = [];
cfg.method           = 'montecarlo';
cfg.statistic        = 'ft_statfun_depsamplesT';
cfg.parameter        = 'pow';
cfg.correctm         = 'cluster';
cfg.numrandomization = 1000;
cfg.alpha            = 0.05;
```

```
cfg.tail             = 0;

nsubj=numel(alphaAAavg);
cfg.design(1,:) = [1:24 1:24];
cfg.design(2,:) = [ones(1,24)*1 ones(1,24)*2];
cfg.uvar        = 1; % row of design matrix that contains unit
   variable (in this case: subjects)
cfg.ivar        = 2; % row of design matrix that contains independent
   variable (the conditions)

delta_conxemo_dep = ft_sourcestatistics(cfg, delta_con, delta_emo);
theta_conxemo_dep = ft_sourcestatistics(cfg, theta_con, theta_emo);
alpha_conxemo_dep = ft_sourcestatistics(cfg, alpha_con, alpha_emo);
beta_conxemo_dep = ft_sourcestatistics(cfg, beta_con, beta_emo);
gamma1_conxemo_dep = ft_sourcestatistics(cfg, gamma1_con, gamma1_emo);
gamma2_conxemo_dep = ft_sourcestatistics(cfg, gamma2_con, gamma2_emo);

% interpolate
cfg            = [];
cfg.downsample = 2;
cfg.parameter  = 'stat';

delta_conxemo_dep_int  = ft_sourceinterpolate(cfg, delta_conxemo_dep,
   mri);
theta_conxemo_dep_int  = ft_sourceinterpolate(cfg, theta_conxemo_dep,
   mri);
alpha_conxemo_dep_int  = ft_sourceinterpolate(cfg, alpha_conxemo_dep,
   mri);
beta_conxemo_dep_int  = ft_sourceinterpolate(cfg, beta_conxemo_dep,
   mri);
gamma1_conxemo_dep_int  = ft_sourceinterpolate(cfg,
   gamma1_conxemo_dep, mri);
gamma2_conxemo_dep_int  = ft_sourceinterpolate(cfg,
   gamma2_conxemo_dep, mri);

```